

UC Davis

Technical Memoranda

Title

Test Method Selection and Validation to Replace the R-Value Test

Permalink

<https://escholarship.org/uc/item/88c7551g>

Authors

Louw, Stephanus
Tom, Heather
Hammack, Joseph
[et al.](#)

Publication Date

2024-11-01

DOI

10.7922/G20V8B4W

Test Method Selection and Validation to Replace the R-Value Test

Authors:

Stephanus Louw, Heather Tom, Joseph Hammack, Jeffrey Buscheck, John Harvey,
and David Jones

Partnered Pavement Research Center (PPRC) Project Number 2.12 (DRISI Task 3830):
Long Term Research

PREPARED FOR:

California Department of Transportation
Division of Research, Innovation and System Information
Office of Materials and Infrastructure Roadway Research

PREPARED BY:

University of California
Pavement Research Center
UC Davis and UC Berkeley



TECHNICAL REPORT DOCUMENTATION PAGE

1. REPORT NUMBER UCPRC-TM-2023-07	2. GOVERNMENT ASSOCIATION NUMBER	3. RECIPIENT'S CATALOG NUMBER
4. TITLE AND SUBTITLE Test Method Selection and Validation to Replace the R-Value Test		5. REPORT PUBLICATION DATE October 2024
		6. PERFORMING ORGANIZATION CODE
7. AUTHOR(S) Stephanus Louw (ORCID 0000-0002-1021-7110) Heather Tom (ORCID 0000-0001-6982-7493) Joseph Hammack (ORCID: 0000-0002-2410-0896) Jeffery Buscheck (ORCID 0000-0002-0930-6861) John Harvey(ORCID 0000-0002-8924-6212) David Jones (ORCID 0000-0002-2938-076X)		8. PERFORMING ORGANIZATION REPORT NO. UCPRC-TM-2023-07 UCD-ITS-RR-23-82
		10. WORK UNIT NUMBER
9. PERFORMING ORGANIZATION NAME AND ADDRESS University of California Pavement Research Center Department of Civil and Environmental Engineering, UC Davis 1 Shields Avenue Davis, CA 95616		11. CONTRACT OR GRANT NUMBER 65A0628
		13. TYPE OF REPORT AND PERIOD COVERED Technical Memorandum
12. SPONSORING AGENCY AND ADDRESS California Department of Transportation Division of Research, Innovation, and System Information P.O. Box 942873 Sacramento, CA 94273-0001		14. SPONSORING AGENCY CODE
15. SUPPLEMENTAL NOTES DOI: 10.7922/G20V8B4W		
16. ABSTRACT <p>This technical memorandum summarizes a study that investigated the use of a confined compressive strength (CCS) test to replace the R-value test currently used for some pavement design and for quality control/quality assurance in California. The report covers a literature review, development of an alternative test, and a comparison of the results from the proposed test with R-value results.</p> <p>The following are conclusions made based on the findings. First, California Test 216 needs revision. The compaction density reported by the test method is lower than the physical density of the compacted specimen in the CT 216 apparatus. The reported CT 216 density is approximately 88% of Modified Proctor density. Second, the proposed specimen compaction procedure, using Modified Proctor as the reference density, produced unbound specimens that could be handled and tested in a triaxial cell. Third, there is no correlation between the R-value test and the CCS test for the materials tested to date because the limited range of R-values produced by the 22 base and one subbase materials is too small to define a relationship with the CCS test. Most of the R-values of the materials tested were just above the minimum specified value of 78 for Class 2 aggregate base. Fourth, the suggested preliminary CCS criteria for replacement of the R-value specification for Class 2 aggregate base are minimum 101 psi peak stress at 5 psi confinement and minimum 144 psi peak stress at 10 psi confinement.</p> <p>The following interim recommendations are made based on the testing, the documented low test precision of the R-value test, and the limitations of developing a correlation between R-value and the CCS test. First, additional testing of four or five subbase materials with R-values between 40 and 60 should be completed to refine the CCS test criteria. If these materials are not available from producers, they can be manufactured in the UCPRC laboratory by blending available materials. Second, material properties, including gradation, flakiness, crushed faces, sand equivalence, Atterberg limits, and moisture sensitivity (i.e., shape of the optimum moisture content curve) should be considered when analyzing any correlations.</p>		
17. KEYWORDS R-value test, confined compressive strength test		18. DISTRIBUTION STATEMENT No restrictions. This document is available to the public through the National Technical Information Service, Springfield, VA 22161
19. SECURITY CLASSIFICATION (of this report) Unclassified	20. NUMBER OF PAGES 111	21. PRICE None

Reproduction of completed page authorized

UCPRC ADDITIONAL INFORMATION

1. DRAFT STAGE Final	2. VERSION NUMBER 1
3. UCPRC STRATEGIC PLAN ELEMENT NUMBER 2.12	4. CALTRANS TASK NUMBER 3830
5. CALTRANS TECHNICAL LEAD AND REVIEWER(S) Deepak Maskey	6. FHWA NUMBER CA243830

7. PROPOSALS FOR IMPLEMENTATION
None

8. RELATED DOCUMENTS
None

9. VERSION UPDATES
None

10. LABORATORY ACCREDITATION
The UCPRC laboratory is accredited by AASHTO re:source and CCRL for the laboratory testing discussed in this report.



11. SIGNATURES

S. Louw FIRST AUTHOR	J.T. Harvey TECHNICAL REVIEW	C. Fink EDITOR	J.T. Harvey PRINCIPAL INVESTIGATOR	D. Maskey CALTRANS TECH. LEAD	T.J. Holland CALTRANS CONTRACT MANAGER
--------------------------------	--	--------------------------	--	---	--

Reproduction of completed page authorized

DISCLAIMER

This document is disseminated in the interest of information exchange. The contents of this report reflect the views of the authors who are responsible for the facts and accuracy of the data presented herein. The contents do not necessarily reflect the official views or policies of the State of California or the Federal Highway Administration. This publication does not constitute a standard, specification, or regulation. This report does not constitute an endorsement by the Department of any product described herein.

ACKNOWLEDGMENTS

The University of California Pavement Research Center acknowledges the following individuals and organizations who contributed to the project:

- California Department of Transportation
- Engeo Geotechnical Testing Laboratories
- George Reed, Inc.
- Graniterock
- Teichert Aggregates
- Vulcan Materials Company
- UCPRC laboratory operations team and Camille Fink, UCPRC publications manager

PROJECT OBJECTIVES

The objective of this project was to identify a replacement test for the R-value test. This would be achieved through the following tasks:

- Recommend an alternative test to the R-value test for characterization and quality control/quality assurance of unbound base and subbase aggregate materials in California.
- Develop a correlation between the R-value and selected test results based on testing of a range of commercially available base and subbase materials.
- Recommend provisional criteria for acceptance.

This technical memorandum covers all tasks.

EXECUTIVE SUMMARY

This technical memorandum summarizes a study that investigated the use of a confined compressive strength (CCS) test to replace the R-value test currently used for some pavement design and for quality control/quality assurance in California. The report covers a literature review, development of an alternative test, and a comparison of the results from the proposed test with R-value results. Testing was limited to aggregate base and subbase materials. The new test method is based on a current Texas Department of Transportation test. However, the specimen preparation and test methods were updated based on the work done in this study.

Although materials with a wide range of R-values were sought, 22 of the 28 materials provided by suppliers fell within a small range that exceeded the minimum Caltrans Class 2 aggregate base specification, with the remaining material only just falling below the specification requirement but easily exceeding the minimum subbase requirements. This was an indication that subbase materials are not being widely produced in California at this time. To have a wider range of materials for comparison of the CCS test and the R-value test, five materials were then manufactured to create materials with lower R-values closer to the minimum specifications for aggregate subbase materials.

The literature review found that the R-value test has relatively low precision and that the precision increases as the R-value increases. However, there is still a risk of failing high quality materials and a higher risk of passing low quality materials.

The development of a CCS test is discussed, including the validation of a simplified confinement cell. The simple CCS test proposed for an R-value replacement test includes the use of a predetermined confinement pressure. Comparing the R-value to CCS for the materials tested to date showed that there is weak correlation between the tests, which was attributed to the known poor precision of the R-value test and the difference in test conditions between the two tests.

Confining pressures between 0 and 20 psi were used in the study. It is logical that a test should have a positive correlation with the R-value such that minimum strength values can be recommended to distinguish between different materials. This would lead to selecting a confinement pressure of either 15 or 20 psi. A lower confinement can be recommended, such as

0 psi or 3 psi, but low confining pressure does not engage the aggregate friction of an aggregate material that will perform well in the field and therefore also have a positive correlation with the R-value. At confining pressures below 15 psi, the materials with more fines and more plasticity (ASB2, ASB3, AB3) showed better peak stress (strength) values than the materials with fewer fines and less plasticity (AB2), largely due to cohesion because friction was not engaged, and had a negative correlation between the R-value and CCS. It is therefore not possible to recommend a minimum CCS value for different material groups for CCS tests run with less than 15 psi confining pressure. Additional parameters would be required to distinguish between material groups.

The following conclusions are made based on the findings:

- California Test 216 needs revision. The compaction density reported by the test method is lower than the density determined by measuring the dimensions of the compacted specimen in the CT 216 apparatus. The reported CT 216 density is approximately 88% of Modified Proctor density.
- The proposed specimen compaction procedure, using Modified Proctor as the reference density, produced unbound specimens that could be handled and tested in a triaxial cell.
- A confining stress of 15 or 20 psi should be used. Confining stresses less than 15 psi showed negative correlations with the R-value and better CCS values for materials with finer gradations and more plasticity.
- The suggested preliminary CCS criteria for replacement of the R-value specification are presented in the following table.
- It must be emphasized that the CCS test, as a replacement for the R-value test, will require additional calibration with resilient modulus before it can be used in mechanistic design.

Recommended Preliminary CCS Specification Values

Parameter	Material				
	AB2	AB3	ASB1	ASB2	ASB3
Min. R-value	78	50	60	50	40
Min. CCS at 15 psi confinement (psi)	206	181	190	181	171
Min. CCS at 20 psi confinement (psi)	242	199	215	199	184
Min. friction angle (degrees)	54	40	45	40	35

The following interim recommendations are made based on the testing discussed in this report, the documented low test precision of the R-value test, and the limitations of developing a

correlation between the R-value and the CCS test using the set of materials considered in this study:

- Material properties, including gradation, flakiness, crushed faces, sand equivalence, Atterberg limits, and moisture sensitivity (i.e., shape of the optimum moisture content curve) should be considered when analyzing any correlations.
- Friction angle can be used as a criterion to replace the R-value, but shear testing is required using multiple confinement pressures to calculate the shear properties.
- The CCS test can be moved forward for specifying aggregate base and subbase materials. The suggested preliminary CCS criteria should be updated once additional testing is completed.

TABLE OF CONTENTS

PROJECT OBJECTIVES	iv
EXECUTIVE SUMMARY	v
LIST OF FIGURES	x
LIST OF TABLES	xiii
LIST OF ABBREVIATIONS	xiv
TEST METHODS CITED IN THE TEXT	xv
1 INTRODUCTION	1
1.1 Background of the Study	1
1.2 Project Objectives	1
1.3 Report Layout.....	2
2 LITERATURE REVIEW	3
2.1 Test Method for Resistance R-Value and Expansion Pressure of Compacted Soils	3
2.1.1 Development of the R-Value Test.....	3
2.1.2 R-Value Test Precision Reported in Test Methods.....	5
2.1.3 R-Value Test Precision from Interlaboratory Proficiency Sample Programs	5
2.1.4 R-Value Test Precision Reported in the Literature.....	7
2.1.5 Previous Correlation Studies Between R-Value and Texas Triaxial Test.....	8
2.2 Alternative Test Methods to the R-Value Test	10
2.2.1 California Bearing Ratio	10
2.2.2 Monotonic Triaxial Shear Testing	12
2.2.3 Modified Triaxial Testing (Texas Triaxial Testing)	12
2.2.4 Resilient Modulus	14
2.2.5 Specimen Size	15
2.3 Proposed Test to Replace R-Value	17
2.4 Summary	17
2.5 Conclusion.....	17
3 EXPERIMENTAL PLAN AND MATERIAL SAMPLING	18
3.1 Experimental Plan	18
3.2 Material Sampling	18
3.3 Material Characterization	20
3.3.1 Gradation.....	21
3.3.2 R-Value Results.....	25
3.3.3 Sand Equivalence.....	27
3.3.4 Durability	28
3.3.5 Final Classification	29
3.4 Specimen Compaction Method Determination.....	30
4 TEST DEVELOPMENT	33
4.1 Introduction	33
4.2 Specimen Size	33
4.2.1 Specimen Diameter	34
4.2.2 Slenderness Ratio	34
4.3 Material Compaction	34

4.3.1	Reference Density Selection	34
4.4	Confinement Cell Comparison.....	37
4.4.1	Conventional Triaxial Cell	37
4.4.2	Wirtgen Confinement Cell	39
4.4.3	Peak Load and Stress Results.....	41
4.4.4	Data Analysis	41
4.4.5	Discussion.....	43
4.5	Effect of Specimen Diameter.....	45
4.6	Summary.....	46
5	CORRELATION OF CONFINED COMPRESSION AND R-VALUE TEST RESULTS	48
5.1	Introduction	48
5.2	Confined Compressive Strength Results.....	48
5.2.1	Compaction Results	48
5.2.2	Strength Results	48
5.3	Tex 117-E Material Classification	50
5.4	Correlation Results.....	52
5.4.1	Relationship Between R-Value and CCS.....	54
5.5	Discussion	57
5.5.1	R-Value Correlation	57
5.5.2	Confined Compressive Strength Test Precision	60
5.5.3	Recycled Aggregate Base Observations.....	60
5.5.4	Potential Confined Compressive Strength Test Criteria.....	60
5.6	Summary.....	62
6	CONCLUSIONS AND RECOMMENDATIONS	64
6.1	Conclusions	64
6.2	Recommendations	65
	REFERENCES	66
	APPENDIX A MATERIAL PROPERTIES.....	68
	APPENDIX B STANDARD OPERATING PROCEDURE FOR CCS TEST	72
	APPENDIX C DENSITY RESULTS.....	75
	APPENDIX D CONFINED COMPRESSIVE STRENGTH TEST RESULTS	85

LIST OF FIGURES

Figure 2.1: Schematic of Hveem stabilometer.	4
Figure 2.2: Stabilometer (CT 301).....	4
Figure 2.3: Within-laboratory standard deviation for R-value tests.	6
Figure 2.4: Relationship between Texas triaxial strength classes and R-value at 300-psi.	9
Figure 2.5: Nomograph of correlations between different material properties.....	11
Figure 2.6: California Bearing Ratio test schematic.	12
Figure 2.7: Texas Triaxial material classes (Tex 117-E).	13
Figure 2.8: Schematic of Texas triaxial test setup and confinement cell (Tex 117-E).	13
Figure 2.9: Triaxial test setup with on-specimen LVDTs and a radial extensometer.	14
Figure 3.1: Sampled aggregate materials that meet Class 2 aggregate base 0.75 in. maximum aggregate size gradation band.	22
Figure 3.2: Sampled aggregates that meet Class 2 aggregate base 1.5 in. maximum aggregate size gradation band.	22
Figure 3.3: Class 3 aggregate base material gradations.	23
Figure 3.4: Class 2 aggregate subbase material gradations.....	23
Figure 3.5: Class 3 aggregate subbase material gradations.....	24
Figure 3.6: Relationship between SE and R-value.	28
Figure 4.1: Traditional triaxial cell.	38
Figure 4.2: Disassembled Wirtgen confinement cell.	39
Figure 4.3: Assembled Wirtgen confinement cell with the new loading platen.	39
Figure 4.4: Original and new loading platen for Wirtgen cell (new platen on left).....	40
Figure 4.5: Original and new base plate for Wirtgen cell (new plate on left).	40
Figure 4.6: Fitting tangent plane for stress states.	42
Figure 4.7: Linear regression to fit failure plane through stress and shear strength points.	42
Figure 4.8: Mohr’s diagram for the comparison tests between the three cells.....	43
Figure 4.9: Effect of specimen diameter on failure envelope (red is 4 inch, blue is 6 inch).....	46
Figure 5.1: Box and whisker plot of wet densities versus target wet density.....	49
Figure 5.2: Average compaction time per lift (six lifts per specimen).	49
Figure 5.3: Failure envelopes results on Texas triaxial classification plot.....	51
Figure 5.4: Texas Triaxial class classification.	52
Figure 5.5: Correlation matrix plot of study results.....	53
Figure 5.6: Relationship between R-value and peak stress (strength) at 0 psi confinement.	55
Figure 5.7: Relationship between R-value and peak stress (strength) at 3 psi confinement.	55
Figure 5.8: Relationship between R-value and peak stress (strength) at 5 psi confinement.	55
Figure 5.9: Relationship between R-value and peak stress (strength) at 10 psi confinement.	55
Figure 5.10: Relationship between R-value and peak stress (strength) at 15 psi confinement. ...	56
Figure 5.11: Relationship between R-value and peak stress (strength) at 20 psi confinement. ...	56
Figure 5.12: Relationship between R-value and cohesion.....	56
Figure 5.13: Relationship between R-value and friction angle.	56
Figure 5.14: Standard deviation results for R-value tests results previously reported.....	58
Figure 5.15: Prediction interval range of average California R-value results.	59
Figure A.1: Class 2 aggregate base material gradations for supplied materials.	68

Figure A.2: Class 1 aggregate subbase material gradations for supplied materials.....	69
Figure A.3: Class 2 aggregate subbase material gradations for supplied materials.....	69
Figure A.4: Class 3 aggregate subbase material gradations for supplied materials.....	70
Figure A.5: P209 material gradations for supplied materials.	70
Figure C.1: Density results for Material #1.....	76
Figure C.2: Density results for Material #2.....	76
Figure C.3: Density results for Material #3.....	76
Figure C.4: Density results for Material #4.....	76
Figure C.5: Density results for Material #5.....	77
Figure C.6: Density results for Material #6.....	77
Figure C.7: Density results for Material #7.....	77
Figure C.8: Density results for Material #8.....	77
Figure C.9: Density results for Material #9.....	78
Figure C.10: Density results for Material #10.....	78
Figure C.11: Density results for Material #11.....	78
Figure C.12: Density results for Material #12.....	78
Figure C.13: Density results for Material #13.....	79
Figure C.14: Density results for Material #14.....	79
Figure C.15: Density results for Material #15.....	79
Figure C.16: Density results for Material #16.....	79
Figure C.17: Density results for Material #17.....	80
Figure C.18: Density results for Material #18.....	80
Figure C.19: Density results for Material #19.....	80
Figure C.20: Density results for Material #20.....	80
Figure C.21: Density results for Material #21.....	81
Figure C.22: Density results for Material #22.....	81
Figure C.23: Density results for Material #23.....	81
Figure C.24: Density results for Material #24.....	81
Figure C.25: Density results for Material #25.....	82
Figure C.26: Density results for Material #26.....	82
Figure C.27: Density results for Material #27.....	82
Figure C.28: Density results for Material #28.....	82
Figure C.29: Density results for Material #29.....	83
Figure C.30: Density results for Material #30.....	83
Figure C.31: Density results for Material #31.....	83
Figure C.32: Density results for Material #32.....	83
Figure C.33: Density results for Material #33.....	84
Figure D.1: Mohr-Coulomb plots for Material #1.....	86
Figure D.2: Mohr-Coulomb plots for Material #2.....	86
Figure D.3: Mohr-Coulomb plots for Material #3.....	86
Figure D.4: Mohr-Coulomb plots for Material #4.....	86
Figure D.5: Mohr-Coulomb plots for Material #5.....	87
Figure D.6: Mohr-Coulomb plots for Material #6.....	87
Figure D.7: Mohr-Coulomb plots for Material #7.....	87
Figure D.8: Mohr-Coulomb plots for Material #8.....	87

Figure D.9: Mohr-Coulomb plots for Material #9	88
Figure D.10: Mohr-Coulomb plots for Material #10	88
Figure D.11: Mohr-Coulomb plots for Material #11	88
Figure D.12: Mohr-Coulomb plots for Material #12	88
Figure D.13: Mohr-Coulomb plots for Material #13	89
Figure D.14: Mohr-Coulomb plots for Material #14	89
Figure D.15: Mohr-Coulomb plots for Material #15	89
Figure D.16: Mohr-Coulomb plots for Material #16	89
Figure D.17: Mohr-Coulomb plots for Material #17	90
Figure D.18: Mohr-Coulomb plots for Material #18	90
Figure D.19: Mohr-Coulomb plots for Material #19	90
Figure D.20: Mohr-Coulomb plots for Material #20	90
Figure D.21: Mohr-Coulomb plots for Material #21	91
Figure D.22: Mohr-Coulomb plots for Material #22	91
Figure D.23: Mohr-Coulomb plots for Material #23	91
Figure D.24: Mohr-Coulomb plots for Material #24	91
Figure D.25: Mohr-Coulomb plots for Material #25	92
Figure D.26: Mohr-Coulomb plots for Material #25	92
Figure D.27: Mohr-Coulomb plots for Material #27	92
Figure D.28: Mohr-Coulomb plots for Material #28	92
Figure D.29: Mohr-Coulomb plots for Material #29	93
Figure D.30: Mohr-Coulomb plots for Material #30	93
Figure D.31: Mohr-Coulomb plots for Material #31	93
Figure D.32: Mohr-Coulomb plots for Material #32	93
Figure D.33: Mohr-Coulomb plots for Material #33	94

LIST OF TABLES

Table 2.1: ASTM D2844/D2844M-18 Test Precision.....	5
Table 2.2: AASHTO Resource R-Value Proficiency Sample Program Test Precision Results	6
Table 2.3: Test Precision Result for California Test 216.....	7
Table 3.1: Aggregate Subbase and Base Materials Tested in the Study	19
Table 3.2: Caltrans 2022 Standard Specification for Aggregate Subbase Properties.....	21
Table 3.3: Caltrans 2022 Standard Specification for Aggregate Base Properties.....	21
Table 3.4: Reclassified Material Types Against Caltrans Specifications Based on Gradation.....	24
Table 3.5: R-Value Results	26
Table 3.6: Sand Equivalence Results	27
Table 3.7: Durability Results.....	28
Table 3.8: Maximum Classifications for Supplied Materials	29
Table 3.9: Modified Proctor Compaction Results.....	31
Table 3.10: CT 216 Compaction Results	32
Table 4.1: Difference Between Modified Proctor and CT 216 Density Results.....	35
Table 4.2: Triaxial Equipment Details	39
Table 4.3: Triaxial Cell Comparison Test Results	41
Table 4.4: ANOVA Results to Evaluate Effect of Cell Type on Major Principal Stress	44
Table 4.5: ANOVA Results to Evaluate Effect of Cell Type on Shear Stress.....	44
Table 4.6: Regression Results for Equation 4.6	45
Table 5.1: Confined Compressive Strength Peak Stress and Shear Properties	50
Table 5.2: Material Type and Texas Triaxial Class Classification.....	52
Table 5.3: Passable Minimum and Maximum Average R-Value Materials	59
Table 5.4: CCS Test Criteria Using 15 psi Results.....	61
Table 5.5: CCS Test Criteria Using 20 psi Results	61
Table 5.6: Friction Angle Test Criteria Using Multiple Confinement Pressures	62
Table 5.7: Recommended Preliminary CCS Specification Values.....	62
Table A.1: Sand Equivalence, Durability, and OMC for Supplied Materials	71

LIST OF ABBREVIATIONS

AASHTO	American Association of State Highway and Transportation Officials
AB	Aggregate base
ASB	Aggregate subbase
ANOVA	Analysis of variance
CBR	California Bearing Ratio
CCS	Confined compressive strength
DCP	Dynamic cone penetrometer
LVDT	Linear variable differential transformer
OMC	Optimum moisture content
PMPC	Pavement Materials Partnering Committee
PSP	Proficiency sample program
RVE	Representative volume element
SE	Sand equivalent
UCS	Unconfined compressive strength

TEST METHODS CITED IN THE TEXT

AASHTO

- T 180 Standard Method of Test for Moisture-Density Relations of Soils Using a 4.54-kg (10-lb) Rammer and a 457-mm (18-in.) Drop
- T 190 Standard Method of Test for Resistance R-Value and Expansion Pressure of Compacted Soils
- T 307 Standard Method of Test for Determining the Resilient Modulus of Soils and Aggregate Materials

ASTM

- D1557 Standard Test Methods for Laboratory Compaction Characteristics of Soil Using Modified Effort (56,000 ft-lbf/ft³ (2,700 kN-m/m³))
- D2844 Standard Test Method for Resistance R-Value and Expansion Pressure of Compacted Soils

California Test Methods

- CT 216 Method of Test for Relative Compaction of Untreated and Treated Soils and Aggregates
- CT 217 Method of Test for Sand Equivalent
- CT 229 Method of Test for Durability Index
- CT 231 Method of Test for Relative Compaction of Untreated and Treated Soils and Aggregates Using Nuclear Gages
- CT 234 Method of Test for Uncompacted Void Content of Fine Aggregates
- CT 301 Method of Test for Determining the Resistance R-Value of Treated and Untreated Bases, Subbases, and Basement Soils by the Stabilometer

Texas Test Methods

- Tex-117-E Triaxial Compression for Disturbed Soils and Base Materials

CONVERSION FACTORS

APPROXIMATE CONVERSIONS TO SI UNITS				
Symbol	When You Know	Multiply By	To Find	Symbol
LENGTH				
in.	inches	25.40	millimeters	mm
ft.	feet	0.3048	meters	m
yd.	yards	0.9144	meters	m
mi.	miles	1.609	kilometers	km
AREA				
in ²	square inches	645.2	square millimeters	mm ²
ft ²	square feet	0.09290	square meters	m ²
yd ²	square yards	0.8361	square meters	m ²
ac.	acres	0.4047	hectares	ha
mi ²	square miles	2.590	square kilometers	km ²
VOLUME				
fl. oz.	fluid ounces	29.57	milliliters	mL
gal.	gallons	3.785	liters	L
ft ³	cubic feet	0.02832	cubic meters	m ³
yd ³	cubic yards	0.7646	cubic meters	m ³
MASS				
oz.	ounces	28.35	grams	g
lb.	pounds	0.4536	kilograms	kg
T	short tons (2000 pounds)	0.9072	metric tons	t
TEMPERATURE (exact degrees)				
°F	Fahrenheit	(F-32)/1.8	Celsius	°C
FORCE and PRESSURE or STRESS				
lbf	pound-force	4.448	newtons	N
lbf/in ²	pound-force per square inch	6.895	kilopascals	kPa
APPROXIMATE CONVERSIONS FROM SI UNITS				
Symbol	When You Know	Multiply By	To Find	Symbol
LENGTH				
mm	millimeters	0.03937	inches	in.
m	meters	3.281	feet	ft.
m	meters	1.094	yards	yd.
km	kilometers	0.6214	miles	mi.
AREA				
mm ²	square millimeters	0.001550	square inches	in ²
m ²	square meters	10.76	square feet	ft ²
m ²	square meters	1.196	square yards	yd ²
ha	hectares	2.471	acres	ac.
km ²	square kilometers	0.3861	square miles	mi ²
VOLUME				
mL	milliliters	0.03381	fluid ounces	fl. oz.
L	liters	0.2642	gallons	gal.
m ³	cubic meters	35.31	cubic feet	ft ³
m ³	cubic meters	1.308	cubic yards	yd ³
MASS				
g	grams	0.03527	ounces	oz.
kg	kilograms	2.205	pounds	lb.
t	metric tons	1.102	short tons (2000 pounds)	T
TEMPERATURE (exact degrees)				
°C	Celsius	1.8C + 32	Fahrenheit	°F
FORCE and PRESSURE or STRESS				
N	newtons	0.2248	pound-force	lbf
kPa	kilopascals	0.1450	pound-force per square inch	lbf/in ²

*SI is the abbreviation for the International System of Units. Appropriate rounding should be made to comply with Section 4 of ASTM E380.
(Revised April 2021)

1 INTRODUCTION

1.1 Background of the Study

The California Department of Transportation (Caltrans) requested that the University of California Pavement Research Center (UCPRC) identify a replacement test for the California R-value test (California Test 301 [CT 301]), which uses Hveem stabilometer equipment, for the specification testing of aggregate base and subbase materials used in pavement layers. The Pavement Materials Partnering Committee (PMPC) task group provided the following reasons for replacing the R-value test:

- The equipment is becoming increasingly difficult to procure and maintain.
- The test results have a high degree of reliance on the person doing the test.
- The test does not directly provide information that can be used to estimate stiffness for mechanistic-empirical pavement design.

The UCPRC performed a literature review of alternative tests with the following criteria:

- The equipment should not be difficult to procure and maintain.
- The test and specimen preparation required for the test should be practical for use in district laboratories and aggregate producer's laboratories in terms of simplicity, time to complete the testing, and cost.
- The test should have reasonable within- and between-laboratory variability and should have low between-operator variability.
- The test results should correlate with stiffness results.

This technical memorandum documents the results of the project completed in response to the Caltrans request. The test method recommended by the UCPRC is a version of the Texas Triaxial Strength test with some changes in the laboratory specimen preparation method and the testing procedure made to better meet all the criteria identified by Caltrans.

1.2 Project Objectives

The objective of this project is to identify a replacement test for the R-value. This objective will be achieved through the following tasks:

- Recommend an alternative test to the R-value for characterization and quality control/quality assurance of unbound base and subbase aggregate materials in California.

- Develop a correlation between the R-value and selected test results based on testing of a range of commercially available base and subbase materials.
- Recommend provisional criteria for acceptance.

The scope was limited to the comparison of the R-value and recommended strength test results of commercially available base and subbase materials. Subgrade and fill materials were not included. The effects of other specification and non-specification material properties that may influence the result—including, but not limited to, material classification, gradation, aggregate flakiness, crushed faces, sand equivalence, plasticity (i.e., Atterberg limits), moisture sensitivity (i.e., shape of the optimum moisture content curve), durability, specific gravity, cohesion, and friction angle—were not part of the project scope. However, obtaining some of these properties for the materials tested and using them to interpret the results from the new test method were later added to the project scope.

1.3 Report Layout

This technical memorandum is organized as follows:

- Chapter 2 provides an overview of the literature related to the topic.
- Chapter 3 summarizes the experimental design for the laboratory testing, the sampling plan, and the densities of the sampled materials.
- Chapter 4 describes the development of the recommended test method.
- Chapter 5 details the test results and analyses.
- Chapter 6 provides a project summary and the conclusions and recommendations.
- Appendix A contains the generic material property results provided by one of the material suppliers.
- Appendix B contains the compaction results for each material.
- Appendix C contains the triaxial test results for each material.
- Appendix D provides the standard operating procedure developed for the replacement test method.

2 LITERATURE REVIEW

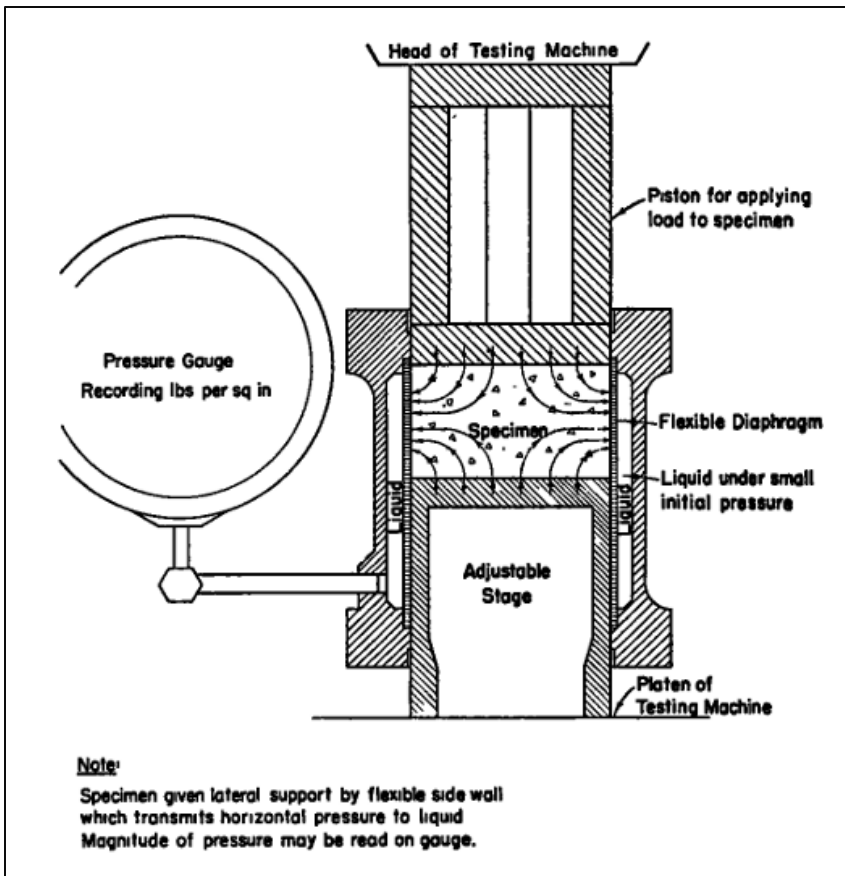
2.1 Test Method for Resistance R-Value and Expansion Pressure of Compacted Soils

2.1.1 Development of the R-Value Test

Caltrans has used the R-value method, based on the Hveem stabilometer equipment, since Francis Hveem and his colleagues developed it at the then California Division of Highways in the 1940s (1). Much of the information regarding development of the stabilometer and R-value test and its use for estimating the shearing resistance of subgrade soils and granular bases and subbases was not published. Conversations with Professor Carl Monismith in the 1990s indicated that Hveem was influenced by work at the US Army Corps of Engineers Waterways Experiment Station in Vicksburg, Mississippi, in the 1930s on development of triaxial testing devices to measure the shear strength and stiffness of soils. The stabilometer is a form of triaxial device where an axial load is applied, and the resulting lateral deformation caused by shearing is measured, shown in Figure 2.1 and Figure 2.2. The deformations are small, as are those in the pavement, and the specimen is not failed.

Hveem developed a flexible pavement design equation based on the R-value test and equivalent single-wheel loads in the late 1940s (and then equivalent single-axle loads in the 1960s) as a replacement for the California Bearing Ratio (CBR) test and design method developed by O.J. Porter, also with the Division of Highways, in the late 1920s. The R-value testing and design method had been the basis for design of California flexible pavements until the 2010s when mechanistic-empirical pavement design using *CalME* started to replace it.

Use of the R-value test and the corresponding flexible pavement design method was adopted in various forms by 13 western states, and Nevada continues with the approach. In the last 20 years, most other states that previously used the R-value have changed to using a version of the AASHTO 1993 empirical pavement design method and/or using the AASHTO mechanistic-empirical design method. Some of these states developed correlations between the R-value and resilient modulus (M_r), primarily for subgrade soils, as part of their transition to either of the AASHTO methods, both of which require a subgrade M_r value for the analysis.



Source: Hveem and Carmany (1948) (1).

Figure 2.1: Schematic of Hveem stabilometer.

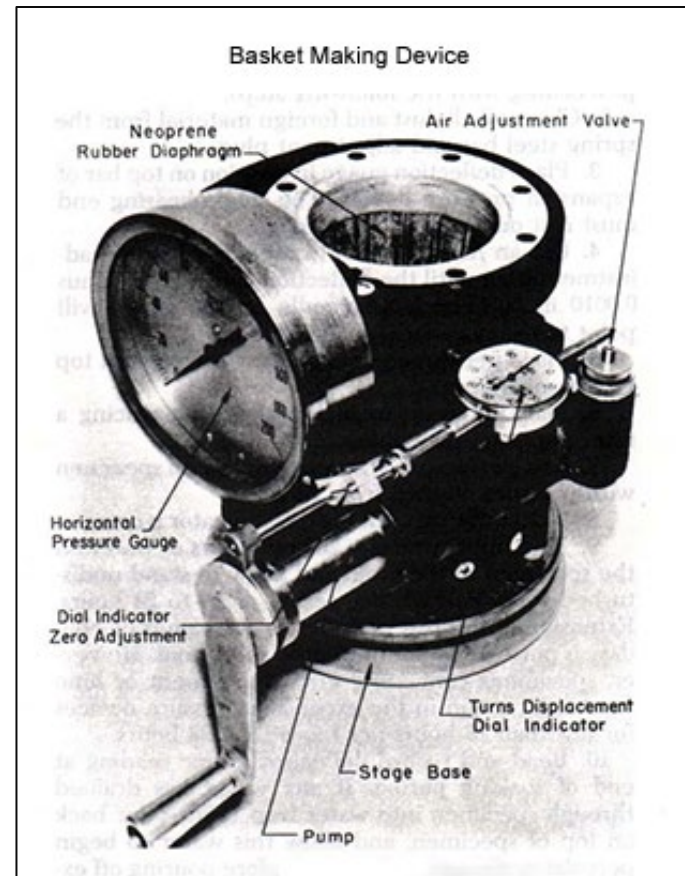


Figure 2.2: Stabilometer (CT 301).

The other 37 states, and much of the rest of the world, adopted the CBR test and design approach and various adaptations of it. The CBR method was adapted by the Army Corps of Engineers for airfield design in the 1940s and then by the Federal Aviation Administration for its empirical pavement design methods, which remain based on CBR to this day.

2.1.2 R-Value Test Precision Reported in Test Methods

The R-value test is subject to large variances. The following test precision information has been reported in available R-value test methods.

ASTM D2844 Standard Test Method for Resistance R-Value and Expansion Pressure of Compacted Soils

The precision and bias statements reported in the ASTM D2844 test method are provided in Table 2.1 for materials with R-values below 50. Estimates for test precision for R-values greater than 50 have not yet been developed as of ASTM D2844/D2844M-18.

Table 2.1: ASTM D2844/D2844M-18 Test Precision

General Error Type (300 psi Exudation Pressure)	R-value	Standard Deviation	Acceptable Range of Two Results
Single-operator precision	5–20	3	8
	21–50	4	12
Multi-laboratory precision	5–20	6	18
	21–50	13	37

AASHTO T 190-22 Standard Method of Test for Resistance R-Value and Expansion Pressure of Compacted Soils

AASHTO T 190 does not provide any test precision and bias statements.

California Test Method 301 Method of Test for Determining the Resistance R-Value of Treated and Untreated Bases, Subbases, and Basement Soils by the Stabilometer

CT 301 does not provide any test precision and bias statements.

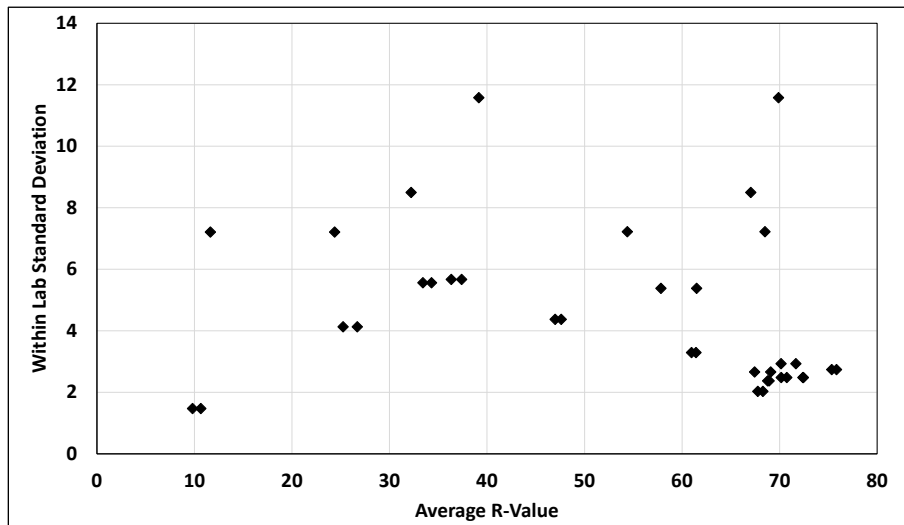
2.1.3 R-Value Test Precision from Interlaboratory Proficiency Sample Programs

AASHTO re:source conducts a yearly proficiency sample program (PSP) to compare individual testing results to a large pool of results (2). This allows laboratories to verify their testing apparatus and operators under actual testing conditions and to show conformance to testing procedures and protocols. R-value testing is part of the PSP program. Every year, AASHTO re:source sends two similar soil samples to different laboratories. The laboratories perform the

R-value test following AASHTO T 190 and report the result back to AASHTO. The material varies from year to year to cover a range of different R-value materials. The test precision results reported for 2006 through 2023 are compiled in Table 2.2 and Figure 2.3.

Table 2.2: AASHTO Re:source R-Value Proficiency Sample Program Test Precision Results

PSP Sample	Average	Between Lab Std. Dev.	Within Lab Std. Dev	Sample Size	Year	PSP Sample	Average	Between Lab Std. Dev.	Within Lab Std. Dev	Sample Size	Year
RVL 153	67.77	5.94	2.03	128	2006	RVL 171	70.74	5.3	2.48	132	2015
RVL 154	68.29	5.75	2.03	128	2006	RVL 172	70.17	5.42	2.48	132	2015
RVL 155	9.80	3.93	1.47	122	2007	RVL 173	71.67	3.73	2.93	127	2016
RVL 156	10.66	4.03	1.47	122	2007	RVL 174	70.15	5.19	2.93	127	2016
RVL 157	75.35	4.97	2.74	131	2008	RVL 175	69.08	4.99	2.66	131	2017
RVL 158	75.84	5.33	2.74	131	2008	RVL 176	67.43	5.85	2.66	131	2017
RVL 159	32.22	14.05	8.5	136	2009	RVL 177	33.43	15.66	5.56	126	2018
RVL 160	67.05	9.31	8.5	136	2009	RVL 178	34.31	15.41	5.56	126	2018
RVL 161	72.44	5.35	2.48	136	2010	RVL 179	25.25	12.94	4.13	131	2019
RVL 162	72.39	4.72	2.48	136	2010	RVL 180	26.70	13.85	4.13	131	2019
RVL 163	61.49	13.63	5.38	137	2011	RVL 181	36.33	15.32	5.67	137	2020
RVL 164	57.83	15.41	5.38	137	2011	RVL 182	37.39	15.73	5.67	137	2020
RVL 165	24.37	12.01	7.21	128	2012	RVL 183	68.77	5.53	2.37	132	2021
RVL 166	11.63	5.95	7.21	128	2012	RVL 184	68.92	5.66	2.37	132	2021
RVL 167	69.89	5.51	11.58	136	2013	RVL 185	46.98	15.09	4.37	131	2022
RVL 168	39.16	17.66	11.58	136	2013	RVL 186	47.60	14.67	4.37	131	2022
RVL 169	68.50	5.71	7.22	132	2014	RVL 187	61.42	7.48	3.29	127	2023
RVL 170	54.38	11.32	7.22	132	2014	RVL 188	60.97	8.17	3.29	127	2023



Source: AASHTO (66).

Figure 2.3: Within-laboratory standard deviation for R-value tests.

The results show that the precision varies according to the range of materials tested. For the reported average R-value results and standard deviations, low R-value materials yielded less precise results than high R-value materials.

2.1.4 R-Value Test Precision Reported in the Literature

Benson and Ames determined the test precision for different aggregate test methods used by Caltrans in 1975 (3). The test methods included sieve analysis, percent crushed particles, sand equivalence, Los Angeles abrasion, cleanness value, durability index, and R-value. The report provides operator error and between-laboratory error for each test method and discusses possible causes that could contribute to the error. For the R-value test, two aggregate base and two aggregate subbase materials were tested. California Test Method 301 was followed to conduct the R-value test. The test precision for the R-value results are provided in Table 2.3. For the range of materials tested, the low R-value material had lower precision test results compared to the higher R-value material. The distributions of error were 20% for the between-operator results and 30% for the between-laboratory results. The residual error was 50%. Additional scale type errors were also observed, which were attributed to improperly calibrated stabilometer readings. The intricate fabrication of specimens could also have contributed to a large portion of the residual error.

Table 2.3: Test Precision Result for California Test 216

General Error Type	R-Value	Variance	Standard Deviation	Acceptable Range of Two Results
Single-operator precision	30	38.5	6.21	18.0
	40	27.9	5.28	15.0
	50	18.9	4.35	12.0
	60	11.7	3.42	10.0
	70	6.2	2.49	7.0
	80	2.4	1.56	4.0
Multi-laboratory precision	30	76.4	8.74	25.0
	40	55.2	7.43	21.0
	50	37.5	6.12	17.0
	60	23.2	4.81	14.0
	70	12.3	3.51	10.0
	80	4.8	2.20	6.0

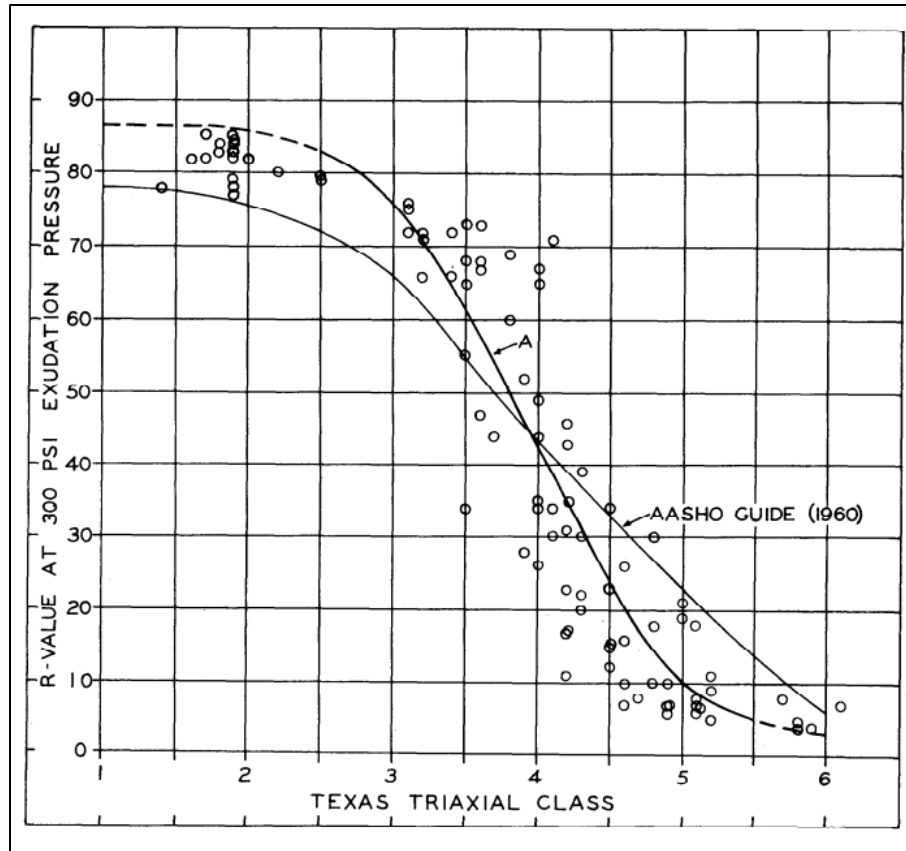
Source: Benson and Ames (3).

Miller analyzed 8,165 historical records of R-value test results of base, subbase, and subgrade soils in Idaho (4). Based on the test results, the following errors in the R-value results were reported:

- An error of 15% to 20% for R-values between 5 and 40
- An error of 10% to 15% for R-values between 40 and 60
- An error of 5% to 10% for R-values between 60 and 80

2.1.5 Previous Correlation Studies Between R-Value and Texas Triaxial Test

Roland conducted a research project in 1963 to determine the relationship between the R-value and Texas triaxial tests in Louisiana (5). The materials tested covered common Louisiana soils as well as artificially produced materials that comply with Texas triaxial Class 2 materials. The relationship between the Texas triaxial strength classes and R-value at 300 psi exudation pressure is shown in Figure 2.4. The coefficient of determination and standard error for the fit are 0.87 and 10.195, respectively. The best fit relationship between the two parameters is described by a third-order polynomial (curve A in Figure 2.4), particularly between the Texas triaxial Class 3 to Class 5. Beyond this range, the curve flattens out, showing low sensitivity to a change in R-value for different Texas triaxial strength class materials. The upper extremity of curve A in Figure 2.4 is dashed due to the inherent possibility of rupturing the specimen upon transfer into the stabilometer. The lower extremity is dashed given that material in this range is extremely difficult to mold with any degree of consistency.



Source: Roland (1963) (5).

Figure 2.4: Relationship between Texas triaxial strength classes and R-value at 300-psi.

Jones and Harvey developed relationships between R-value results and dynamic cone penetrometer (DCP) derived stiffness and shear strength (6). They noted that “the relative complexity of the R-value test, coupled with the potentially doubtful reproducibility and repeatability implies that added caution would be required in the development of this test and DCP penetration.” The report further discussed how the DCP provides a more economical and comprehensive evaluation of projects compared to R-value testing. In the report, they showed how resilient moduli of the subgrade, subbase, and base layers estimated from R-value testing using correlations charts developed by Van Til et al. as part of National Cooperative Highway Research Program (NCHRP) 128 and the correlation equations developed by Huang do not provide consensus on material stiffness (7,8).

Miller developed regression models to determine the material properties that best predict the R-value of the material (4). In this study, the material unified soil classification code, percent fines, and plasticity index of plastic soils produced regression models with correlation coefficients

between 0.61 and 0.70. Non-plastic soils had correlation coefficients of less than 0.25 using the same explanatory variables.

Fragomeni and Hedayat developed prediction models for the R-value and resilient modulus using a database of over 2,600 R-value and 200 resilient modulus results (9). The multiple regression models include specific gravity; absorption; maximum dry density; liquid limit; plastic limit; plasticity index; percent passing the No. 4, No. 10, No. 40, and No. 200 sieves; difference in R-value test moisture and optimum moisture content multiplied by the plasticity index; and exudation pressure. If the moisture content at the exudation pressure was known, the model was able to predict the R-value within $\pm 20\%$. Since the moisture content that provides an exudation pressure of 300 psi is not always known, they considered models without this variable. The prediction error increased significantly for some soils.

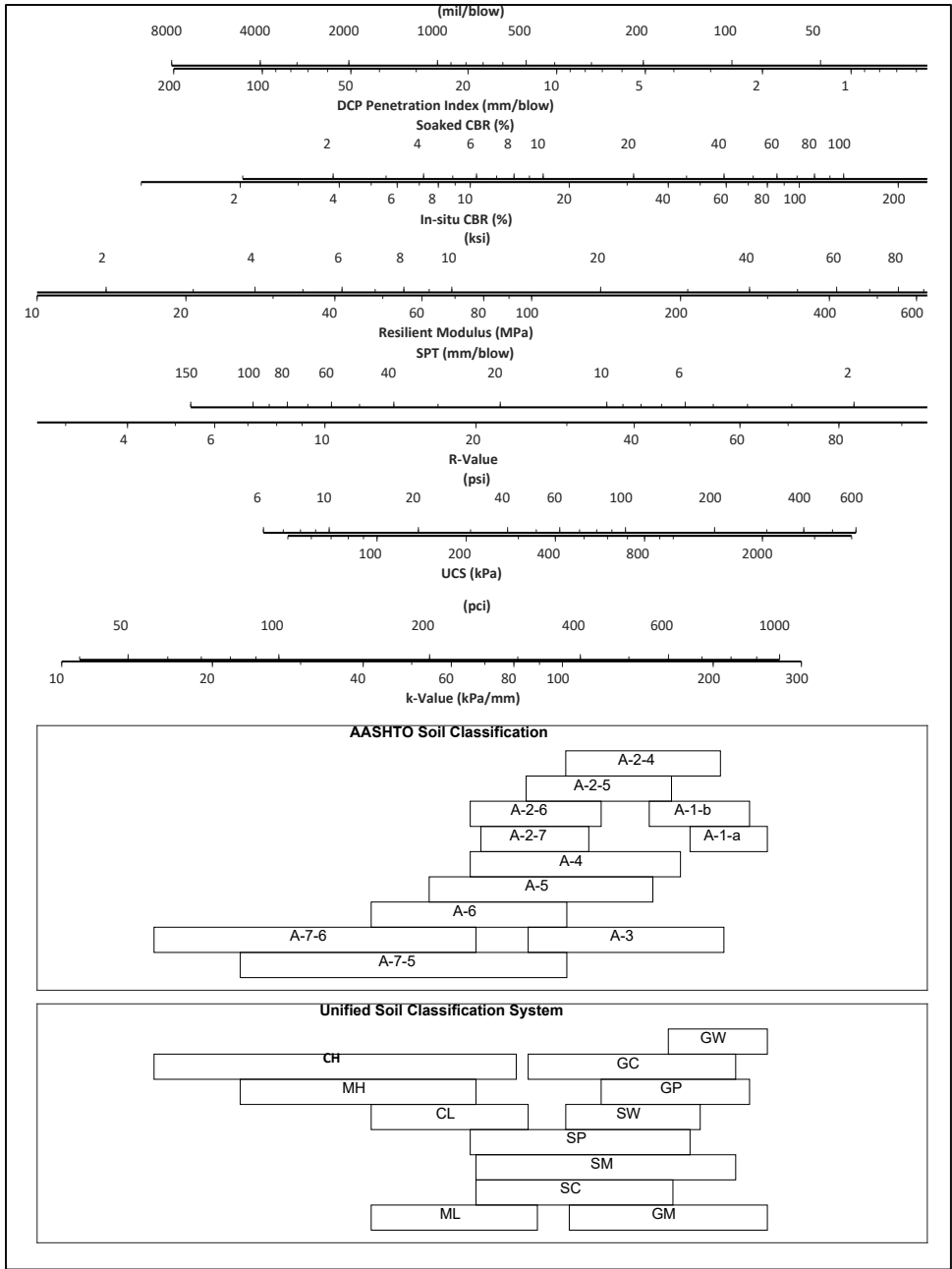
Lea et. al. performed a meta-analysis of published relationships between various test methods to correlate the DCP test, which is widely used worldwide to characterize the top 800 mm (31.5 in.) of the granular layers in a pavement, with CBR, R-value, resilient modulus, unconfined compressive strength (UCS), and the AASHTO and ASTM soil classification systems (10). The relationships were combined on a nomograph, shown in Figure 2.5.

2.2 Alternative Test Methods to the R-Value Test

The alternative test methods that were considered for this project include CBR, monotonic triaxial shear, modified triaxial, and resilient modulus and are described below.

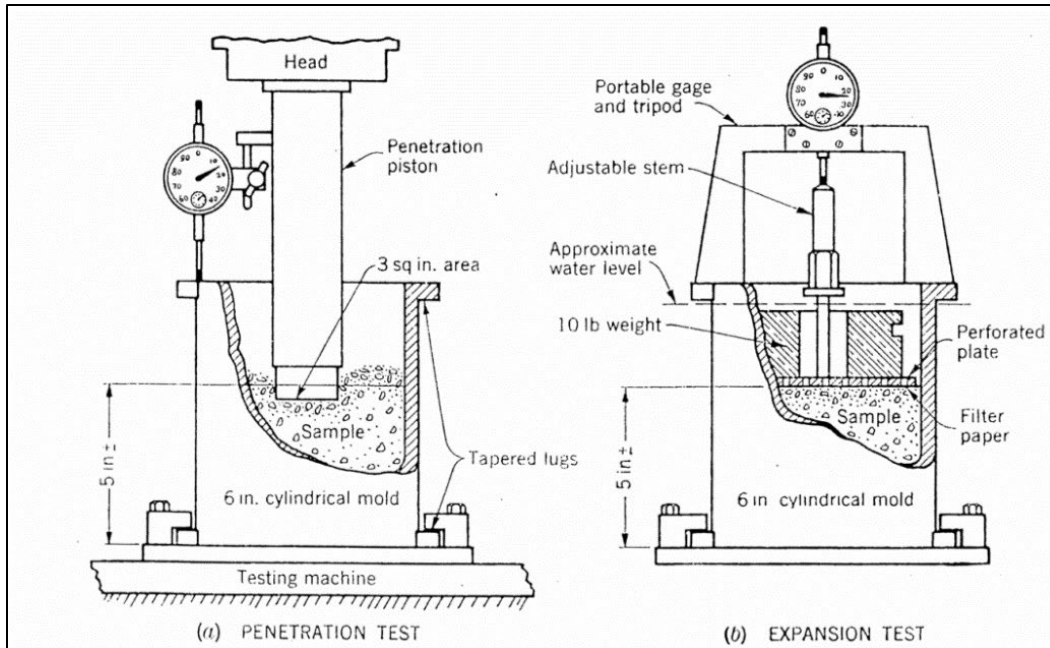
2.2.1 California Bearing Ratio

The California Bearing Ratio (CBR) test was developed in 1929 by the California Division of Highways to eliminate the deficiencies of field loading tests and to provide a fast method for comparing local base and subbase materials (11). The method consists of subjecting confined compacted specimens to four days in a water bath with a surcharge that represents the weight of the pavement. This allows the specimen to swell and absorb water, with possible reduction in the strength of the material. After soaking, the confined specimen is penetrated to determine the resistance to lateral displacement, thus measuring the influence of cohesion and internal friction. The resistance to penetration is expressed as a percentage of the resistance of a standard crushed stone with a CBR value of 100%. The penetration and expansion tests are shown in Figure 2.6.



Source: Lea et al. (2023) (10).

Figure 2.5: Nomograph of correlations between different material properties.



Source: Porter (1950) (11).

Figure 2.6: California Bearing Ratio test schematic.

2.2.2 Monotonic Triaxial Shear Testing

Monotonic triaxial testing can be used to measure the bearing capacity of unbound materials. It is performed in a triaxial cell at different confinement pressures at a constant loading rate to determine the peak strength. Typical confinement pressures range between 0 and 29 psi (12) and loading rates between 1 in./min. and 2 in./min. The results are used to determine the shear properties of the material.

2.2.3 Modified Triaxial Testing (Texas Triaxial Testing)

The Texas triaxial test method (Tex 117-E, Triaxial Compression for Disturbed Soils and Base Materials) is a modified triaxial test that is used to classify unbound aggregate material in one of six accepted classes (Figure 2.7). The test uses 6 × 8 in. specimens for base materials and 4 × 6 in. specimens for subgrade specimens, compacted in a Proctor compaction apparatus. The method provides for multiple specimen conditioning procedures and confinement pressures to determine the failure plane, friction angle, and cohesion, which are used to classify the material. A schematic of the test setup is provided in Figure 2.8.

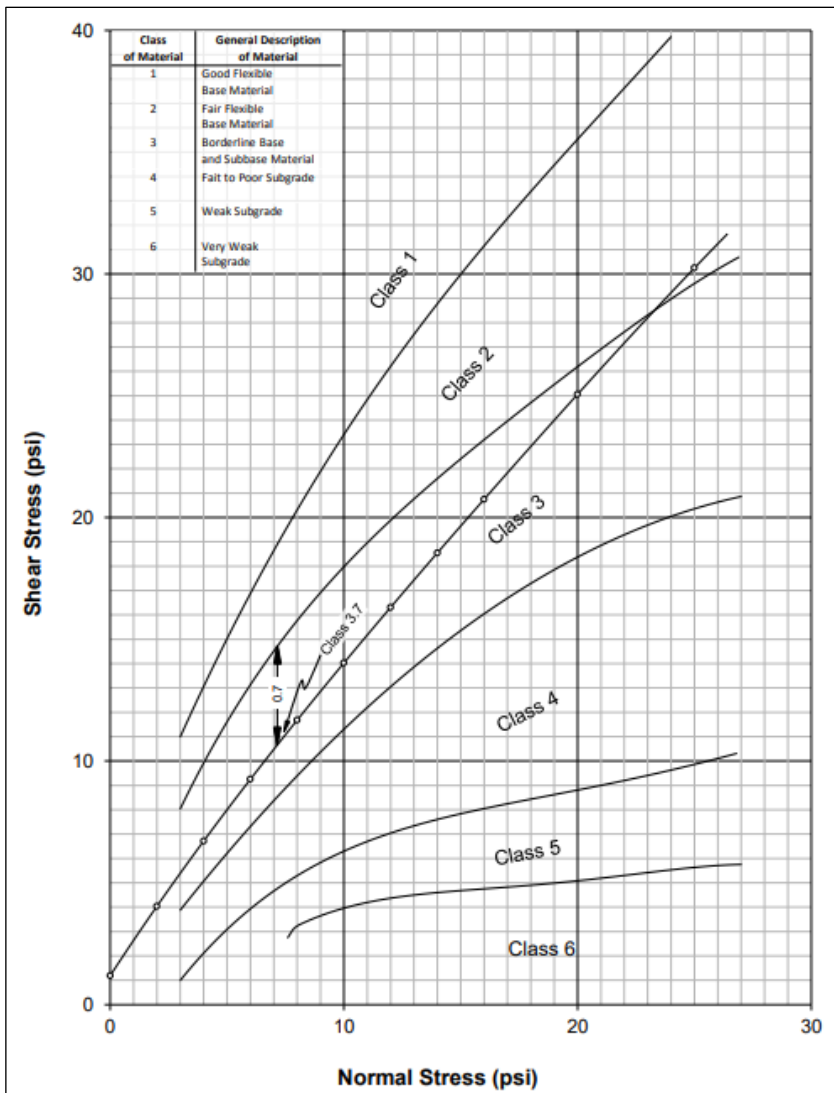


Figure 2.7: Texas Triaxial material classes (Tex 117-E).

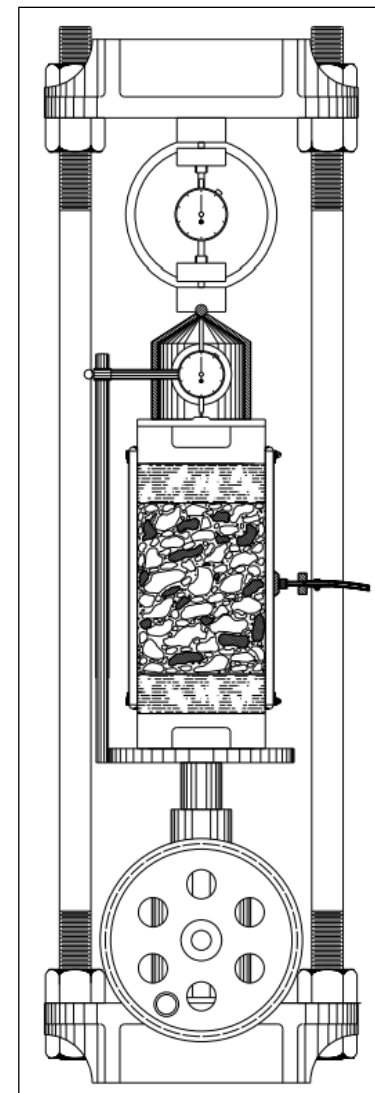


Figure 2.8: Schematic of Texas triaxial test setup and confinement cell (Tex 117-E).

2.2.4 Resilient Modulus

Resilient modulus testing is a triaxial test method that measures the stiffness response of unbound materials at different loading frequencies and deviatoric stresses. A common unbound material resilient modulus test is provided in AASHTO T 307. The test uses a 6 × 12 in. specimen. Figure 2.9 shows the test setup with on-specimen linear variable differential transformers (LVDTs) and a radial extensometer. Vibratory compaction of the specimen is prescribed, with specimens compacted to a predetermined target density and moisture content, typically based on AASHTO T 180. One benefit of the resilient modulus test is the ability to use the results directly in mechanistic pavement design.



Figure 2.9: Triaxial test setup with on-specimen LVDTs and a radial extensometer.

Groeger et al. provided a detailed discussion on AASHTO T 307 and listed several aspects for consideration for an updated version of the specification (13). Issues including load cell location, deformation measurement, and the number of LVDTs were discussed. The following actions were recommended:

- The load cell should be located inside the triaxial cell, provided that the LVDTs are mounted on the specimen. The load cell works by means of strain measurement, which should be external of the LVDT strain measurements.

- The LVDTs should be mounted on the specimen to “negate any slop in the system” if the deflection is measured outside the cell and to alleviate any stress concentrations at the ends of the specimen.
- Two or more LVDTs should be mounted at equal spacing around the specimen.

2.2.5 Specimen Size

Specimen Slenderness Ratio

Moore and Hoover reviewed available literature on the effect of the slenderness ratio (height-to-diameter ratio) of triaxial test specimens in 1966 (14). The study found that slenderness ratios less than 1.5 resulted in the whole specimen being restrained by the friction at the end loading platens and, at ratios greater than 3.0, the specimen is at risk of buckling. The recommended ratio was 2.0, which was found in that study to give sufficient accuracy and reproducibility while allowing the complete development of cones that do not intersect or interfere with the strength through columnar action.

Maximum Aggregate Size to Diameter

Moore and Hoover suggested that the maximum aggregate size-to-specimen diameter ratio of 1:5 developed for sand might also be applicable to aggregate materials (14). Hoffman provided mathematical reasoning to support a maximum aggregate size-to-specimen diameter ratio of 1:6 and reported that the use of end conditions with low friction does not reduce the need for this 1:6 ratio (15).

Specimen Diameter

The specimen diameter for the Texas triaxial test method can either be 4 in. or 6 in. The specimen diameter is selected based on the classification of the material. Base materials are typically compacted in 6 in. molds, and subgrade and backfill materials are classified following the laboratory classification of soils for engineering purposes in Tex 142e. The specimen diameters for subgrade and fill materials are as follows:

- 6 in. diameter: Plastic and coarse grained soils with Tex-142-E classifications of GM, GC, SM, and SC
- 4 in. diameter: Clean, cohesionless sands with Tex-142-E classifications of SW and SP
- 4 in. diameter: Plastic and fine grained soils with Tex-142-E classifications of ML, MH, CL, and CH

The equipment manufacturer, Rainhart, sells 4 in. and 6 in. triaxial confinement cells specifically for the specimen's dimensions required in Tex-117-E.

The effect of specimen diameter on triaxial testing has been investigated by several researchers (16,17,18,19). The studies on the effect of specimen diameter on the shear strength of granular materials have shown the following:

- Very loose Ottawa sands soils exhibited higher shear strengths and friction angles compared to larger diameter specimens (18).
- The shear strength of non-cohesive materials such as graded sands are not affected by specimen diameter when subjected to consolidated, drained triaxial testing (16). Specimen diameters of 2 in. (50 mm) and 4 in. (100 mm) were used, with a slenderness ratio of 2.0.
- The cohesion of materials with cohesive properties can be affected by the specimen diameter, while the friction angle does not change.
 - Zarei et al. (19) did not find a consistent trend in cohesion and friction angle as the specimen diameter increased of CL and CH materials tested with consolidated undrained triaxial testing. Specimen diameters of 1.5 in. (38 mm), 2 in (50 mm), and 2.43 in. (61.8 mm), with a slenderness ratio of 2.0, were used in this study. The authors recommended using the largest possible diameter for triaxial testing.
 - Skuodis et al. (16) reported an increase in cohesion of an over-consolidated sandy-silty-clay material subjected to consolidated drained triaxial testing as the diameter increased from 2 in. (50 mm) to 4 in. (100 mm), with slenderness ratios of 2.0.

The effect of the specimen diameter does not appear to be consistent, but the general consensus from the studies on the effect of specimen size is to use the larger specimen size for more conservative shear properties (17,18,19). For this project the specimen diameter will be kept consistent at 6 in. throughout the study. However, experience with the vibratory hammer has shown that it can be difficult to compact fine grained cohesive materials in a 6 in. diameter mold to Modified Proctor density. If compaction issues are encountered, the specimen diameter will be reduced to 4 in. to increase the pressure the compactor induces during compaction, since this is allowed in Tex 117-E.

2.3 Proposed Test to Replace R-Value

The PMPC working group proposed the resilient modulus test as a replacement for the R-value, since it provides mechanistic results that could be used in the *CalME* pavement design software. The Caltrans Pavement Program was in favor of a simple confined compressive strength (CCS) test, similar to the Texas triaxial test, using a predetermined confinement pressure. This test is easier to perform than the resilient modulus test, and it does not require complex equipment and test setup procedures.

2.4 Summary

This part of the study reviewed available literature on the R-value test and potential alternative tests that could replace it. The review indicated the following:

- The R-value test is a low strain test.
- R-value results have relatively high variability, with variability increasing as the R-value decreases. Variability is attributed in part to specimen fabrication, compaction, and testing procedures.
- The test precision of the R-value test increases as the material's R-value increases.
- There are several feasible alternative test methods that could be used to replace the R-value test method-value test.
- The recommended specimen slenderness ratio for triaxial test specimens is 2:1, with a maximum aggregate size-to-specimen diameter ratio of 1:6.

2.5 Conclusion

The preferred test to replace the R-value is a CCS test. Based on this conclusion, the UCPRC was directed by Caltrans to proceed with calibrating the Texas triaxial test to R-value results and to identify a practical and technically appropriate specimen preparation procedure. The CCS test, which is based on triaxial testing, has established specimen compaction procedures and test methods that have been successfully used to classify aggregate materials. The proposed specimen compaction equipment (discussed in Section 4.3) is easy to maintain and can be used with little experience. The proposed test is relatively simple and can easily be implemented in district laboratories with limited requirements for new equipment. There is no information on test precision of the CCS test and or stiffness correlations with other tests.

3 EXPERIMENTAL PLAN AND MATERIAL SAMPLING

3.1 Experimental Plan

The following experimental plan was developed for this study:

- Collect at least 20 aggregate samples from across California. The aggregate samples should include Class 2 aggregate base, aggregate subbase, and recycled aggregate base. The plan was later modified to state that if a material type cannot be sourced commercially, a material will be manufactured to achieve the goal of the study.
- Contract with an outside laboratory to determine the R-value for each aggregate material.
- Determine the optimum density and moisture content for compacting specimens for confined compressive strength (CCS) testing.
- Validate the simplified confinement cell that will be proposed for use in the CCS test against a traditional triaxial cell. Use confinement pressures of 0, 7, 15, and 29 psi and a loading rate of 2 in. per min for this validation.
- Determine CCS of each aggregate at 0, 3, 5, 10, 15, and 20 psi using a loading rate of 2 in. per minute in the simplified confinement cell.
- Develop a relationship between the R-value and CCS.

3.2 Material Sampling

The aggregate base and subbase materials used in this study were provided by the following aggregate material suppliers in California:

- George Reed, Inc.
- Graniterock
- Teichert Aggregates
- Vulcan Materials Company

Aggregate base and subbase materials were requested from each supplier. The suppliers had several sources of material that conformed to Caltrans Class 2 aggregate base specifications but no aggregate subbase materials with low R-values since it is more economical to manage fewer stockpiles and to supply Class 2 aggregate base materials when aggregate subbase materials are requested. Once it became clear that subbase materials could not be sourced commercially with R-values near the minimum specification value for aggregate subbases, materials from other aggregate streams were sourced and tested, and blends were manufactured to produce materials with lower R-values. When aggregate subbase materials were supplied, the materials

were sent for R-value testing before any additional laboratory testing was performed on the material. If the material had a high R-value (>70), additional laboratory testing was not performed.

The material suppliers shipped approximately 600 lb. of each of the materials listed in Table 3.1 to the UCPRC, with the exception of the exception of Materials #17 and #18, which the UCPRC already had stockpiles of for other testing (20). The material numbers listed in Table 3.1 are used as a reference throughout this report.

The suppliers provided material property test results for each of the supplied materials. These results are provided in Appendix A.

Table 3.1: Aggregate Subbase and Base Materials Tested in the Study

Material Number	Supplier	Location	Material ID	Date Received
1	Graniterock	Aromas	Aromas - Wilson 3/4 Virgin Class 2 Base	5/23/2023
2	Graniterock	Aromas	Aromas - 3/4 Class 2 Aggregate Subbase	5/23/2023
3	Vulcan	Palmdale	Vulcan Palmdale CAB/AB	11/30/2022
4	Vulcan	Anaheim	Vulcan Anaheim Class 2	11/30/2022
5	Vulcan	San Bernardino	Vulcan San Bernardino Recycled Base	11/30/2022
6	Vulcan	Irwindale	Vulcan Reliance Stone P209	11/30/2022
7	Vulcan	Chula Vista	Vulcan Chula Vista CAB/AB	11/30/2022
8	Vulcan	Chula Vista	Vulcan Chula Vista P209	11/30/2022
9	Vulcan	Irwindale	Vulcan Reliance Stone 3/4 CAB	11/30/2022
10	Vulcan	San Bernardino	Vulcan San Bernardino CAB	11/30/2022
11	Graniterock	Highway 25/156	Graniterock Screeded Road Grindings Recycle Class I ASB	5/23/2023
12	Teichert	Vernalis	Teichert Vernalis Virgin Class II AB	8/30/2023
13	Teichert	Vernalis	Teichert Vernalis Recycled Class II AB	8/30/2023
14	Teichert	Perkins	Teichert Perkins Virgin Class II AB	9/30/2023
15	Teichert	Perkins	Teichert Perkins Recycled Class II AB	9/8/2023
16	Teichert	Graniteline	Teichert Graniteline Virgin Class II AB	9/8/2023
17	Teichert	Woodland	Teichert Woodland Virgin Class II AB (2019)	2/1/2019
18	Teichert	Woodland	Teichert Woodland Virgin Class II AB (2023)	9/29/2023
19	Teichert	Bear River	Teichert Bear River Virgin Class II AB	9/8/2023
20	Teichert	Spanish Springs	Teichert Spanish Springs Virgin Class II AB	9/23/2023
21	Teichert	Marysville	Teichert Western Aggregate Marysville Virgin Class II AB	9/23/2023
22	Teichert	Martis	Teichert Martis Virgin Class II AB	9/23/2023

Material Number	Supplier	Location	Material ID	Date Received
23	George Reed	Jackson Valley	George Reed Jackson Valley Class II AB	10/4/2023
24	Teichert	Perkins	Teichert Perkins 1/4" x Dust (Washed)	1/19/2024
25	Teichert	Perkins	Teichert Perkins 1/4" x Dust (Unwashed)	1/19/2024
26	Teichert	Perkins	Teichert Perkins 50/50 AB/Soil Blend	1/19/2024
27	Teichert	Perkins	Teichert Perkins Soil	1/19/2024
28	UCPRC	Blend	Blend 1A-Concrete Control with 38% Soil (15% #200)	2/12/2024
29	UCPRC	Blend	Blend 2B-Concrete Agg with 67% Soil (25% #200)	2/12/2024
30	UCPRC	Blend	Blend 5A-Perkins AB with 70% Soil (30% #200)	2/12/2024
31	UCPRC	Blend	Blend 8A - Unwashed 1/4" x Dust + Clay + 2% Bentonite	3/21/2024
32	UCPRC	Blend	Blend 8B - Unwashed 1/4" x Dust + Clay + 5% Bentonite	3/21/2024
33	Western Nevada Materials	Sparks, NV	Tracy Clark 3/8" Select AB Fill	4/16/2024

3.3 Material Characterization

The aggregate subbase and base material requirements in the Caltrans 2022 standard specifications are shown in Table 3.2 and Table 3.3. The supplied material was characterized using the material property results provided by the suppliers that included gradation, durability, and sand equivalence.

There are no requirements for Atterberg limits or crushed faces in the specifications, both of which are likely to influence strength and shear test results. The only language that is provided is that the material must be clean and consist of any combination of the following:

- Broken stone
- Crushed gravel
- Natural rough-surfaced gravel
- Sand
- Processed reclaimed asphalt concrete, portland cement concrete, lime treated base, and/or cement treated base.

Table 3.2: Caltrans 2022 Standard Specification for Aggregate Subbase Properties

Property	Sieve Size	Class 1	Class 2	Class 3	Class 4	Class 5
Gradation	3 in.	100	100	100	N/A	N/A
	2.5 in.	87-100	87-100	87-100	N/A	N/A
	No. 4	30-75	35-95	45-100	N/A	N/A
	No. 200	0-23	0-29	0-34	N/A	N/A
Sand Equivalency	N/A	18	18	18	N/A	N/A
R-value (min)	N/A	60	50	40	N/A	N/A

Table 3.3: Caltrans 2022 Standard Specification for Aggregate Base Properties

Property	Sieve Size	Class 2 (1.5 in. max)	Class 2 (0.75 in. max)	Class 3 (1.5 in. max)	Class 3 (0.75 in. max)
Gradation	2 in.	100	N/A	100	N/A
	1.5 in.	87-100	N/A	87-100	N/A
	1.0 in.	N/A	100	N/A	100
	0.75 in.	45-90	90-100	45-95	87-100
	No. 4	20-50	35-60	20-65	35-75
	No. 30	6-29	5-35	6-39	7-45
	No. 200	0-12	0-12	0-19	0-19
Sand Equivalency	N/A	22	22	18	18
R-value (min)	N/A	78	78	50	50
Durability Index (min)	N/A	35	35	N/A	N/A

3.3.1 Gradation

The gradation results were compared against Caltrans 2022 standard specifications for aggregate base and aggregate subbase to determine if the number of material groups can be reduced for the analysis. All the materials that were reported as Class 2 aggregate base materials are provided in Figure 3.1 against the Class 2 aggregate base range. The results show that all the Class 2 aggregate base conforms to the minimum gradation requirements for Class 2 aggregate base for 0.75 in. maximum aggregate size. The P209 materials (Materials #6 and #8) and the Class 1 aggregate subbase material (Material #2) generally conform to the Class 2 aggregate base gradation for 1.5” maximum aggregate size (Figure 3.2). The Class 2 aggregate subbase material (Material #2) conformed to the Class 2 aggregate subbase gradation (Figure 3.4). Based on the gradation results, the number of material types can be reduced to four groups (Table 3.4):

- 22 Class 2 aggregate base materials (Figure 3.1 and Figure 3.2)
- 1 Class 3 aggregate base material (Figure 3.3)
- 3 Class 2 aggregate subbase material (Figure 3.4)
- 7 Class 3 aggregate subbase materials (Figure 3.5)

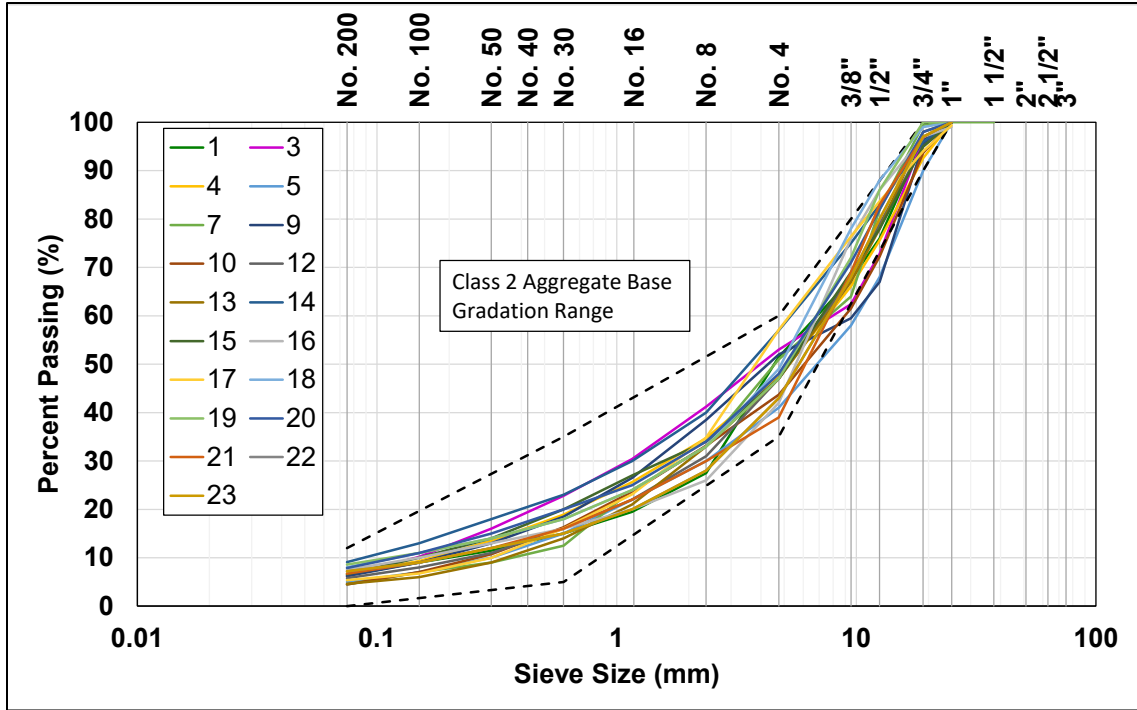


Figure 3.1: Sampled aggregate materials that meet Class 2 aggregate base 0.75 in. maximum aggregate size gradation band.

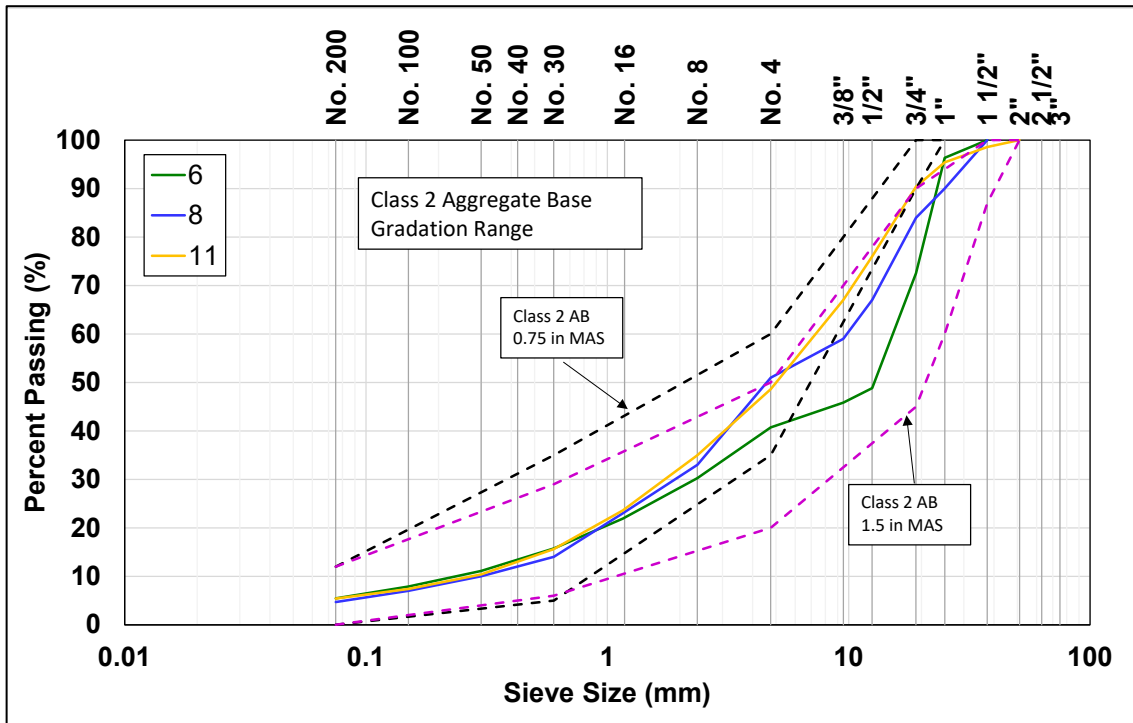


Figure 3.2: Sampled aggregates that meet Class 2 aggregate base 1.5 in. maximum aggregate size gradation band.

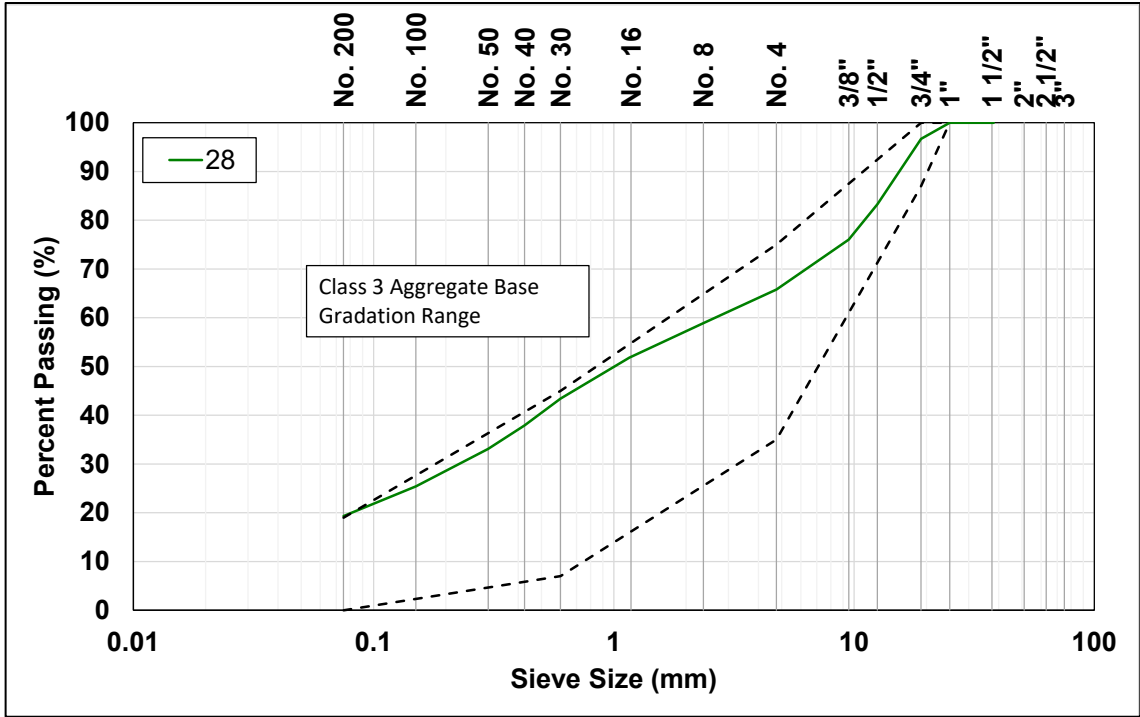


Figure 3.3: Class 3 aggregate base material gradations.

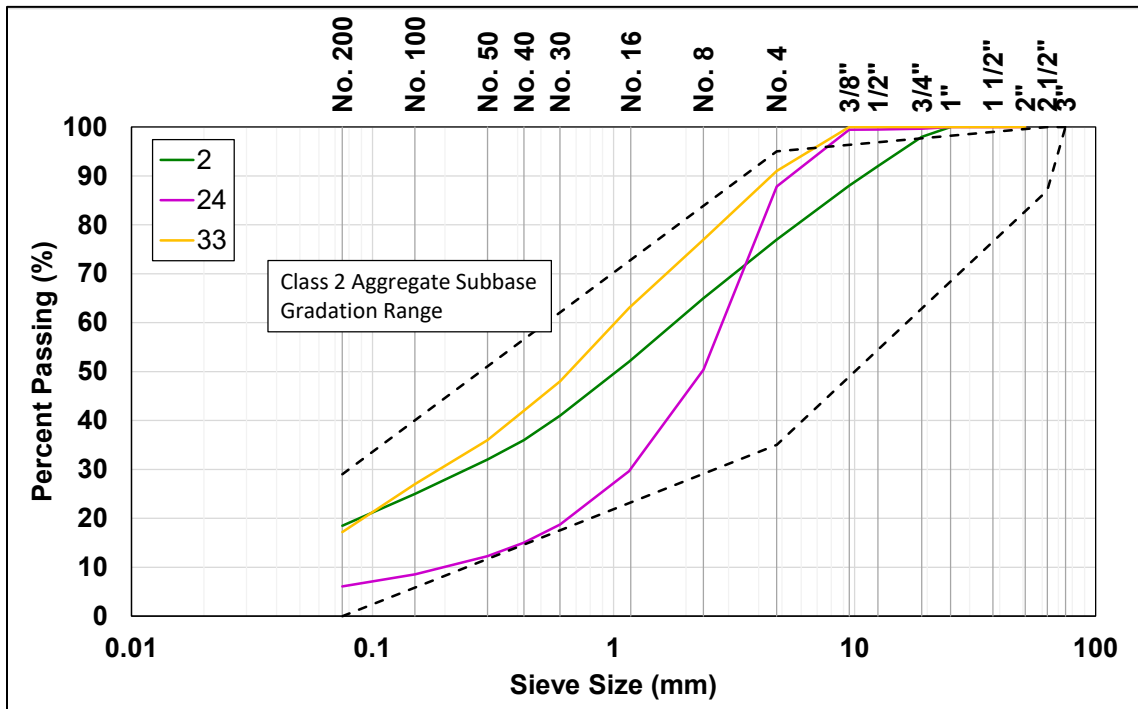


Figure 3.4: Class 2 aggregate subbase material gradations.

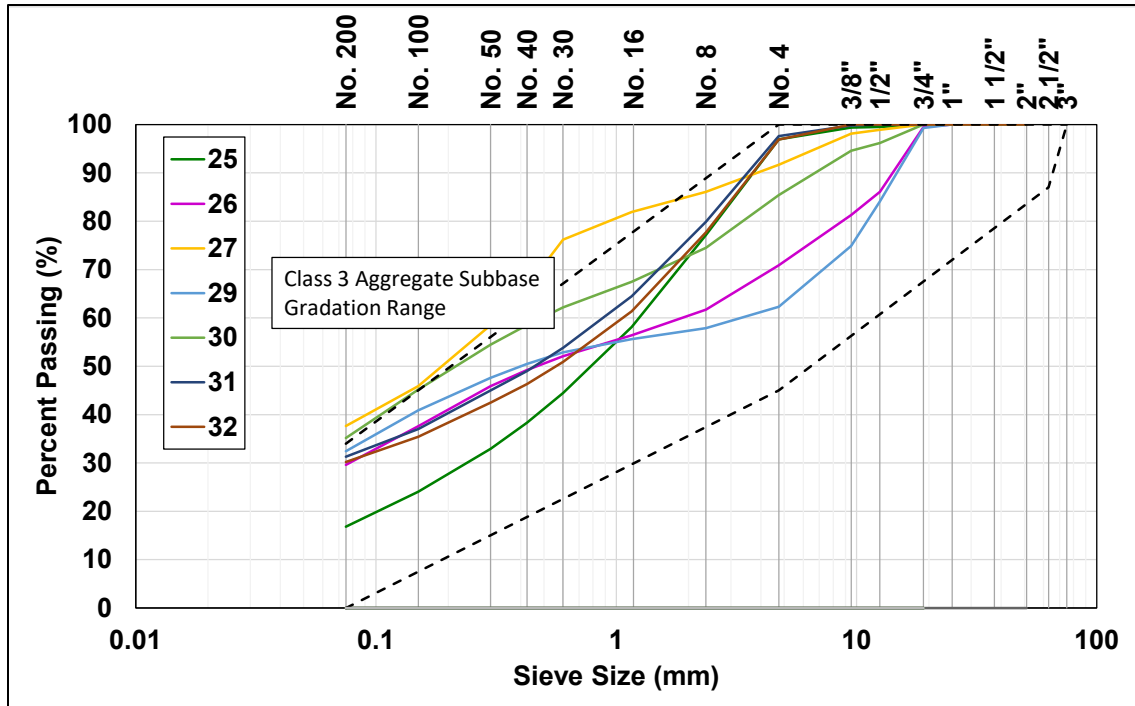


Figure 3.5: Class 3 aggregate subbase material gradations.

Table 3.4: Reclassified Material Types Against Caltrans Specifications Based on Gradation

Material Number	Reported Caltrans Classification	Maximum Caltrans Classification	Material Number	Reported Caltrans Classification	Maximum Caltrans Classification
1	AB2	AB2	18	AB2	AB2
2	ASB2	ASB2	19	AB2	AB2
3	AB2	AB2	20	AB2	AB2
4	AB2	AB2	21	AB2	AB2
5	AB2	AB2	22	AB2	AB2
6	P209	AB2	23	AB2	AB2
7	AB2	AB2	24	N/A	ASB2
8	P209	AB2	25	N/A	ASB3
9	AB2	AB2	26	N/A	ASB3
10	AB2	AB2	27	N/A	ASB3
11	ASB1	AB2	28	N/A	AB3
12	AB2	AB2	29	N/A	ASB3
13	AB2	AB2	30	N/A	ASB3
14	AB2	AB2	31	N/A	ASB3
15	AB2	AB2	32	N/A	ASB3
16	AB2	AB2	33	N/A	ASB2
17	AB2	AB2		N/A	

3.3.2 R-Value Results

The materials tested in the study cover an R-value range from 36 to 84. Independent testing laboratories were contracted to perform the R-value tests on the sampled materials. At the start of the project, Material #1 was sent to the first laboratory. The R-value result on the material was 61. The test results were questioned by the supplier. A second sample of the material was sampled and tested at a second laboratory, with a result of 79, which was consistent with routine testing conducted by the supplier. All subsequent samples were sent to the second laboratory to ensure consistent testing across all samples. The other material suppliers provided R-value results determined by their preferred testing laboratories. All the R-value test results are provided in Table 3.5. The minimum specified R-value results for aggregate to classify as aggregate base and subbase are as follows:

- Class 1 aggregate subbase (ASB1): 60
- Class 2 aggregate subbase (ASB2): 50
- Class 3 aggregate subbase (ASB3): 40
- Class 2 aggregate base (AB2): 78
- Class 3 aggregate base (AB3): 50
- P209: No requirement

Using the results from Laboratory 2, five of the 22 reclassified Class 2 aggregate base materials failed to meet minimum R-value of 78. Four of these materials did meet the minimum criteria based on Laboratory 3 test results. The blended materials (Materials#28 to #32) were manufactured using a range of different materials to meet AB3 and ASB3 specifications. The R-values of the blended materials were decreased by increasing the fines and plasticity of the material.

Table 3.5: R-Value Results

Material Number	Maximum Classification ^a	R-Value		
		Lab. 1	Lab. 2	Lab. 3
1	AB2	61^b	79	N/A
2	ASB2	N/A	75	N/A
3	AB2	N/A	78	N/A
4	AB2	N/A	77^b	N/A
5	AB2	N/A	80	N/A
6	AB2	N/A	81	N/A
7	AB2	N/A	78	N/A
8	AB2	N/A	81	N/A
9	AB2	N/A	78	N/A
10	AB2	N/A	78	N/A
11	AB2	N/A	84	N/A
12	AB2	N/A	79	82
13	AB2	N/A	79	80
14	AB2	N/A	78	82
15	AB2	N/A	80	81
16	AB2	N/A	77^b	81
17	AB2	N/A	71^b	79
18	AB2	N/A	77^b	78
19	AB2	N/A	79	81
20	AB2	N/A	80	79
21	AB2	N/A	72^b	81
22	AB2	N/A	79	77^b
23	AB2	N/A	81	N/A
24	ASB2	N/A	75	N/A
25	ASB3	N/A	75	N/A
26	ASB3	N/A	76	N/A
27	ASB3	N/A	47	N/A
28	AB3	N/A	76	N/A
29	ASB3	N/A	64	N/A
30	ASB3	N/A	59	N/A
31	ASB3	N/A	41	N/A
32	ASB3	N/A	36^b	N/A
33	ASB2	N/A	67	N/A

^a Based on gradation envelopes.

^b R-values that did not meet the minimum R-value for the classification.

3.3.3 Sand Equivalence

The sand equivalence (SE) results are provided in Table 3.6. The minimum SE requirements are the following:

- Class 2 aggregate base: 22
- Class 3 aggregate base: 18
- Class 2 aggregate subbase: 18
- Class 3 aggregate subbase: 18

Based on the reported results, all the materials pass the minimum requirements, except Material #29. There is a non-linear relationship between sand equivalence and R-value (Figure 3.6), but the R-value test is not sensitive to changes in SE with materials with R-values greater than 70.

Table 3.6: Sand Equivalence Results

Material Number	Maximum Classification ^a	Sand Equivalence (%)	Material Number	Maximum Classification ^a	Sand Equivalence (%)
1	AB2	59	18	AB2	32
2	ASB2	38	19	AB2	26
3	AB2	73	20	AB2	36
4	AB2	N/A	21	AB2	54
5	AB2	52	22	AB2	61
6	AB2	51	23	AB2	29
7	AB2	63	24	ASB2	100
8	AB2	40	25	ASB3	91
9	AB2	54	26	ASB3	28
10	AB2	61	27	ASB3	14^b
11	AB2	57	28	AB3	28
12	AB2	31	29	ASB3	15^b
13	AB2	37	30	ASB3	18
14	AB2	54	31	ASB3	22
15	AB2	47	32	ASB3	21
16	AB2	69	33	ASB2	28
17	AB2	31	N/A	N/A	N/A

^a Based on gradation envelopes.

^b R-values that did not meet the minimum R-value for the classification.

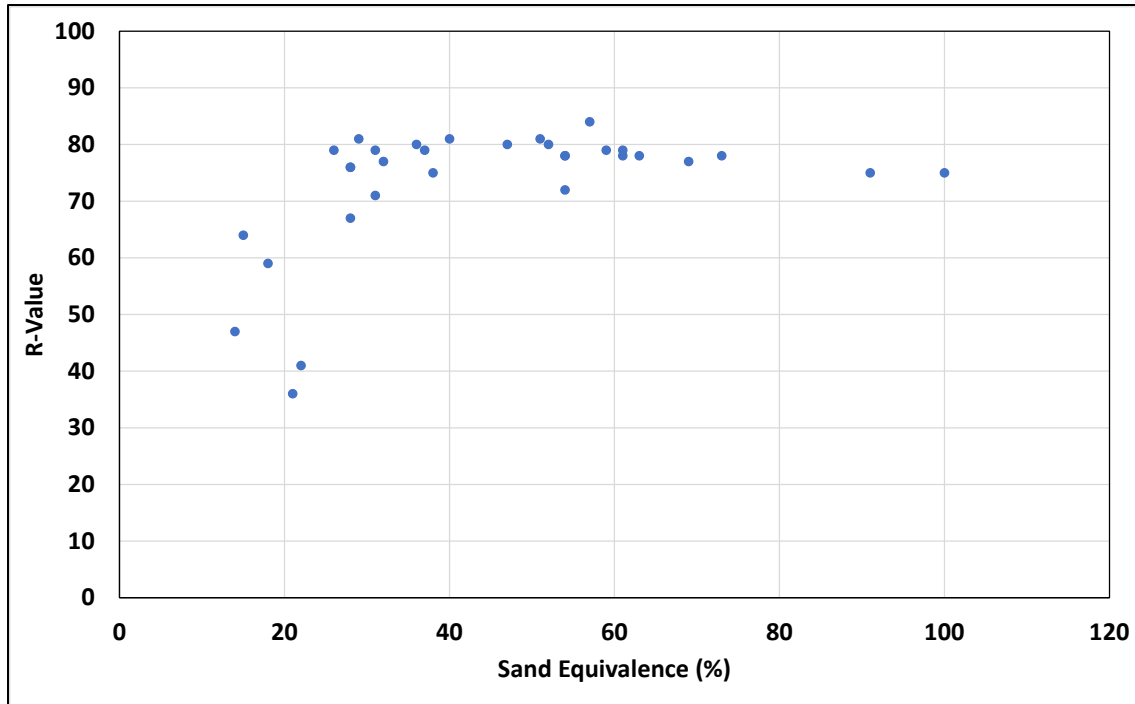


Figure 3.6: Relationship between SE and R-value.

3.3.4 Durability

The reported durability index results based on California Test Method 229 are provided in Table 3.7. The minimum durability index requirement for Class 2 aggregate base is 35. There is no minimum requirement for aggregate subbase materials.

Table 3.7: Durability Results

Material Number	Maximum Classification ^a	Coarse Fraction	Fine Fraction	Minimum
1	AB2	79.3	66	35
2	ASB2	49	45	N/A
3	AB2	N/A	N/A	35
4	AB2	N/A	N/A	35
5	AB2	N/A	N/A	35
6	AB2	N/A	N/A	35
7	AB2	N/A	N/A	35
8	AB2	N/A	N/A	35
9	AB2	N/A	N/A	35
10	AB2	N/A	N/A	35
11	AB2	N/A	N/A	35
12	AB2	N/A	42	35

Material Number	Maximum Classification ^a	Coarse Fraction	Fine Fraction	Minimum
13	AB2	N/A	N/A	35
14	AB2	N/A	73	35
15	AB2	N/A	47	35
16	AB2	N/A	N/A	35
17	AB2	N/A	40	35
18	AB2	86	70	35
19	AB2	61	39	35
20	AB2	78	47	35
21	AB2	N/A	67	35
22	AB2	65	38	35
23	AB2	N/A	61	35

^a Based on gradation envelopes

3.3.5 Final Classification

The reported material classifications are summarized in Table 3.8 along with the conclusions drawn by UCPRC regarding the classification based on the properties reported above from the material results provided by the suppliers and the independent testing performed by the UCPRC.

Table 3.8: Maximum Classifications for Supplied Materials

Material Number	Reported Classification	Maximum Classification ^a	UCPRC Conclusion and Comment
1	AB2	AB2	Has low R-value from at least one laboratory
2	ASB2	ASB2	Met all criteria
3	AB2	AB2	Met all criteria
4	AB2	AB2	Has low R-value from at least one laboratory
5	AB2	AB2	Met all criteria
6	P209	AB2	Met all criteria
7	AB2	AB2	Met all criteria
8	P209	AB2	Met all criteria
9	AB2	AB2	Met all criteria
10	AB2	AB2	Met all criteria
11	ASB1	AB2	Met all criteria
12	AB2	AB2	Met all criteria
13	AB2	AB2	Met all criteria
14	AB2	AB2	Met all criteria
15	AB2	AB2	Met all criteria
16	AB2	AB2	Has low R-value from at least one laboratory

Material Number	Reported Classification	Maximum Classification ^a	UCPRC Conclusion and Comment
17	AB2	AB2	Has low R-value from at least one laboratory
18	AB2	AB2	Has low R-value from at least one laboratory
19	AB2	AB2	Met all criteria
20	AB2	AB2	Met all criteria
21	AB2	AB2	Has low R-value from at least one laboratory
22	AB2	AB2	Has low R-value from at least one laboratory
23	AB2	AB2	Met all criteria
24	N/A	ASB2	Met all criteria
25	N/A	ASB3	Met all criteria
26	N/A	ASB3	Met all criteria
27	N/A	ASB3	Did not meet SE requirement
28	N/A	AB3	Met all criteria
29	N/A	ASB3	Did not meet SE requirement
30	N/A	ASB3	Met all criteria
31	N/A	ASB3	Met all criteria
32	N/A	ASB3	Has low R-value from at least one laboratory
33	N/A	ASB2	Met all criteria

^a Based on gradation envelopes.

3.4 Specimen Compaction Method Determination

The test methods considered for determining the material density included two versions of the Modified Proctor compaction method, AASHTO T 180 and ASTM D1557, and the Caltrans compaction method CT 216. At the start of the project, AASHTO T 180 was used to determine the maximum dry density of the materials that were collected early in the study. This method was selected since it allows the use of 100% passing 0.75 in. material in a 4 in. mold, which reduced the amount of material required for density characterization.

During the project, in a meeting with Caltrans, the Pavement Program requested that CT 216 be used as the target density. As discussed later in Section 4.3.1, the CT 216-determined density was too low to produce specimens with a vibratory hammer, which was selected as the most practical compaction method for the study. The specimens could not be extracted and handled without damaging them. A proposal was therefore made to Caltrans to change the reference density back to Modified Proctor. Caltrans requested that ASTM D1557 be used for the remainder of the materials. ASTM D1557 requires a maximum size of 0.75 in. for 6 in. diameter specimens.

The maximum dry and wet density and optimum moisture contents determined using Modified Proctor and CT 216 are provided in Table 3.9 and Table 3.10, respectively. Only the Class 2 AB materials were tested for CT216. The Modified Proctor (either AASHTO T 180 or ASTM D1557) wet density and optimum moisture content results were used as the basis for compacting specimens for CCS testing with a vibratory hammer.

Table 3.9: Modified Proctor Compaction Results

Material Number	AASHTO T 180			ASTM D1557		
	Wet Density (pcf)	Optimum Moisture Content (%)	Dry Density (pcf)	Wet Density (pcf)	Optimum Moisture Content (%)	Dry Density (pcf)
1	152.3	6.8	142.6	149.1	6.3	140.3
2	150.7	6.4	141.6	N/A	N/A	N/A
3	146.6	5.9	138.5	N/A	N/A	N/A
4	133	10	120.9	N/A	N/A	N/A
5	135.3	9.5	123.6	N/A	N/A	N/A
6	149	7.4	138.8	N/A	N/A	N/A
7	143.5	4.3	137.6	N/A	N/A	N/A
8	144.9	5.2	137.8	N/A	N/A	N/A
9	146.8	5	139.8	N/A	N/A	N/A
10	144.4	5.4	137	N/A	N/A	N/A
11	N/A	N/A	N/A	149.6	5.4	141.9
12	N/A	N/A	N/A	145.1	5	138.2
13	N/A	N/A	N/A	139.3	7.1	130.1
14	N/A	N/A	N/A	151.5	5.5	143.6
15	N/A	N/A	N/A	141.8	7.2	132.3
16	N/A	N/A	N/A	147.6	4.9	140.7
17	144.2	5.5	136.7	N/A	N/A	N/A
18	N/A	N/A	N/A	143.8	5.2	136.7
19	N/A	N/A	N/A	147.7	5	140.7
20	N/A	N/A	N/A	147.5	5.8	139.4
21	N/A	N/A	N/A	143.7	4.8	137.1
22	N/A	N/A	N/A	136.1	8.5	125.4
23	N/A	N/A	N/A	148	4.7	141.4
24	N/A	N/A	N/A	130.6	3.1	126.7
25	N/A	N/A	N/A	144.4	6.3	135.8
26	N/A	N/A	N/A	146.8	6.1	138.4
27	N/A	N/A	N/A	134.6	7.4	125.3
28	N/A	N/A	N/A	148.4	7.2	138.4
29	N/A	N/A	N/A	144.4	7.7	134.1
30	N/A	N/A	N/A	141.7	7.7	131.6
31	N/A	N/A	N/A	148.5	7.3	138.4
32	N/A	N/A	N/A	145.7	7.4	135.7
33	N/A	N/A	N/A	N/A	N/A	N/A

Table 3.10: CT 216 Compaction Results

Material Number	Wet Density (pcf)	Optimum Moisture Content (%)	Dry Density (pcf)
1	138.6	6.3	130.4
2	148.0	7.7	137.4
3	134.3	5.1	127.8
4	120.5	9.7	109.9
5	123.0	11.7	110.1
6	Not tested		
7	129.9	4.1	124.7
8	Not tested		
9	Not tested		
10	136.1	5.1	129.5
11	142.3	5.4	135.0
12	136.7	4.3	131.1
13	128.6	7.0	120.2
14	Not tested		
15	132.4	7.4	123.3
16	137.9	5.8	130.3
17	137.3	5.8	129.8
18	Not tested		
19	134.2	3.5	129.7
20	Not tested		
21	Not tested		
22	Not tested		
23	Not tested		

4 TEST DEVELOPMENT

4.1 Introduction

The test proposed to replace the R-value test is a confined compressive strength (CCS) test adapted from the Texas triaxial test. There is currently no standard test method for this test or a method to easily and consistently compact the specimens for the test. This chapter reviews the development of the methodology to compact and prepare the specimens for unconfined and confined testing. The UCPRC's standard operating procedure developed for the test is provided in Appendix B.

The CCS test considers aspects of the monotonic Texas triaxial testing method (based on its success in classifying aggregate materials) and the Quick Shear Test described in Section 9.3.9 of the AASHTO T 307 triaxial testing method. The specimen size selected for this test considers aspects of the aggregate material designated for the test.

4.2 Specimen Size

The ideal specimen size is larger than the representative volume element (RVE), which is defined as the smallest material volume large enough such that the global characteristics of the material remain constant, regardless of the location of the testing sample from a larger completely homogenous sample (21). Harvey et al. (22) noted that, when the specimen is smaller than the RVE, random results occur (i.e., the variability in the results increase).

The proposed test should evaluate the largest fraction of the material. The material used for the R-value test is passed through the No. 4 sieve to accommodate the relatively small sample size prescribed in CT 301 (4 in. diameter x 2.5 in. height). This means the R-value does not represent the full gradation.

The specimen size should also consider readily available triaxial confinement cells, a number of which are available for geotechnical testing. Traditional triaxial cells can accommodate any specimen size up to 6 in. in diameter and 12 in. in height. Simple confinement cells are available that can only accommodate one specimen size. Traditional triaxial tests can be complex to set up, and the equipment is typically more expensive than those that use simple confinement cells.

The scope for developing this test required that it should be relatively simple and be performed by any materials laboratory with limited experience and budgets.

The simple confinement cells available at the time of writing this report included the following:

- Rainhart Part Number 721, for 4 in. diameter specimens, up to 9 in. in height
- Rainhart Part Number 720, for 6 in. diameter specimens, up to 12 in. in height
- Wirtgen triaxial cell, for 6 in. diameter specimens, up to 12 in. in height

The UCPRC was already equipped with traditional and Wirtgen triaxial cells, and these were used for the testing.

4.2.1 Specimen Diameter

The specimen diameter selected for this study was 6 in. This allows testing of aggregate with a maximum aggregate size of up to 1 in. with a maximum aggregate size-to-specimen diameter ratio of 1:6, to provide material properties representative of as large a portion of the aggregate gradation as possible.

4.2.2 Slenderness Ratio

Based on the literature, an aspect ratio of 2:1 was selected to ensure repeatability and to minimize the effects of end-friction on the test results. This slenderness ratio is larger than that prescribed in Texas triaxial test (Tex 117-E), which may negate the possibility of using the material classes listed in the method.

4.3 Material Compaction

The method recommended for specimen compaction is a vibratory hammer, similar to the device described in AASHTO T 307 but with a height control device to assist in controlling compaction density. The vibratory hammer cannot compact to a standard energy level like Proctor, gyratory, or Marshall compaction devices, but it can replicate a target density. This compaction method is fast, requiring between 20 and 240 seconds to compact a 6 × 12 in. specimen, depending on the aggregate properties.

4.3.1 Reference Density Selection

The required relative compaction of aggregate subbase and base materials in the California standard specifications is 95% relative to CT 216 as measured with a nuclear gauge following

CT 231. At the onset of this study, CT 216 was selected as the target density since it is the reference density used for field compactions. CT 216 testing was conducted on 14 of the 23 materials used in the study. As part of the study, Modified Proctor densities (AASHTO T 180 or ASTM D1557) were also determined for each material.

An attempt was made to compact a 6 × 12 in. specimen to CT 216 density using Material #17. Specimen densities were too low to allow them to be extracted from the mold without disintegrating. Compactions were repeated using the Modified Proctor method, which produced specimens that could be successfully extracted from the mold immediately after compaction and then handled and prepared for testing without any damage.

This prompted an investigation regarding the appropriateness of using the CT 216 method and the possible impacts of using the specimens, if they could be retrieved from the mold, for determining the triaxial strength. For each of the CT 216 compactions, two density readings were taken. The first, referred to as the “stick reading” in this report, is the rod reading that is translated to a density based on the mass of the material used for compaction. The second, referred to as the “measured density,” was based on the physical measurements of the specimen, which depended on it being intact after extraction from the mold. The specimen was weighed and measured for diameter and height to determine the wet and dry density. The density results are provided in Appendix C and summarized in Table 4.1. Materials #24 to #33 were not tested for CT 216.

Table 4.1: Difference Between Modified Proctor and CT 216 Density Results

Material Number	Dry Density (pcf)			% Relative Compaction to Modified Proctor		
	Modified Proctor	CT 216 Stick	CT 216 Measured	CT 216 Stick (%)	CT 216 Measured (%)	95% of CT 216 Stick (%)
1	141.5	130.4	135.1	92	95	88
2	141.6	137.4	139.8	97	99	92
3	138.5	127.8	133.1	92	96	88
4	120.9	109.9	116.2	91	96	86
5	123.6	110.1	121.6	89	98	85
6	Not tested for CT 216					
7	137.6	124.7	128.6	91	93	86
8	Not tested for CT 216					
9	Not tested for CT 216					

Material Number	Dry Density (pcf)			% Relative Compaction to Modified Proctor		
	Modified Proctor	CT 216 Stick	CT 216 Measured	CT 216 Stick (%)	CT 216 Measured (%)	95% of CT 216 Stick (%)
10	137.0	129.5	136.3	95	100	90
11	141.9	135.0	137.2	95	97	90
12	138.2	131.1	135.2	95	98	90
13	130.1	120.2	126.3	92	97	88
14	Not tested for CT 216					
15	132.3	123.3	126.6	93	96	89
16	140.7	130.3	135.8	93	97	88
17	136.7	129.8	137.9	95	101	90
18	Not tested for CT 216					
19	140.7	129.7	133.4	92	95	88
20	Not tested for CT 216					
21	Not tested for CT 216					
22	Not tested for CT 216					
23	Not tested for CT 216					

The results show that the stick reading is on average 4% lower than the measured density and 7% lower than the Modified Proctor density. Based on these results, 95% relative compaction of CT 216 is approximately 88% of Modified Proctor, which explains why specimens could not be satisfactorily compacted with the vibratory hammer when the stick density was targeted.

After discussions with the Caltrans Pavement Program, it was concluded that the density calculation in the CT 216 method is different from the typical method for calculation of density and the CT 216 method was developed to expedite preparation of specimens in the field during construction. Extracting specimens compacted following CT 216 is difficult and will likely result in damage to the specimens. The method was not intended to produce specimens for testing, only for determination of density. The UCPRC proposed using Modified Proctor (ASTM D1557) as the target density for the study since it provided intact specimens that could be tested. This request was approved, which mitigated any further issues with specimen compaction and handling. It was acknowledged that the proposed method to remove specimens compacted following ASTM D1557 by pushing them out of the compaction cylinder using a jack may result in some additional compaction.

4.4 Confinement Cell Comparison

As part of this project, results from a simple confinement cell were compared against those from a traditional triaxial cell to validate the simplified approach for determining the material shear strength. Known differences between traditional and simple cells include the following:

- The traditional cell applies confinement on all three dimensions of the specimen. The simple cell only applies confinement to the lateral area of the specimen.
- The traditional cell can be used to evaluate drained and undrained conditions by allowing or preventing the pore pressure to vent to the atmosphere. The simple cell does not have the ability to measure or control pore pressure.
- The traditional cell typically uses a latex membrane that is slipped over the specimen and sealed with o-rings over the loading platens to prevent leaks. The simple cell uses a rubber tube to apply confinement.
- Leaks can develop in the traditional cell confinement system, either past the o-rings or through punctures in the membrane. This is often observed as bubbles where the drain tubes are venting to atmosphere through a water-filled container. The simple cell is less likely to develop leaks since the rubber tube is thicker and more durable than latex membranes. There are also no o-rings seals where leaks can develop. There are some risks associated with the simple cell, including warnings not to inflate the cell without a specimen, which can cause the tube to burst.
- Assembling the traditional cell is more complex than assembling the simple cell as there are more parts in the loading system that have to align. In the traditional cell, the specimen is positioned through a series of aligned rods and platens, whereas in the simple cell, the specimen is loaded directly onto the loading platen.

4.4.1 Conventional Triaxial Cell

The conventional triaxial cell used in this study is shown in Figure 4.1. The major principal stress is determined using Equation 4.1. The mass of the platen, loading shaft, and upward force of the confinement pressure on the actuator are considered in the calculation of the deviatoric stress in Equation 4.2. The masses of the test equipment which contribute to the deviatoric stress are provided in Table 4.2.



Figure 4.1: Traditional triaxial cell.

$$\sigma_1 = q + \sigma_3 \quad (4.1)$$

Where: σ_1 = Major principal stress (MPa)
 σ_3 = Confinement stress (MPa)
 q = Deviatoric stress (MPa)

$$q = \frac{P_L + P_S - P_c}{\pi(D/2)^2} \quad (4.2)$$

Where: P_L = Peak load at break (N)
 P_S = Surcharge weight including weight of platen, loading shaft and ball bearing (N)
 P_c = Upwards force of confinement pressure on loading shaft (N) (Equation 4.3)
 D = Diameter of contact face of top loading platen (mm)

$$P_c = \sigma_c \pi (D_s/2)^2 \quad (4.3)$$

Where: σ_c = Confinement pressure, σ_3 (MPa)
 D_s = Diameter of loading shaft (mm)

Table 4.2: Triaxial Equipment Details

Triaxial Cell Type	Traditional	Traditional	Wirtgen	Wirtgen_Modified
Triaxial cell designation in report	<i>IPC_Light</i>	<i>IPC_Heavy</i>	<i>WTC_150</i>	<i>WTC_Modified</i>
Top loading platen, lb. (g)	2.7 (1,223.7)	2.7 (1,223.7)	10.36 (4,698.8)	3.94(1,787.4)
Loading shaft, lbf (g)	3.57 (1,620.7)	17.01 (7,717.5)	N/A	N/A
Ball bearing, lb. (g)	0.06(27.8)	0.06(27.8)	0.06(27.8)	0.06(27.8)
Top loading platen diameter, in. (mm)	6.00(152.8)	6.00 (152.8)	5.60 (142.3)	6.00(152.8)

4.4.2 Wirtgen Confinement Cell

The Wirtgen confinement cell shown in Figure 4.2 and Figure 4.3 is an example of a simple triaxial cell. The major principal stress can be calculated using Equation 4.4. The mass of the platen is considered in the calculation of the deviatoric stress in Equation 4.5. The loads of the test equipment which contribute to the deviatoric stress are provided in Table 4.2. The Wirtgen cell, as sold, was used for the testing of all 23 materials.

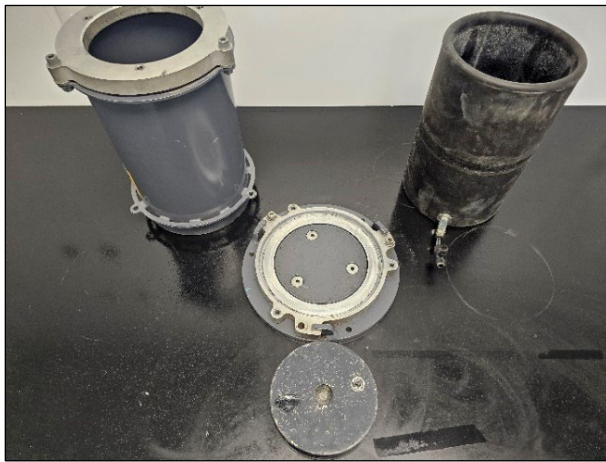


Figure 4.2: Disassembled Wirtgen confinement cell.



Figure 4.3: Assembled Wirtgen confinement cell with the new loading platen.

$$\sigma_1 = q \tag{4.4}$$

Where: σ_1 = Major principal stress (MPa)
 q = Deviatoric stress (MPa) (Equation 4.5)

$$q = \frac{P_L + P_S}{\pi(D/2)^2} \tag{4.5}$$

Where: P_L = Peak load at break (N)
 P_S = Surcharge load including load of platen and ball bearing (N)
 D = Diameter of contact face of top loading platen (mm)

Wirtgen Cell Improvements

The Wirtgen cell has a top loading platen with a contact area of 5.65 in., which is smaller than the 6 in. diameter of the specimens. This increases the applied stress. The base plate also has recesses where bolts attach the base plate to the bottom of the cell. For this study, a new top platen was machined with a contact area of 6 in. The confining cell was also modified to attach the base plate using screws that fasten through the bottom of the cell into blind holes, ensuring a flat surface at the bottom of the specimen. These modifications were completed before any testing was initiated. Figure 4.4 and Figure 4.5 show the original and new loading platen and modified base plate, respectively.



Figure 4.4: Original and new loading platen for Wirtgen cell (new platen on left).



Figure 4.5: Original and new base plate for Wirtgen cell (new plate on left).

4.4.3 Peak Load and Stress Results

The traditional triaxial cell (*IPC_Heavy*), standard Wirtgen cell (*WTC_150*), and the modified Wirtgen cell (*WTC_Modified*) were compared using Material #14, compacted to Modified Proctor density. An unmodified traditional triaxial cell (*IPC_Light*) typically used for 4 in. diameter specimens, or for material that is expected to have lower shear strengths, was available for the study, but it was not included in the triaxial cell comparison since it is similar in design and uses the same loading platens as the *IPC_Heavy* cell. Four specimens were tested with each cell using confinement pressures of 0, 7.25, 14.5, and 29.0 psi. The test results are provided in Table 4.3.

4.4.4 Data Analysis

The data were analyzed by calculating the friction angle and cohesion measured by each cell type using the test results in Table 4.3 and using Equation 4.1 to Equation 4.5 to calculate the minor and major principal stresses. A recursive process was used to determine the failure envelope by fitting a tangent line to each combination of confining pressures (12 combinations in a four-confinement pressure factorial) to produce a set of stress states (normal stress and shear strength combinations). An example is shown in Figure 4.6. Linear regression was then used to fit a linear equation through the array of stress states to determine the friction angle and cohesion of the group of tests for each cell (Figure 4.7). The y-axis intercept of the linear equation is the cohesion, and the angle of the slope of the line is the friction angle.

Table 4.3: Triaxial Cell Comparison Test Results

Cell	Confinement Pressure (psi)	Peak Load (psi)	Peak Stress (psi)	Minor Principal Stress (psi)	Major Principal Stress (psi)
<i>IPC_Heavy</i>	0	2,159	76.4	0.0	76.4
	7.3	4,830	170.4	7.3	177.7
	14.5	6,763	237.6	14.5	252.1
	29	9,826	344.7	29.0	373.7
<i>WTC_150</i>	0	1,669	67.8	0.0	67.8
	7.3	5,430	220.3	7.3	220.3
	14.5	7,782	315.7	14.5	315.7
	29	9,988	405.2	29.0	405.2
<i>WTC_Modified</i>	0	1,124	40.0	0.0	40.0
	7.3	4,753	169.0	7.3	169.0
	14.5	6,630	235.7	14.5	235.7
	29	9,658	343.4	29.0	343.4

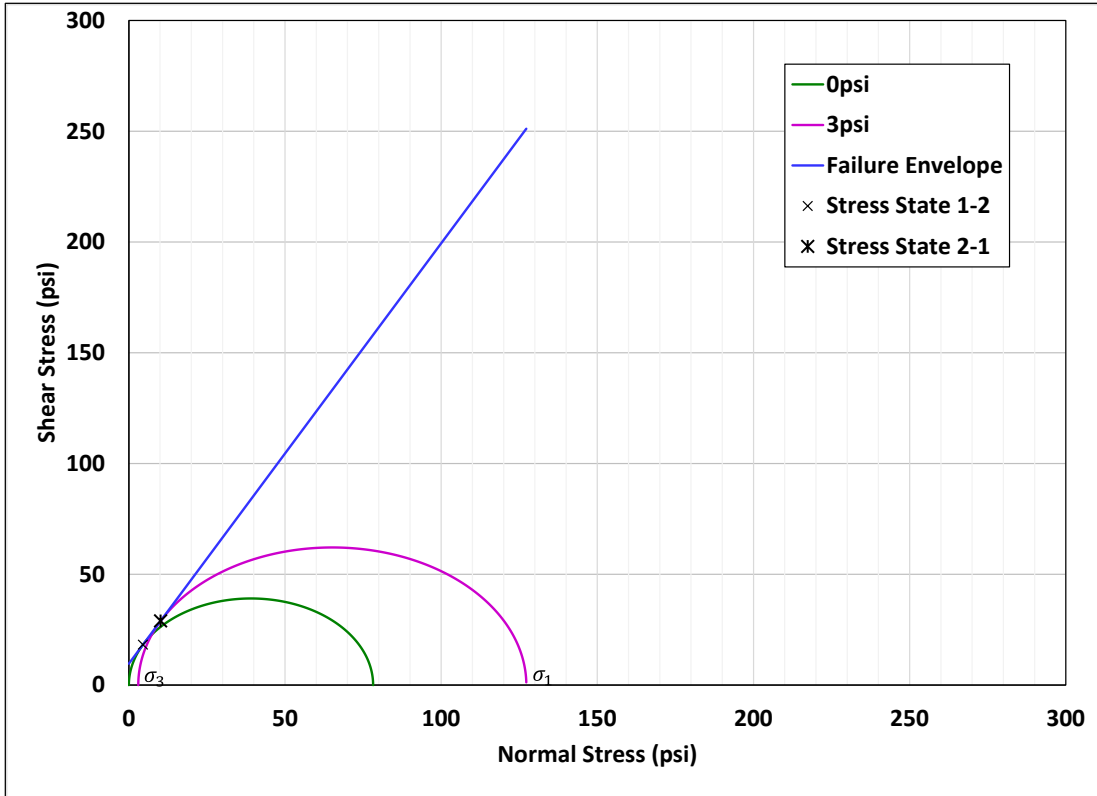


Figure 4.6: Fitting tangent plane for stress states.

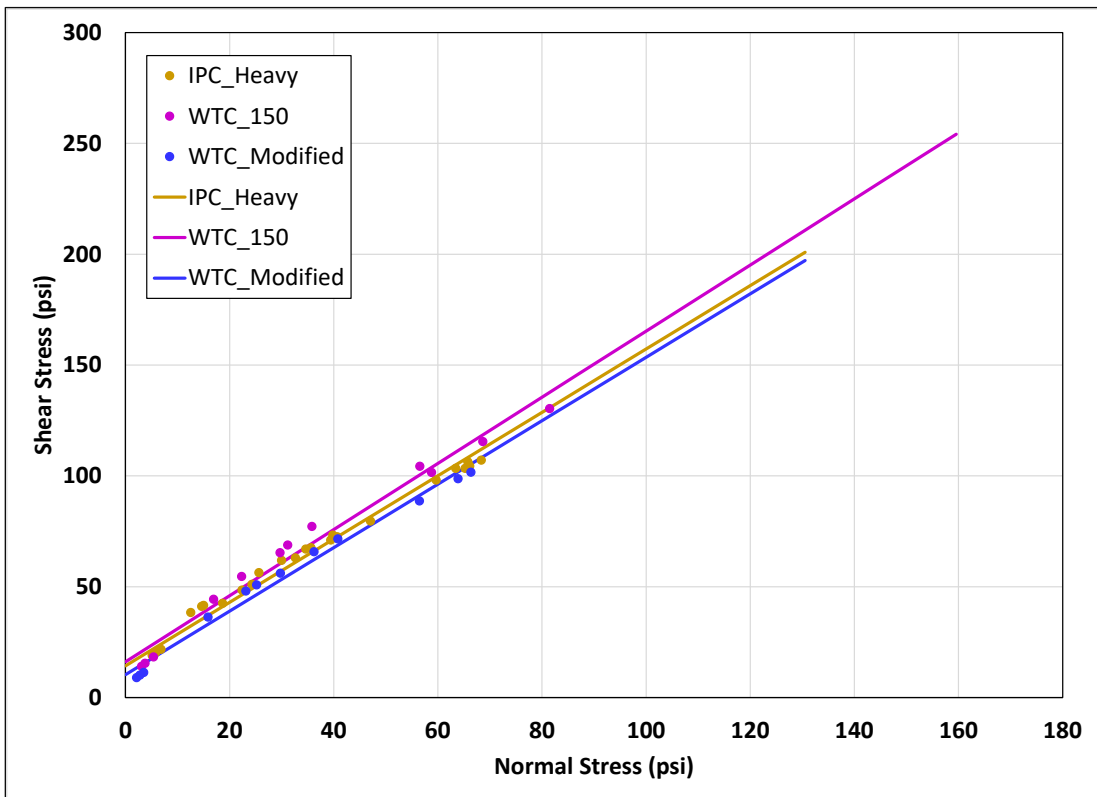


Figure 4.7: Linear regression to fit failure plane through stress and shear strength points.

The different Mohr-Coulomb diagrams using the results from each cell were developed and are shown in Figure 4.8. The results produced using the different triaxial cells were relatively consistent, with the conventional and modified Wirtgen cells producing envelopes that were essentially the same. The failure envelope determined using the original Wirtgen cell appears to be slightly more sensitive to confinement, which is likely a result of using the smaller diameter loading platen.

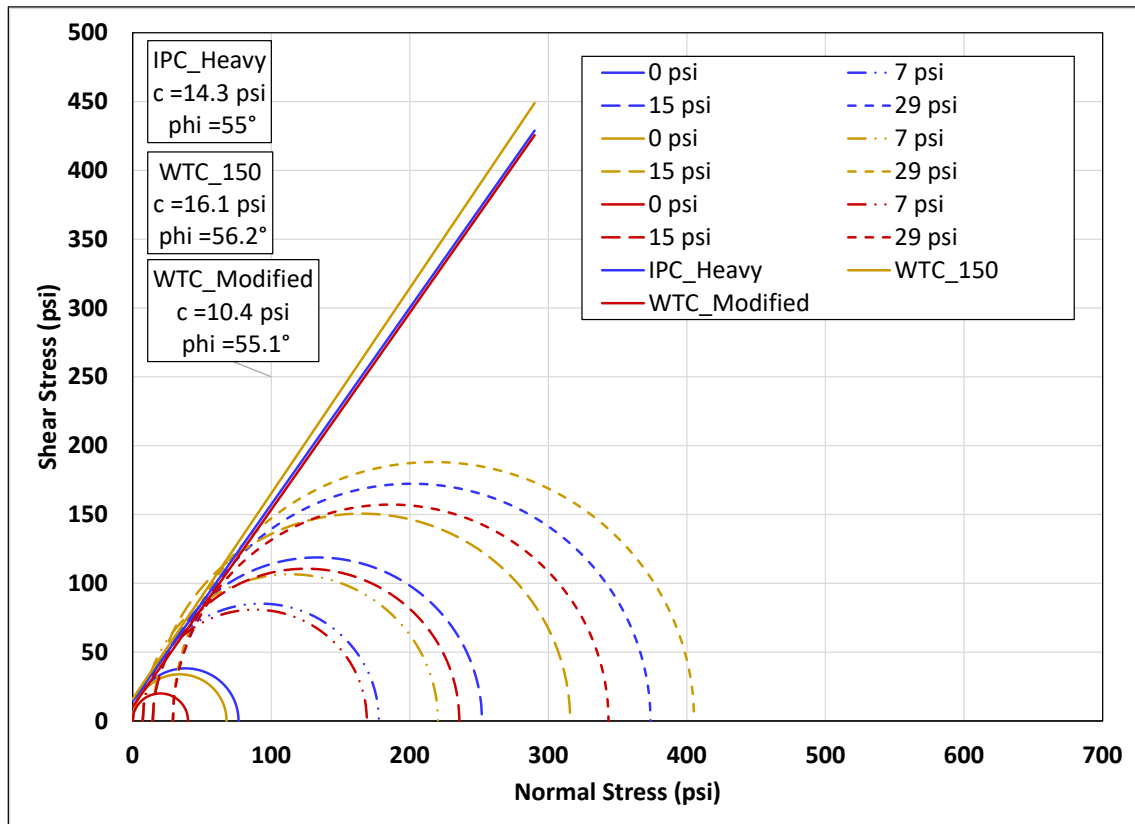


Figure 4.8: Mohr's diagram for the comparison tests between the three cells.

4.4.5 Discussion

The results were evaluated using analysis of variance (ANOVA) tests and regression analysis to determine if a significant difference exists between the results produced by the cells. The analysis considered the effects of cell type, confinement pressure, and the interaction between the cell and confinement pressure on the major principal stress and failure envelope.

Effect on Major Principal Stress

The ANOVA results are provided in Table 4.4. The results show a significant statistical difference in major principal stress for the different confinement stresses at a significance level of 0.05. There is no significant statistical difference for cell types or for the interaction between cell types and confinement stress. Since cell type and the interaction parameter were statistically insignificant, regression analysis was not necessary. The results indicate that, within the scope of this study and the variables considered in the analysis, the major principal stress is only significantly affected by the confinement pressure.

Table 4.4: ANOVA Results to Evaluate Effect of Cell Type on Major Principal Stress

Parameter	Degrees of Freedom	Sum Sq.	Mean Sq.	F Value	Pr(>F)
Confinement Pressure	1	7,090,314	7,090,314	106.505	4.84E-05
Cell	2	29,2751	146,376	2.1987	0.1922
Confinement Pressure:Cell	2	18,254	9,127	0.1371	0.8745
Residuals	6	399,436	66,573	—	—

Effect on Failure Envelope

The ANOVA results to compare the effect the of cell type, the normal stress, and the interaction between cell type and normal stress on the shear strength (Figure 4.7) are provided in Table 4.5. The results show that there is a significant difference in the mean shear strength results for different normal stresses and cell types at a significance level of 0.05, but there is no interaction between the normal stress and cell type. This indicates that the type of triaxial cell used in the study has an effect on the mean of the shear strength results. In order to determine which cell effect is significantly different, regression analysis was performed on Equation 4.6. The regression analysis results are provided in Table 4.6.

$$ShearStress = \beta_0 + \beta_1 * NormalStress + \beta_2 * TestSetup + \beta_2 * NormalStress * TestSetup \quad 4.6$$

Table 4.5: ANOVA Results to Evaluate Effect of Cell Type on Shear Stress

Parameter	Degrees of Freedom	Sum Sq.	Mean Sq.	F Value	Pr(>F)
Normal Stress	1	1.936	1.936	2,126.518	< 2.2e-16
TestSetup	2	0.017	0.008	9.291	0.001
Normal Stress:TestSetup	2	0.001	0.000	0.457	0.638
Residuals	30	0.027	0.001	—	—

Table 4.6: Regression Results for Equation 4.6

Parameter	Estimate	Std. Error	t value	Pr(> t)
β_0	0.099	0.016	6.296	<0.0001
β_1	1.429	0.060	23.861	< 2e-16
$\beta_2 \times \text{WTC}_{150}$	0.012	0.022	0.560	0.580
$\beta_2 \times \text{WTC}_{\text{Modified}}$	-0.027	0.022	-1.266	0.215
$\beta_3 \times \text{NormalStress:WTC}_{150}$	0.063	0.078	0.809	0.425
$\beta_3 \times \text{NormalStress:WTC}_{\text{Modified}}$	0.002	0.083	0.027	0.979

The results show that the coefficient for the normal stress is statistically significant at $p < 0.05$. However, neither the coefficients for the triaxial cell type (β_2) nor the interaction term (β_3) are statistically significant. This means that, even though the ANOVA show that triaxial cell type has an effect on the shear stress (i.e., that the means of the shear stress for the different cells are different), the regression analysis shows that the relationship between the predictor variables and the shear stress are not significantly varied. It can thus be shown that, for this study, based on the variables considered in the modeling, that the original Wirtgen cell, the modified Wirtgen cell, and the conventional cell all produce results that are not statistically significantly different.

4.5 Effect of Specimen Diameter

A small shear test factorial was included to compare the effect of specimen diameter on the shear strength when it was realized that the vibratory compaction hammer could not compact the cohesive materials in 6 in. diameter molds to Modified Proctor density. The vibratory hammer was able to compact the cohesive materials in 4 in. diameter molds to Modified Proctor density.

Material #28 was used for this comparison. This material classified as a Class 3 aggregate base, with an SE of 28 and R-value of 76. The shear strength results are provided in Figure 4.9. The results show that the 6 in. diameter specimens had a lower cohesion but higher friction angle, resulting in higher shear strengths at higher confinement pressures. The literature has shown that specimen diameter should not affect non-cohesive materials, and there was conflicting information specimen diameter had on cohesive materials.

Experience has shown that the vibratory hammer is not always able to compact cohesive materials in a 6 in. mold to Modified Proctor density. Since Tex 117-E uses different specimen diameters based on the material type, the decision was made to compact the cohesive materials

(Materials #28 to #32) in 4 in. molds. This is not an ideal solution for this study based on the comparison results and literature review for this study. This might be the motivation required to use 4 in. diameter specimens for future testing to reduce variables while working within the equipment limits.

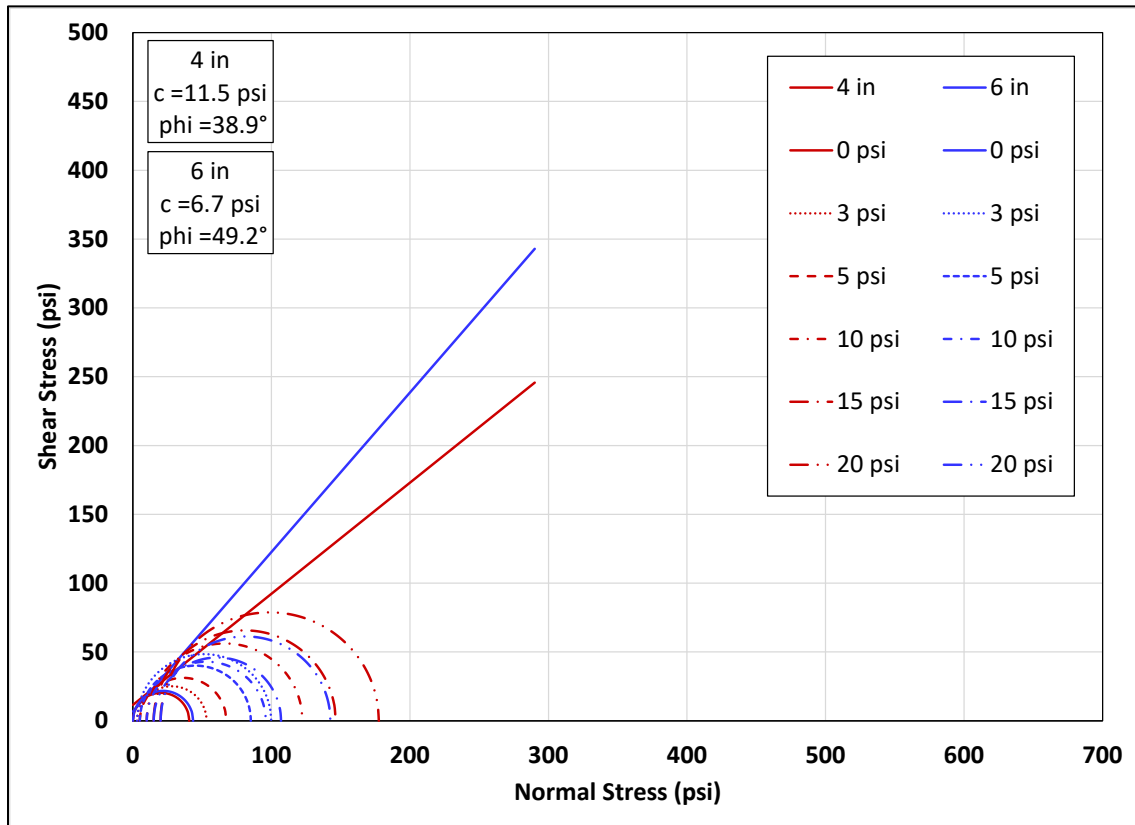


Figure 4.9: Effect of specimen diameter on failure envelope (red is 4 inch, blue is 6 inch).

4.6 Summary

This chapter provides details of the development and validation of the proposed CCS test. The following observations were made:

- The specimen size selected for the CCS test is 6 × 12 in., which can accommodate a maximum aggregate size of up to 1 in.
- The CT 216 relative compaction method resulted in a lower density measured when using the rod reading compared to the physical measurements of the compacted specimen, which resulted in test specimens that were not sufficiently compacted to survive handling after removal from the compaction mold.

- The minimum specified relative compaction required for aggregate base and aggregate subbase materials is 95% of CT 216. This is approximately 88% of Modified Proctor.
- The Modified Proctor method is recommended for determining the density and moisture content for specimen compaction for the CCS test.
- The simple triaxial cell provides similar shear strength results to the traditional triaxial cell.

5 CORRELATION OF CONFINED COMPRESSION AND R-VALUE TEST RESULTS

5.1 Introduction

The confined compression strength (CCS) and R-value test results that were used to correlate the two tests and develop benchmarks for the CCS test based on current R-value based specifications are provided in this chapter. The testing followed the plan discussed in Chapter 3.

5.2 Confined Compressive Strength Results

The compaction density results, compaction times, CCS results, and shear properties are discussed in this section. CCS testing of Material #7 could not be completed because insufficient material was available to prepare the required number of specimens.

Materials #24, #26, #27, and #33 were sampled as part of an effort to obtain materials for aggregate subbase materials.

5.2.1 Compaction Results

The CCS specimen compaction density results are summarized in Figure 5.1. The compaction times per lift for each material are summarized in Figure 5.2.

5.2.2 Strength Results

The CCS results, following the test plan in Section 3.1, are provided in Table 5.1 and include the friction angle and cohesion for each material. The peak stress is reported as measured during the CCS test. The cohesion and friction angle for each material were calculated based on the methodology described in Section 4.4.4.

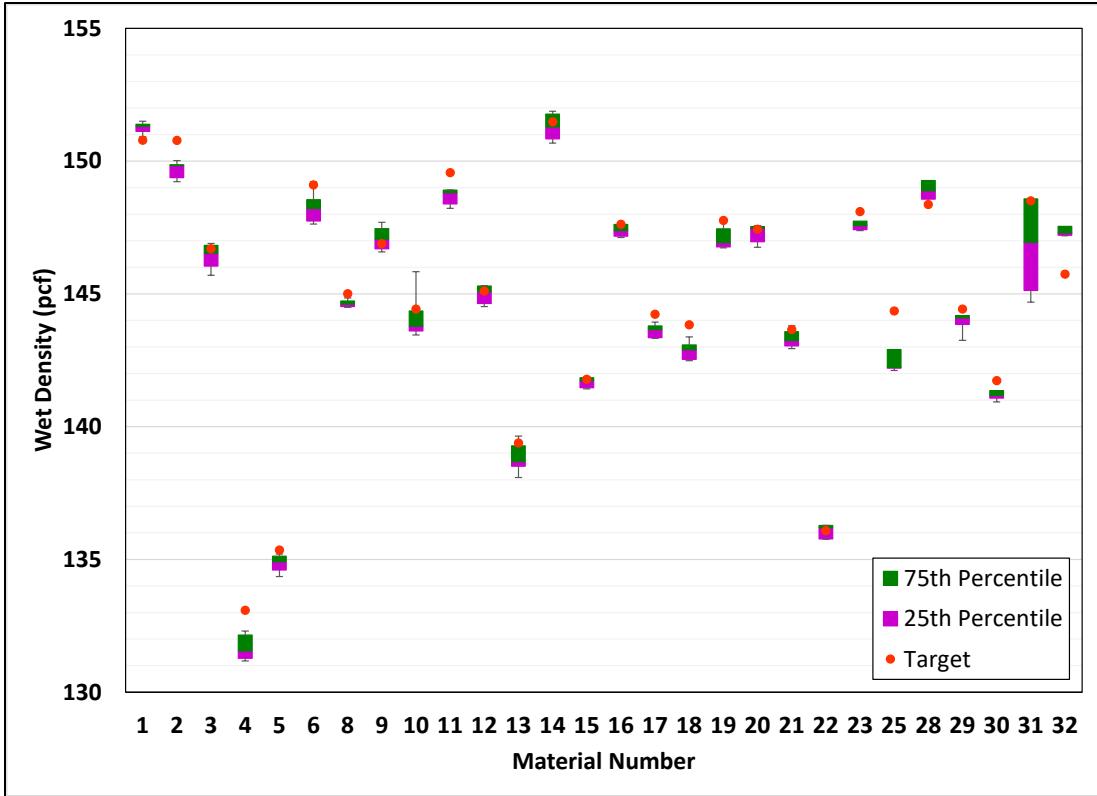


Figure 5.1: Box and whisker plot of wet densities versus target wet density.

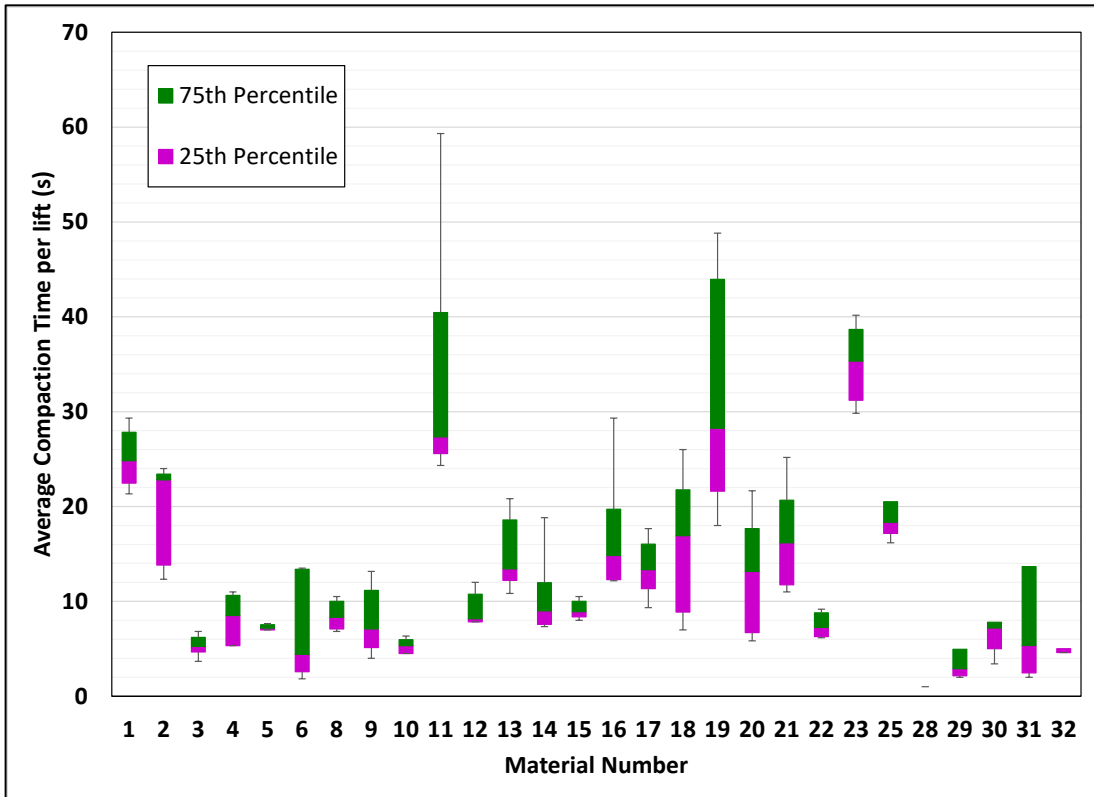


Figure 5.2: Average compaction time per lift (six lifts per specimen).

Table 5.1: Confined Compressive Strength Peak Stress and Shear Properties

Material Number	Material Type	Confinement Pressure (psi)						Cohesion (psi)	Friction Angle (°)
		0	3	5	10	15	20		
1	AB2	43.4	80.6	136.3	190.3	237.6	262.5	9.3	55.7
2	ASB2	93.7	110.2	158.7	182.7	233.4	253.3	16.9	50.9
3	AB2	31.2	87.6	101.1	168.2	226.7	266.7	6.3	57.3
4	AB2	21.1	93.7	124.8	173.4	229.7	248.5	9.3	54.2
5	AB2	34.4	100.1	134.9	186.9	241.1	262.9	10.3	55.1
6	AB2	14.7	57.8	102.4	146.5	176.1	224.8	4.6	55.0
7	AB2	Not Tested							
8	AB2	32.0	88.8	126.1	156.9	215.2	258.5	7.3	56.2
9	AB2	28.3	71.7	109.7	174.1	215.8	265.3	5.8	57.4
10	AB2	12.1	59.7	106.3	144.7	197.5	254.1	3.6	57.4
11	AB2	33.3	87.9	116.9	149.2	209.2	240.0	8.0	54.7
12	AB2	31.4	85.1	101.1	175.5	202.2	234.0	7.8	54.4
13	AB2	43.1	86.4	123.9	171.5	182.6	227.5	12.3	49.3
14	AB2	25.8	76.5	129.3	185.0	226.5	269.4	6.4	57.6
15	AB2	35.3	84.1	121.1	162.3	211.4	243.2	8.2	55.0
16	AB2	35.3	87.4	109.6	186.7	232.8	278.5	6.8	57.8
17	AB2	37.3	71.9	92.8	135.3	185.4	202.1	9.1	50.2
18	AB2	19.5	56.5	100.1	134.4	213.2	253.7	3.6	57.4
19	AB2	80.2	104.5	137.6	185.5	222.3	247.4	14.9	51.9
20	AB2	37.6	97.3	113.7	144.3	171.8	231.6	9.1	52.5
21	AB2	46.4	87.0	135.1	194.5	215.4	266.1	9.8	55.1
22	AB2	53.4	89.8	107.9	167.3	198.2	232.9	10.3	52.9
23	AB2	78.6	127.6	140.3	177.6	207.9	258.9	15.3	52.0
24	N/A	Not Tested							
25	ASB3	64.7	112.9	127.1	201.0	237.7	240.1	13.1	53.0
26	N/A	Not Tested							
27	N/A	Not Tested							
28	AB3	43.5	96.8	80.1	85.9	91.9	122.5	11.5	38.9
29	ASB3	58.7	84.1	85.2	98.8	122.9	142.6	14.1	41.1
30	ASB3	138.4	126.3	153.3	186.8	207.6	222.0	25.7	45.7
31	ASB3	123.8	164.9	171.0	200.8	208.1	241.8	29.7	43.3
32	ASB3	113.8	134.2	135.1	147.7	148.8	152.4	36.4	26.7
33	N/A	Not Tested							

5.3 Tex 117-E Material Classification

The shear testing results were used to classify the materials from this study according to the Texas triaxial classes in Tex 117-E. The Tex 117-E triaxial classes are based on materials with a

slenderness ratio of 1.5 and the specimen diameters, which depend on the material type. The specimens in this study had a slenderness ratio of 2.0, and the specimen diameters depended on the material types, with 6 in. diameters for AB materials and 4 in. diameters for fine grained materials. The failure envelopes of the tested materials are plotted on the Texas triaxial class figure (Figure 5.3). Table 5.2 provides the Texas triaxial classes for the individual materials, and Figure 5.4 shows the relationship between the R-value and Texas triaxial classes for the tested materials. Seven of the materials classified as Class 1, seventeen classified as Class 2, and four classified as Class 3.

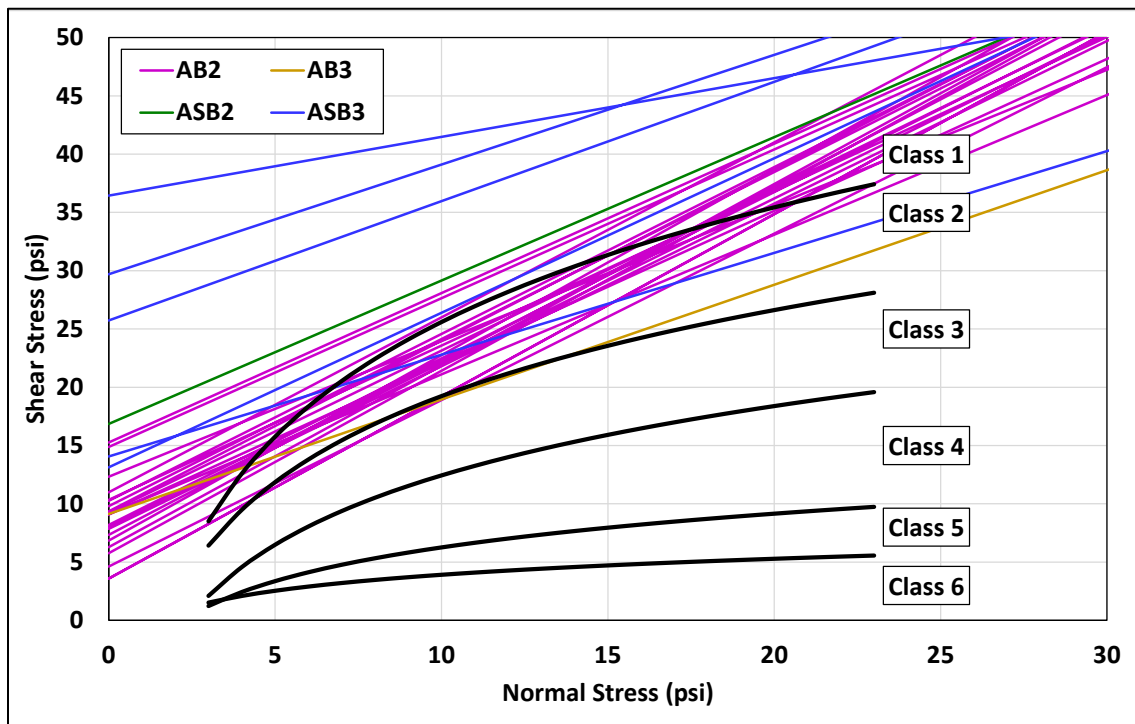


Figure 5.3: Failure envelopes results on Texas triaxial classification plot.

Table 5.2: Material Type and Texas Triaxial Class Classification

Material Number	Material Type	Texas Triaxial Class	Material Number	Material Type	Texas Triaxial Class
1	AB2	2.2	16	AB2	2.5
2	ASB2	1.0	17	AB2	2.7
3	AB2	2.7	18	AB2	3.1
4	AB2	2.4	19	AB2	1.0
5	AB2	2.1	20	AB2	2.5
6	AB2	3.1	21	AB2	2.2
8	AB2	2.5	22	AB2	2.3
9	AB2	2.7	23	AB2	1.0
10	AB2	3.1	25	ASB3	1.0
11	AB2	2.6	28	AB3	3.0
12	AB2	2.6	29	ASB3	2.5
13	AB2	2.2	30	ASB3	1.0
14	AB2	2.6	31	ASB3	1.0
15	AB2	2.5	32	ASB3	1.0

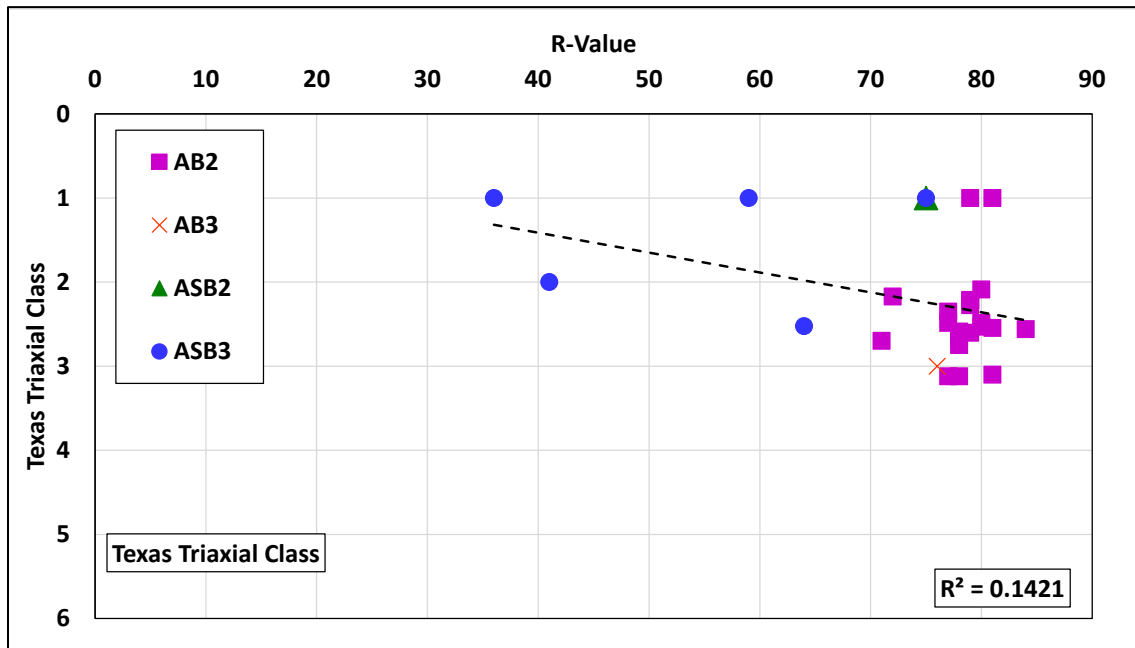
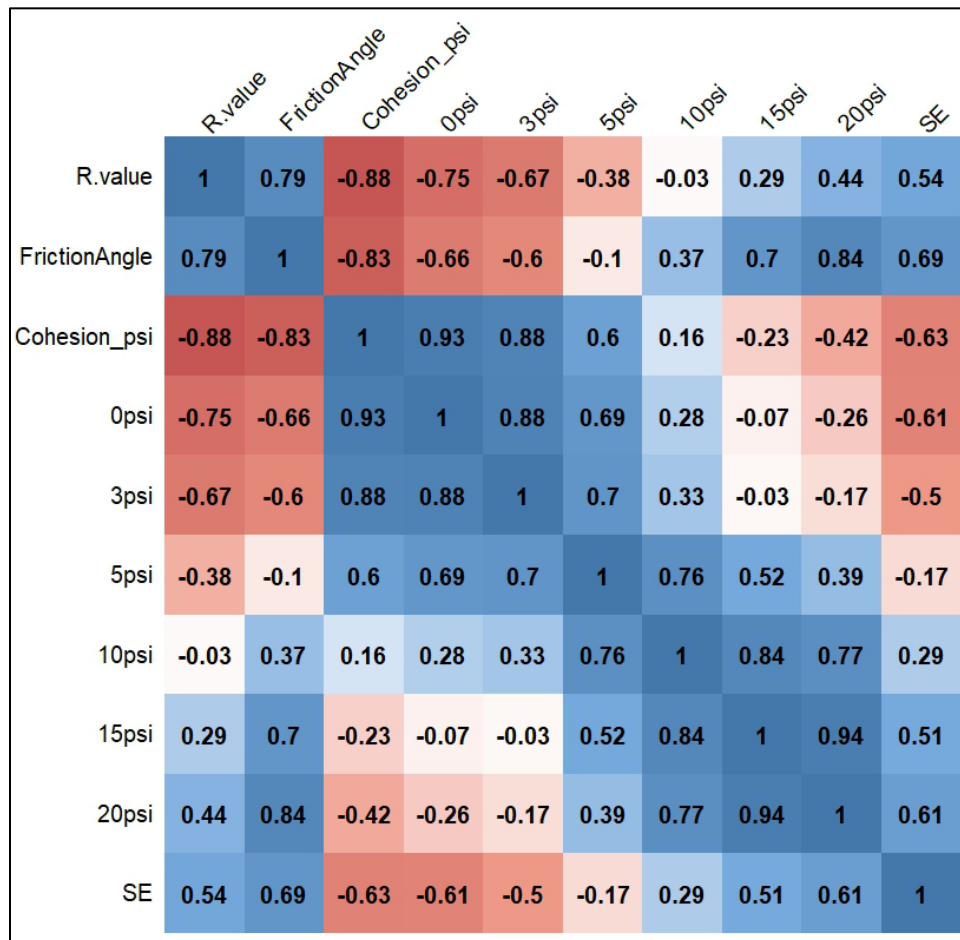


Figure 5.4: Texas Triaxial class classification.

5.4 Correlation Results

A correlation plot of the results from the study is provided in Figure 5.5. The correlation plot shows that the R-value has the highest coefficient of determination with cohesion and friction

angle and that it is poorly correlated with the individual CCS results. The correlation plot further shows that the correlation between the R-value and CCS results changes from a negative correlation at low confinements to a positive correlation at high confinements. This is due to the stress sensitivity of the materials. Aggregate base is more stress sensitive and has lower cohesion, meaning it will have low strength at low confinements but higher strengths at high confinement pressures. The cohesive subbase materials have higher strengths compared to the aggregate base materials at low confinements and lower strengths compared to the aggregate base materials at high confinements. The sand equivalent results had similar correlation results with the shear testing results and the R-value correlations.



Note: The psi refers to CCS strength at the confining stress shown.

Figure 5.5: Correlation matrix plot of study results.

5.4.1 Relationship Between R-Value and CCS

The relationship between the R-value and the different CCS results at each confinement pressure, are provided in Figure 5.6 through Figure 5.11. The relationship between the R-value and cohesion and between the R-value and friction angle are plotted in Figure 5.12 and Figure 5.13, respectively. Linear regression analyses were performed to determine the coefficient of determination between the R-value and CCS or shear parameters (cohesion and friction angle). Similar to the correlation plot in Figure 5.5, the results in Figure 5.6 through Figure 5.11 show that CCS decreases with increasing R-value at low confinements and, inversely, that CCS increases with an increase in the material R-value at high confinement.

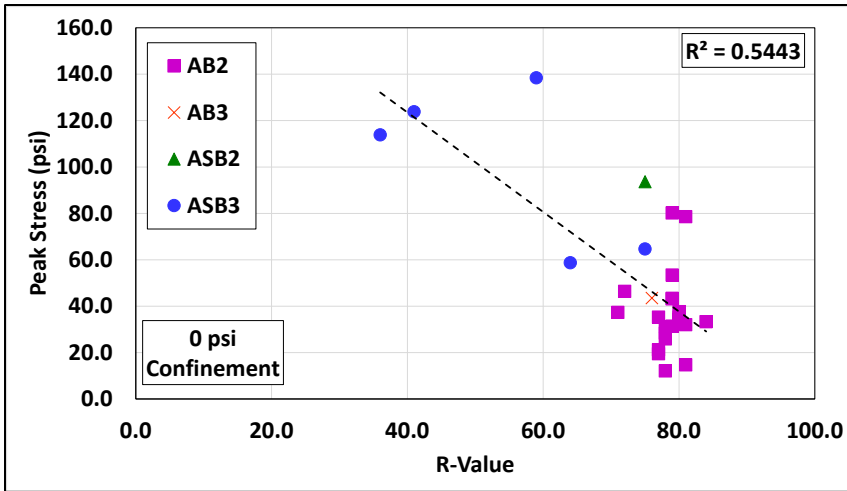


Figure 5.6: Relationship between R-value and peak stress (strength) at 0 psi confinement.

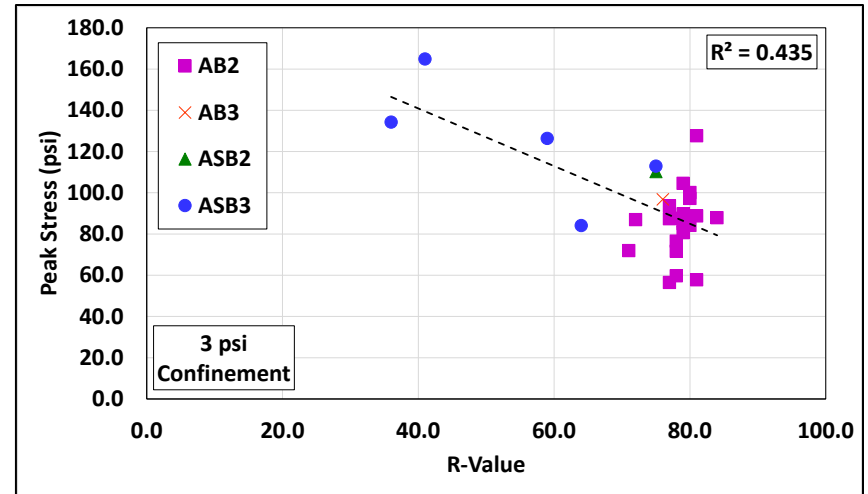


Figure 5.7: Relationship between R-value and peak stress (strength) at 3 psi confinement.

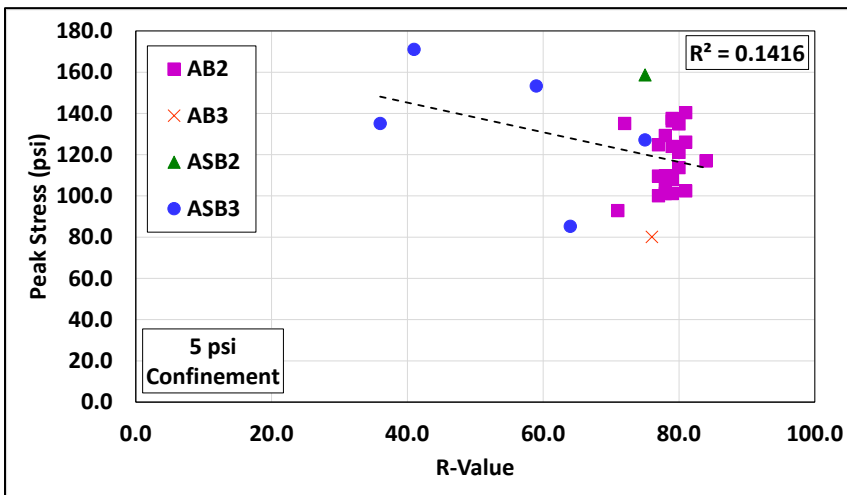


Figure 5.8: Relationship between R-value and peak stress (strength) at 5 psi confinement.

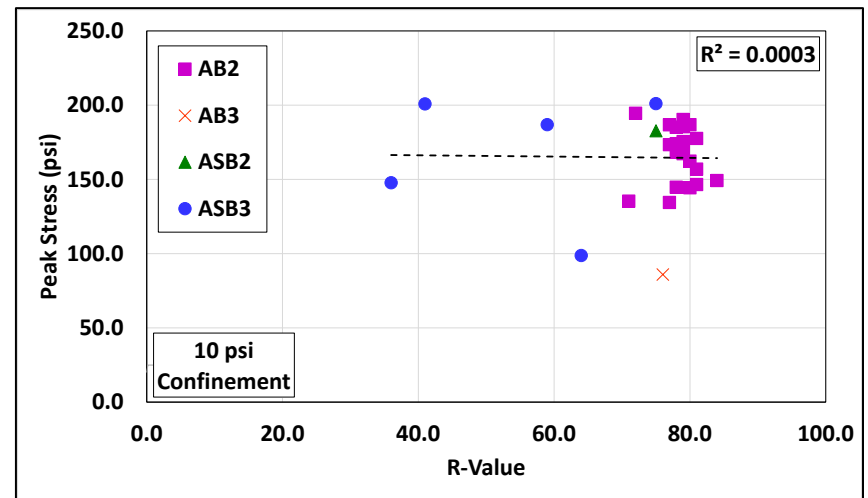


Figure 5.9: Relationship between R-value and peak stress (strength) at 10 psi confinement.

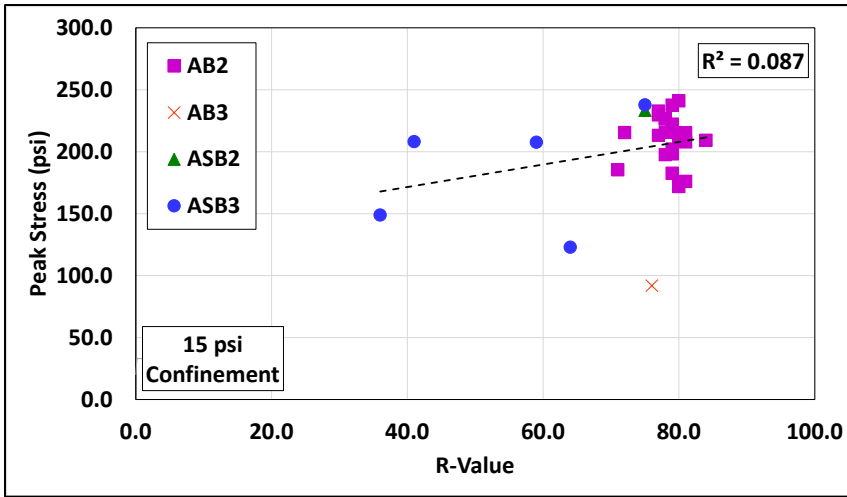


Figure 5.10: Relationship between R-value and peak stress (strength) at 15 psi confinement.

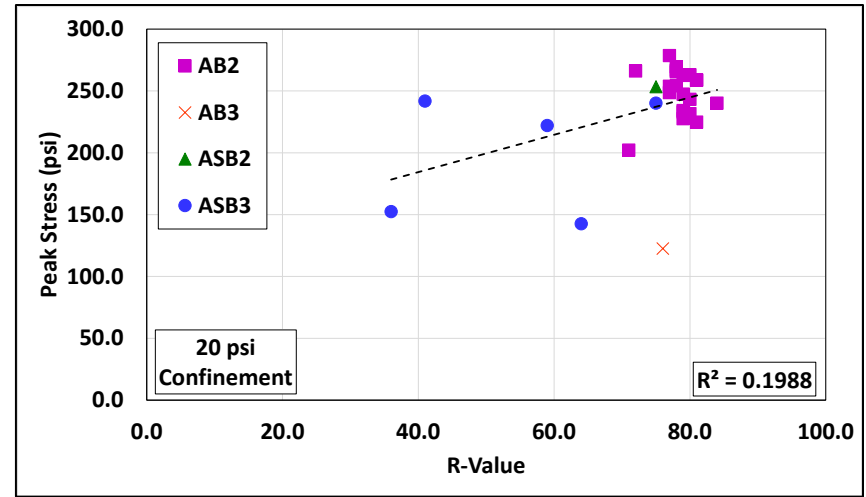


Figure 5.11: Relationship between R-value and peak stress (strength) at 20 psi confinement.

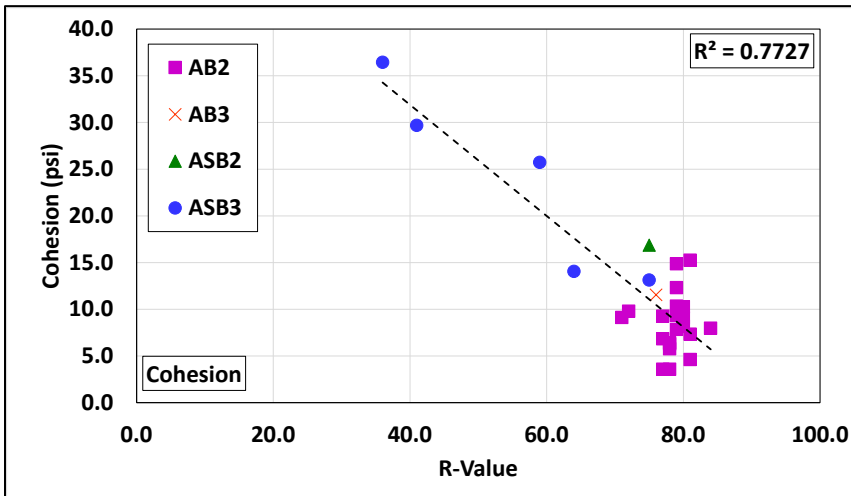


Figure 5.12: Relationship between R-value and cohesion.

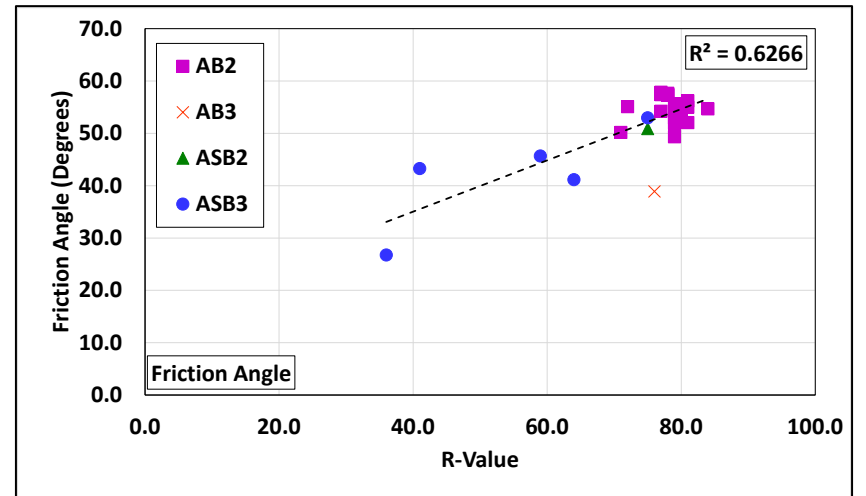


Figure 5.13: Relationship between R-value and friction angle.

5.5 Discussion

5.5.1 R-Value Correlation

The CCS results of the Class 2 aggregate base materials, with R-values between 71 and 84, correlated poorly with the R-value. These findings are supported by the results from Roland (5), where the Texas triaxial Class 1 and 2 materials could not explain the change in the R-value of the material, especially for aggregate base materials with R-values between 75 and 85. The correlation between the R-value and CCS improved slightly with the inclusion of subbase materials, but it is weak. However, the low correlation coefficients, variability in the R-value test results, and the difference in the material response to confinement pressure are significant hurdles to recommending a minimum CCS value at a confinement pressure to replace the R-value test.

The poor correlation between the R-value and the CCS results can be attributed to the following:

- Difference in R-value testing conditions.
- Reported high variability in R-value results.

The shear parameters correlated well with the R-value. However, for a specification to require minimum friction angle or cohesion, multiple shear tests at different confinement pressures are required to calculate the shear parameters. Conducting these multiple shear tests was outside of the scope of the report, but it has been included as alternative option.

Test Condition

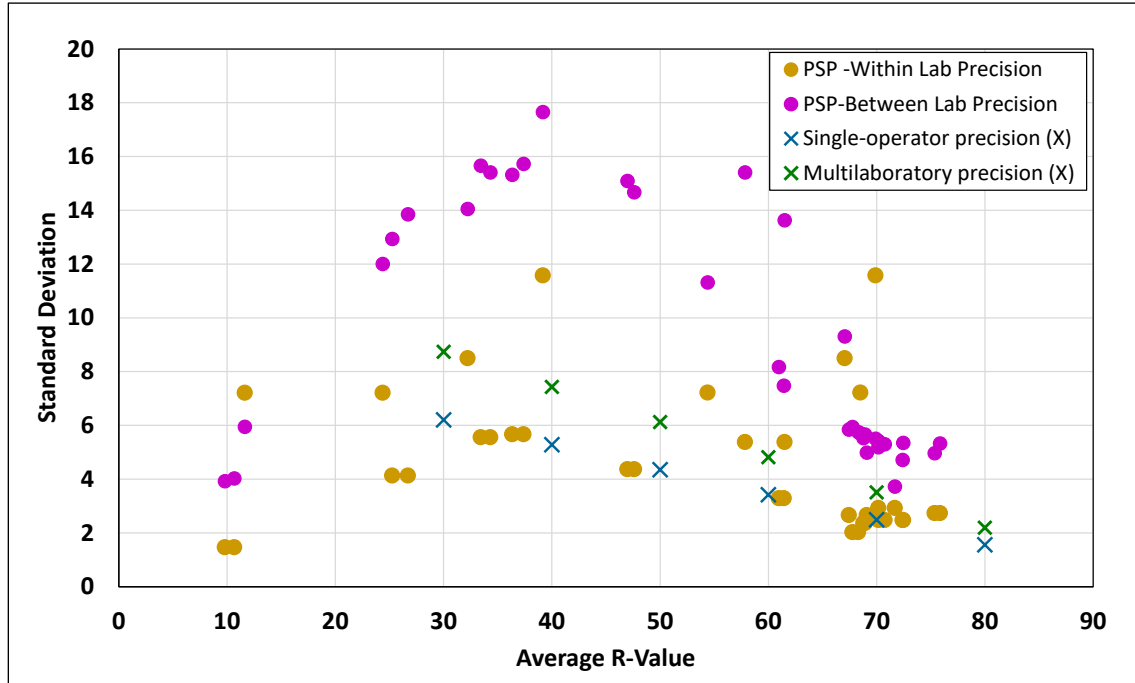
The following two primary differences in testing conditions between the R-value and CCS test are relevant to the interpretation of the results:

- The R-value test is performed on specimens with different moisture contents to determine the R-value at an exudation pressure of 300 psi. The CCS test is performed on material that is at the optimum moisture content and maximum wet density.
- The R-value test is a low strain test that does not fail the specimen, whereas the CCS test takes the material to failure.

Reported R-Value Variability

The literature review provided several sources with R-value variability results. The largest set of data was extracted from the AASHTO re:source database of R-value PSP results. The results from

the Benson and Aimes study (3) are also relevant. Figure 5.14 shows the within-laboratory and between-laboratory standard deviation, reported by the aforementioned sources, over the typical range of R-values for aggregate materials.



Note: Reported in AASHTO (2) and Benson and Ames (3).

Figure 5.14: Standard deviation results for R-value tests results previously reported.

The within-laboratory/single-operator precision reported by the two sources shows some agreement. The between-laboratory, also called the multi-laboratory precision, shows a higher degree of difference. Using the results from the Benson and Aimes results (3), which are based on California materials, the 95% prediction intervals can be determined assuming a large population size. This provides an estimate of the range of values that would contain a single observation based on the standard deviation and the assumed sample size. The prediction interval range, based on the standard deviation results reported by Benson and Aimes, is provided in Figure 5.15. The results show that the test precision decreases for materials with lower R-values.

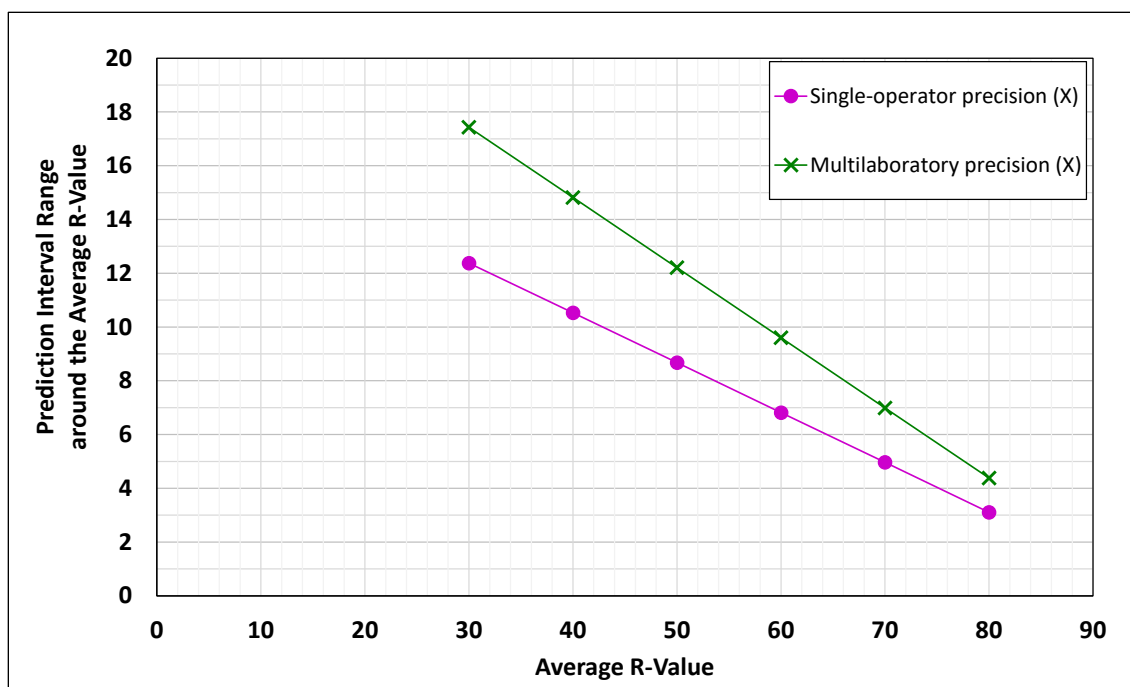


Figure 5.15: Prediction interval range of average California R-value results.

Table 5.3 provides the minimum and maximum average R-value materials that could pass the minimum R-value specification for different classes of material, based on the 95% prediction interval using the conservative test precision results from Benson and Aimes (3). The results show that a Class 2 aggregate base material that has historically produced an average R-value of 80.9 based on single-operator variance could have a minimum R-value of 78. Conversely, a material with an historical average of 73.7 could also have an R-value of 78. These results emphasize the range of materials that can feasibly pass the minimum R-value specifications, the risk of failing a high quality material, and the risk of passing a low quality material. As noted in the literature review, variability increases as R-value decreases, which implies that the range of non-passing materials that might be accepted could increase for subbase materials.

Table 5.3: Passable Minimum and Maximum Average R-Value Materials

Material	Class	Min. Specified R-Value	Single-Operator		Multi-Laboratory	
			Max. Avg. R-Value	Min. Avg. R-Value	Max. Avg. R-Value	Min. Avg. R-Value
Aggregate Subbase	1	60	65.8	51.6	67.6	47.0
Aggregate Subbase	2	50	57.3	39.4	59.7	33.5
Aggregate Subbase	3	40	48.9	27.1	51.8	19.9
Aggregate Base	2	78	80.9	73.7	81.9	71.4

5.5.2 Confined Compressive Strength Test Precision

No test precision results for the CCS test were identified during the literature review, and the scope of the project did not include developing these test precision results. The number of specimens at each confinement pressure is not sufficient for determining the standard deviation of the test. Therefore, at this time, test precision cannot be provided for the CCS test.

5.5.3 Recycled Aggregate Base Observations

The recycled aggregate base materials tested in this study could contain reclaimed asphalt concrete and/or cement concrete. The presence of these crushed materials could result in recementation in aggregate bases, but this was not observed in any of the compacted specimens at the time of testing.

5.5.4 Potential Confined Compressive Strength Test Criteria

The proposed test for an R-value replacement test is a simple CCS test at a predetermined confinement pressure. It is logical that a test should have a positive correlation with the R-value such that minimum strength values can be recommended to distinguish between different materials. This would lead to selecting a confinement pressure of either 15 or 20 psi. A lower confinement can be recommended, such as 0 psi or 3 psi, but low confining pressure does not engage the aggregate friction of an aggregate material that will perform well in the field and therefore also have a positive correlation with the R-value. At confining pressures below 15 psi, the materials with more fines and more plasticity (ASB2, ASB3, AB3) showed better peak stress (strength) values than the materials with fewer fines and less plasticity (AB2), largely due to cohesion because friction was not engaged, and had a negative correlation between the R-value and CCS. It is therefore not possible to recommend a minimum CCS value for different material groups for CCS tests run with less than 15 psi confining pressure. Additional parameters would be required to distinguish between material groups.

Using the linear regression results from the 15 psi and 20 psi confinement tests, as well as the friction angle results, a summary of the materials that pass and fail and R-value and CCS requirements is shown in Table 5.4, Table 5.5, and Table 5.6. The test outcome difference in Table 5.4, Table 5.5, and Table 5.6 is defined as the percentage of specimens that did not meet

the minimum R-value but passed the minimum CCS results. The test errors are similar between the 15 psi and 20 psi confinement results.

Table 5.4: CCS Test Criteria Using 15 psi Results

15 psi Confinement Results	AB2	AB3	ASB2	ASB3
Min R-value	78	50	50	40
Fitted CCS (psi)	206	181	181	171
Number of samples	21	1	1	5
Fail min CCS	7	1	0	2
Pass min CCS	14	0	1	3
Pass R-value, Pass min CCS	10	0	1	3
Pass R-value, Fails min CCS	6	1	0	1
Fails R-value, Pass min CCS	4	0	0	0
Fails R-value, Fails min CCS	1	0	0	1
Test outcome difference (%)	40	0	0	0

Table 5.5: CCS Test Criteria Using 20 psi Results

20 psi Confinement Results	AB2	AB3	ASB2	ASB3
Min R-value	78	50	50	40
Fitted CCS (psi)	242	199	199	184
Number of samples	21	1	1	5
Fail min CCS	7	1	0	2
Pass min CCS	14	0	1	3
Pass R-value, Pass min CCS	10	0	1	3
Pass R-value, Fails min CCS	6	1	0	1
Fails R-value, Pass min CCS	4	0	0	0
Fails R-value, Fails min CCS	1	0	0	1
Test outcome difference (%)	40	0	0	0

Table 5.6: Friction Angle Test Criteria Using Multiple Confinement Pressures

Friction Angle Results	AB2	AB3	ASB2	ASB3
Min R-value	78	50	50	40
Fitted friction angle (degrees)	54	40	40	35
Number of samples	21	1	1	5
Fail min friction angle	6	1	0	1
Pass min friction angle	15	0	1	4
Pass R-value, Pass min friction angle	11	0	1	4
Pass R-value, Fails min friction angle	5	1	0	0
Fails R-value, Pass min friction angle	4	0	0	0
Fails R-value, Fails min friction angle	1	0	0	1
Test outcome difference (%)	36.4	0	0	0

The criteria developed for the CCS test will need to be calibrated for use in mechanistic design. A correlation will be required to estimate the stiffness from the CCS results.

- Preliminary CCS criteria are suggested based on the relationship between the R-value and CCS and the R-value and friction angle. The recommended values are provided in Table 5.7 for the different confinement pressures and material types.

Table 5.7: Recommended Preliminary CCS Specification Values

Parameter	Material				
	AB2	AB3	ASB1	ASB2	ASB3
Min. R-value	78	50	60	50	40
Min. CCS at 15 psi confinement (psi)	206	181	190	181	171
Min. CCS at 20 psi confinement (psi)	242	199	215	199	184
Min. friction angle (degrees)	54	40	45	40	35

5.6 Summary

The chapter provides the test results and data analysis comparing the R-value and CCS for the materials included in this study. The results show the following:

- The R-value test has a low test precision, which could result in lower quality material passing the minimum specification, while higher quality material could fail the minimum specification.
- The test precision of the CCS test has not been published in the literature and could not be developed during this study given the limited scope of testing.

- Preliminary recommendations for CCS test specification minimum values were proposed for 15 psi and 20 psi confining stress. Either confining stress can be used in a specification.
- Additional preliminary recommendations for CCS test specifications values were proposed for friction angle of the material based on shear testing using multiple confinement pressures.

6 CONCLUSIONS AND RECOMMENDATIONS

This technical memorandum summarizes a study that investigated the use of a confined compressive strength test to replace the R-value test currently used for some pavement design and for quality control/quality assurance in California. The report covers a literature review, development of an alternative test, and a comparison of the results from the proposed test with R-value results. Testing was limited to aggregate base and subbase materials. The new test method is based on a current Texas Department of Transportation test. However, the specimen preparation and test methods were updated based on the work done in this study.

The literature review found that the R-value test has relatively low precision and that this precision increases as the R-value increases. However, there is still a substantial risk of failing high quality aggregate base and subbase materials and a higher risk of passing low quality materials. The development of a confined compressive strength (CCS) test is discussed, including the validation of a simplified confinement cell. Comparing the R-value to CCS for the materials tested to date showed that there is a poor correlation between the tests, which was attributed in large part the known poor precision of the R-value test, and the difference in test conditions between the two tests.

6.1 Conclusions

The following conclusions are made based on the findings:

- California Test 216 needs revision. The compaction density reported by the test method is lower than the density determined by measuring the dimensions of the compacted specimen in the CT 216 apparatus. The reported CT 216 density is approximately 88% of Modified Proctor density.
- The proposed specimen compaction procedure, using Modified Proctor as the reference density, produced unbound specimens that could be handled and tested in a triaxial cell.
- A confining stress of 15 or 20 psi should be used. Confining stresses less than 15 psi showed negative correlations between the R-value and CCS values for materials with finer gradations and more plasticity.
- The suggested preliminary CCS criteria for replacement of the R-value specification were presented in Table 5.7.
- It must be emphasized that the CCS test, as a replacement for the R-value test, will require additional calibration with the resilient modulus before it can be used in mechanistic design.

6.2 Recommendations

The following interim recommendations are made based on the testing discussed in this report, the documented low test precision of the R-value test, and the limitations of developing a correlation between the R-value and the CCS test using the set of materials considered in this study:

- Material properties, including gradation, flakiness, crushed faces, sand equivalence, Atterberg limits, and moisture sensitivity (i.e., shape of the optimum moisture content curve) should be considered when analyzing any correlations.
- Friction angle can be used as a criterion to replace the R-value, but shear testing is required using multiple confinement pressures to calculate the shear properties.
- The CCS test can be moved forward for specifying aggregate base and subbase materials. The suggested preliminary CCS criteria should be updated once additional testing is completed.

REFERENCES

1. Hveem, F.N. and Carmany, R.M. 1948. "The Factors Underlying the Rational Design of Pavements." In *Proceedings of the Twenty-Eighth Annual Meeting of the Highway Research Board*. Washington, DC, December 7-10, 1948. <https://onlinepubs.trb.org/Onlinepubs/hrbproceedings/28/28-011.pdf>
2. AASHTO. n.d. "View Sample Round Analysis." AASHTO re:source. Accessed October 26, 2023. <http://aashtoresource.org/psp/sample-round-analysis>.
3. Benson, P.E. and Ames, W.H. 1975. "Test Precision of Selected Aggregate Test Methods." *Transportation Research Record*, no. 539: 85–93. <https://onlinepubs.trb.org/Onlinepubs/trr/1975/539/539-009.pdf>.
4. Miller, S.M. 2009. *Developing Statistical Correlations of Soil Properties with R-value for Idaho Pavement Design* (Final Report No. N08-11). Moscow, ID: National Institute for Advanced Transportation Technology. <https://apps.itd.idaho.gov/apps/research/Completed/RP185.pdf>.
5. Roland, H.L. 1963. *Texas Triaxial R Value Correlation* (Research Project 61-1S). Baton Rouge, LA: Louisiana Department of Transportation. https://www3.ltrc.lsu.edu/pdf/2006/old_reports/Report%20008.pdf.
6. Jones, D. and Harvey, J. 2005. *Relationship Between DCP, Stiffness, Shear Strength and R-value* (Technical Memorandum: UCPRC-TM-2005-12). Davis and Berkeley, CA: University of California Pavement Research Center. <https://escholarship.org/uc/item/3cg854dc>.
7. Van Til, C.J., McCullough, B.F., Vallerga, B.A., and Hicks, R.G. 1972, *Evaluation of AASHTO Interim Guides for Design of Pavement Structures* (National Cooperative Highway Research Council Report No. 128: Washington, D.C: Highway Research Board. https://onlinepubs.trb.org/Onlinepubs/nchrp/nchrp_rpt_128.pdf.
8. Huang, Y.H. 1993. *Pavement Analysis and Design*, New York, NY: Prentice Hall Inc.
9. Fragomeni, C.L. and Hedayat, A. 2020. *Construction and Design Soil Property Correlation* (CDOT-2020-10). Denver CO: Colorado Department of Transportation..
10. Lea, J.D., Wu, R., and Harvey, J.T. 2023. "Meta-Analysis of Soil Property Relationships and Construction Platform Design." *Transportation Research Record* 2677, no. 3: 1230–1244.
11. Porter, O.J. 1950. "Development of the Original Method for Highway Design." *Transactions of the American Society of Civil Engineers* 115, no. 1: 461-467.
12. Wirtgen Group. Wirtgen Cold Recycling Technology. 2012. Windhagen, Germany: Wirtgen Group.
13. Groeger, J.L., Rada, G.R., and Lopez, A. 2003. "AASHTO T 307 — Background and Discussion." In *Resilient Modulus Testing for Pavement Components*, edited by Durham, G., DeGroff, W.L., and Marr, A., 16–29. West Conshohocken, PA: ASTM International.

14. Moores, E.R. and Hoover, J.M. 1966. "The Influence of Slenderness Ratios on Triaxial Shear Testing." *Proceedings of the Iowa Academy of Science* 73, no. 1: 285–292.
15. Hoffman, P. 2019. "Triaxial Testing's 1/6th Rule: Particle-Continuum Analysis of Granular Stability During Compression." *E3S Web of Conferences* 92: 1–6. https://www.e3s-conferences.org/articles/e3sconf/pdf/2019/18/e3sconf_isg2019_15009.pdf.
16. Skuodis, Š., Dirgėlienė, N. and Lekstutytė, I., 2019. "Change of Soil Mechanical Properties Due to Triaxial Sample Size. In *Modern Building Materials, Structures, and Techniques*, edited by Juozapaitis, A., Daniūnas, A., and Juknevičius, L. Vilnius, Lithuania, May 16–17, 2019. <https://webu3.vgtu.lt/uni/stf/mbmst/MBMST2019proceedings.pdf>.
17. Monteiro, F.F., de Carvalho, L.M.C., Moura, A.S., de Aguiar, M.F.P., Marques, I.R., and de Matos, Y.M.P., 2016. "Specimen Diameter Influence on Effective Shear Strength Parameters in Triaxial Tests." *Electronic Journal of Geotechnical Engineering* 21: 4049–4060.
18. Omar, T. and Sadrekarimi, A., 2015. "Effect of Triaxial Specimen Size on Engineering Design and Analysis." *International Journal of Geo-Engineering* 6: 1–17.
19. Zarei, C., Soltani-Jigheh, H., and Liu, Y., 2023. "Effects of Strain Rate and Specimen Size on the Behavior of Fine-Grained Soils." *Arabian Journal of Geosciences* 16, no. 4: 244.
20. Jones, D., and Louw, S. 2022. Cold Central Plant Recycling Study: Test Track Construction, Layout, and Instrumentation (Technical Memorandum: UCPRC-TM-2020-05). Davis and Berkeley, CA. <https://doi.org/10.7922/G28G8J25>.
21. Weissman, S.L. and Sackman, J.L. 1997. *The Mechanics of Permanent Deformation in Asphalt-Aggregate Mixtures: A Guide to Laboratory Test Selection*. Berkeley and Davis, CA University of California Pavement Research Center.
22. Harvey, J., Du Plessis, L., Long, F., Shatnawi, S., Scheffy, C., Tsai, B.W., Guada, I., Hung, D., Coetzee, N., Riemer, M., and Monismith, C.L. 1996. *Initial CAL/APT Program: Site Information, Test Pavement Construction, Pavement Materials Characterizations, Initial CAL/APT Test Results, and Performance Estimates*. Davis and Berkeley, CA: University of California Pavement Research Center. <https://escholarship.org/uc/item/8419b23v>.

APPENDIX A MATERIAL PROPERTIES

This appendix includes the material property test results provided by the material suppliers. The properties provided include gradation (Figures A.1 to A.4) and sand equivalence (SE), durability (Los Angeles abrasion), and optimum moisture content (OMC) (Table A.1). The materials are grouped by the suppliers' indicated material classification:

- Figure A.1 – Class 2 aggregate base materials
- Figure A.2 – Class 1 aggregate subbase materials
- Figure A.3 – Class 2 aggregate subbase materials
- Figure A.4 – Class 3 aggregate subbase materials
- Figure A.5 – P209 aggregate

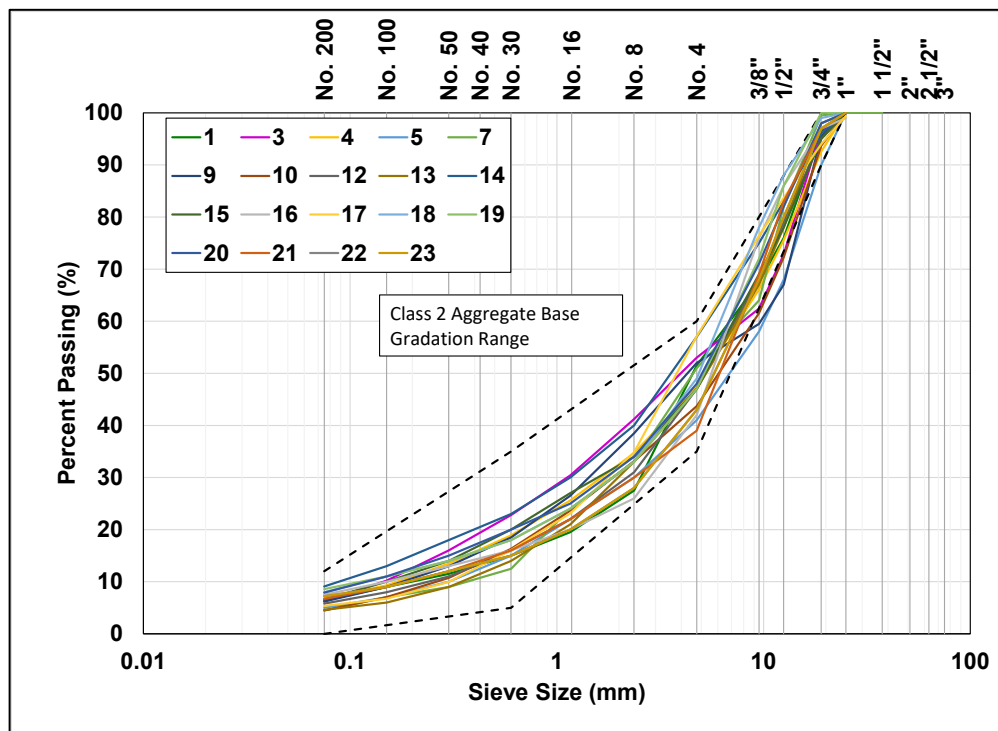


Figure A.1: Class 2 aggregate base material gradations for supplied materials.

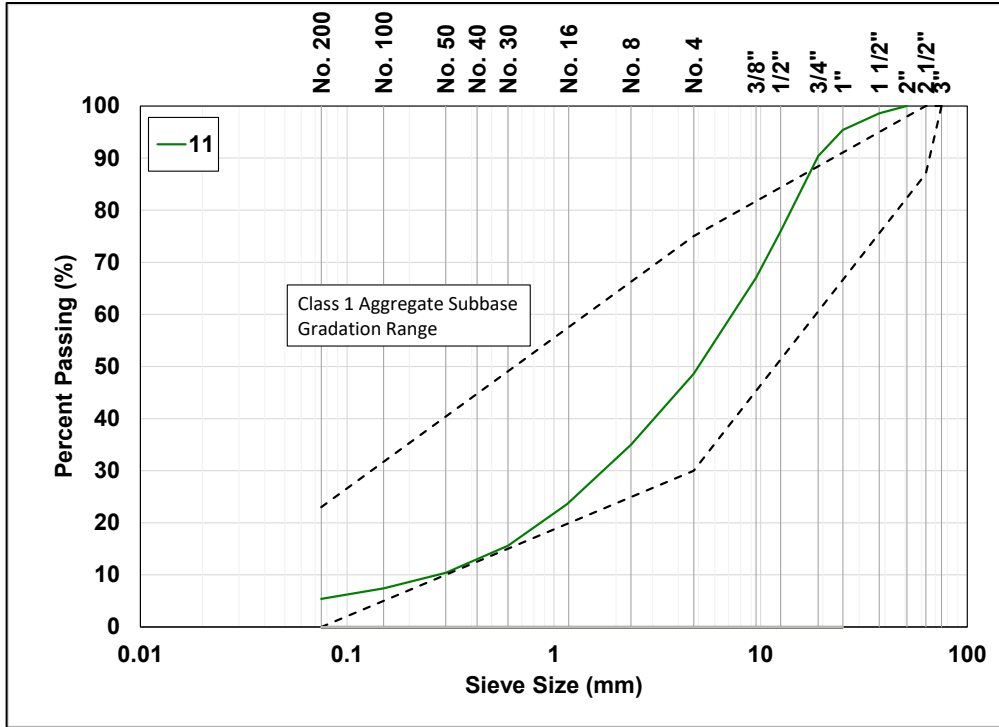


Figure A.2: Class 1 aggregate subbase material gradations for supplied materials.

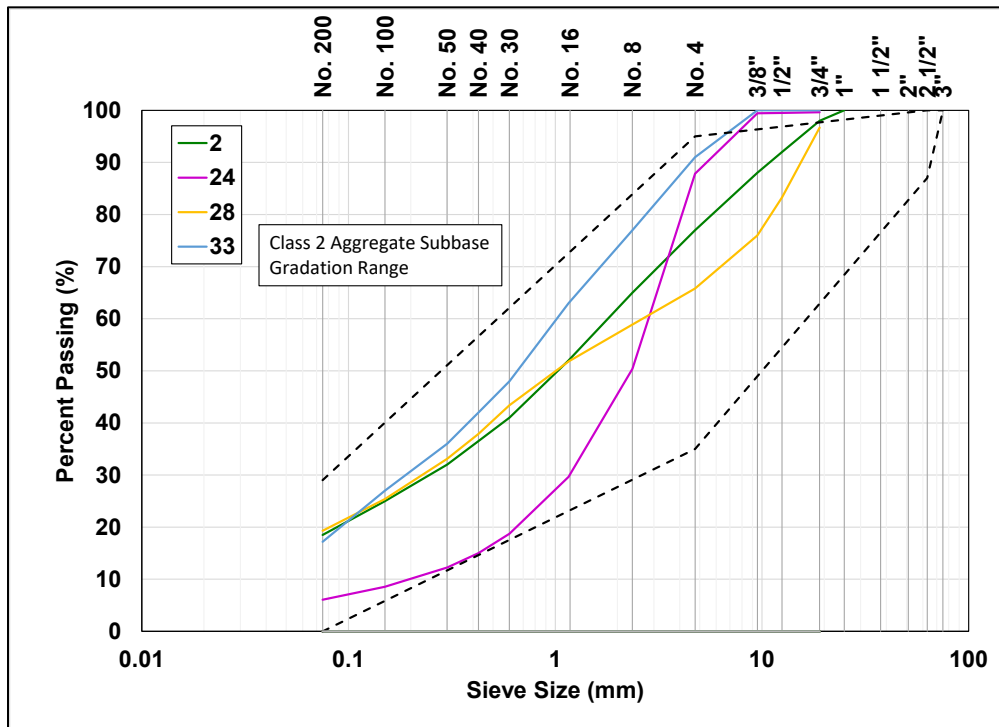


Figure A.3: Class 2 aggregate subbase material gradations for supplied materials.

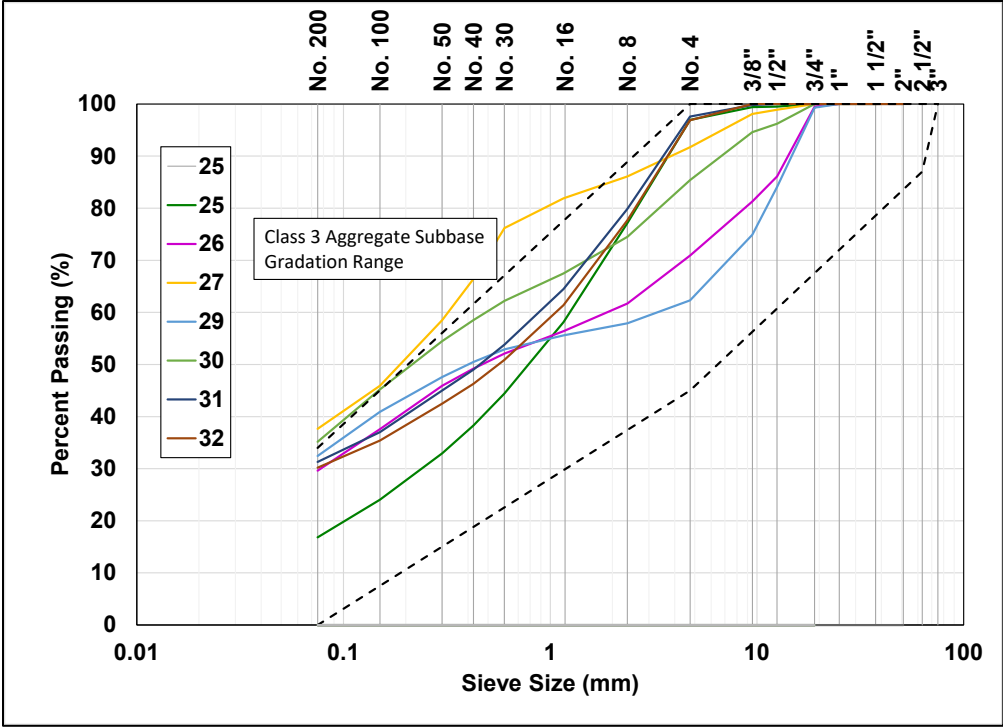


Figure A.4: Class 3 aggregate subbase material gradations for supplied materials.

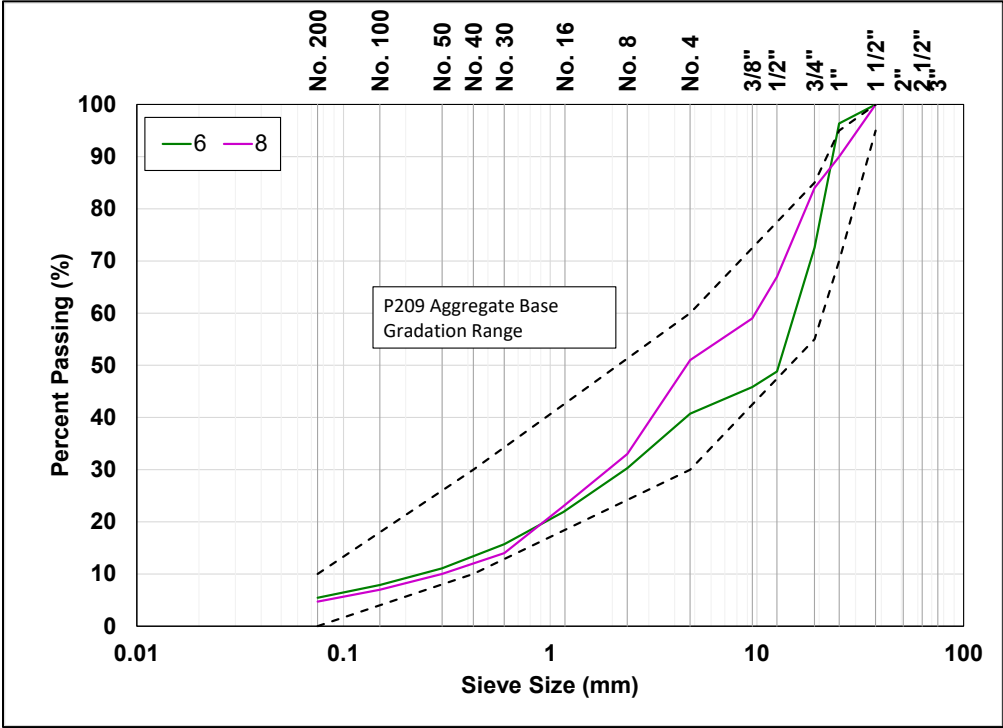



Figure A.5: P209 material gradations for supplied materials.

Table A.1: Sand Equivalence, Durability, and OMC for Supplied Materials

Material		Durability (CT 229)		SE (CT 217)	OMC
#	Supplier's Material Identification	Coarse	Fine	%	%
1	Aromas - Wilson 3/4 Virgin Class 2 Base	79.3	66	59	N/A
2	Aromas - 3/4 Class 2 Agg Subbase	49	45	38	N/A
3	Vulcan Palmdale CAB/AB	N/A	N/A	73	N/A
4	Vulcan Anaheim Class 2	N/A	N/A	N/A	N/A
5	Vulcan San Bernardino Recycled Base	N/A	N/A	52	N/A
6	Vulcan Reliance Stone P209	N/A	N/A	51	N/A
7	Vulcan Chula Vista CAB/AB	N/A	N/A	63	N/A
8	Vulcan Chula Vista P209	N/A	N/A	40	N/A
9	Vulcan Reliance Stone 3/4 CAB	N/A	N/A	53.5	N/A
10	Vulcan San Bernardino CAB	N/A	N/A	60.6	N/A
11	Graniterock SFO Grindings Recycle Class I ASB	N/A	N/A	56.8	N/A
12	Teichert Vernalis Virgin Class II AB	N/A	42	31	4.3
13	Teichert Vernalis Recycled Class II AB	N/A	N/A	37	4.9
14	Teichert Perkins Virgin Class II AB	N/A	73	54	1.5
15	Teichert Perkins Recycled Class II AB	N/A	47	47	6.3
16	Teichert Graniteline Virgin Class II AB	N/A	N/A	69	5.1
17	Teichert Woodland Virgin Class II AB (2019)	N/A	40	31	N/A
18	Teichert Woodland Virgin Class II AB (2023)	86	70	32	5.1
19	Teichert Bear River Virgin Class II AB	61	39	26	0.7
20	Teichert Spanish Springs Virgin Class II AB	78	47	36	8.5
21	Teichert Western Aggregate Marysville Virgin Class II AB	N/A	67	54	N/A
22	Teichert Martis Virgin Class II AB	65	38	61	N/A
23	George Reed Jackson Valley Class II AB	N/A	61	29	N/A
24	Teichert Perkins 1/4" x Dust (Washed)	N/A	N/A	100	N/A
25	Teichert Perkins 1/4" x Dust (Unwashed)	N/A	N/A	91	N/A
26	Teichert Perkins 50/50 AB/Soil Blend	N/A	N/A	28	N/A
27	Teichert Perkins Soil	N/A	N/A	14	N/A
28	Blend 1A-Concrete Control with 38% Soil (15% #200)	N/A	N/A	28	N/A
29	Blend 2B-Concrete Agg with 67% Soil (25% #200)	N/A	N/A	15	N/A
30	Blend 5A-Perkins AB with 70% Soil (30% #200)	N/A	N/A	18	N/A
31	Blend 8A - Unwashed 1/4" x Dust + Clay + 2% Bentonite	N/A	N/A	22	N/A
32	Blend 8B - Unwashed 1/4" x Dust + Clay + 5% Bentonite	N/A	N/A	21	N/A
33	Tracy Clark 3/8" Select AB Fill	N/A	N/A	28	N/A

APPENDIX B STANDARD OPERATING PROCEDURE FOR CCS TEST

UCPRC Standard Operating Procedure, Safety, and Training Orientation Standard Method Test for Standard Practice for CCS Testing		
Overview	Name:	
Responsible person: Heather Tom & Miriam Brichta & Jeffrey Buscheck		
Location and Designated Area		
Room 126		
If in doubt, ask your supervisor.		
Procedure Orientation		
I have reviewed and understood the attached performance checklist.		
Make sure all samples and containers are properly labeled.		
Equipment		
For Fabrication: <ul style="list-style-type: none"> • Scale • 3/4" sieve • Compactor (hammer capable of achieving a compaction height with 6" circular compactor head) • Cylindrical mold capable of molding 12 in. long specimens • Mold collar • 5/8" diameter tamping rod • Interlayer roughening device (Tool with steel spikes capable of breaking up the soil's surface) • Extruder • Airtight containers capable of holding 35 lb. of material • Pans capable of holding 7 lb. of material without loss • Scoop (non-absorbent) • Caliper accurate to 0.01 mm with a minimum jaw length of 3.5 in. capable of measuring a 12 in. length • Plastic wrap For Testing: <ul style="list-style-type: none"> • Loading device equipped with 10 kip load cell capable of maintaining a loading rate of 2% strain/min • Compressed air regulator that can regulate air between 3 to 20 psi to the nearest 1 psi, fitted with push to connect fittings • Triaxial cell with a tubular rubber membrane fitted with a push to connect fitting including flat, metal top and bottom 6 in platens • LVDT capable of measuring 25 mm of displacement accurate to at least 0.025 mm 		
Follow all safety guidelines and warning labels on the equipment.		
All Water used in this procedure is to be distilled or deionized water.		
Pre-Procedure – Equipment Maintenance Check		
Check the maintenance and calibration records of all equipment. Do not use if it is out of date.		
Report all issues or concerns to the laboratory manager.		
Determine the optimum moisture content and maximum dry density according to ASTM D1557 method C.		

Fabrication Procedure	
Calculate the mass required to compact a 6 in. x 12 in. specimen at maximum dry density.	
Prepare enough material passing the 3/4" sieve required to fabricate 6 specimens and reduce the sample into 6 portions.	
Weigh mixture into 6 equal portions and place into an airtight container.	
Pour the material into the mold and distribute it evenly. Rod the material 15 times.	
Lower the compactor onto the surface of the material. Compact each lift to a 50 mm height.	
Scour the surface between lifts with the interlayer roughening device to help layers adhere to each other.	
Repeat compaction procedure until all lifts have been compacted. Do not scour the final lift. (Suction may develop between the compactor head and the specimen. Carefully twist the compactor head to break the seal to avoid damage to the specimen. It may also be necessary to break up suction by testing the mold.)	
Extrude the specimen. Use a jack press or other suitable device to break the suction between the mold and specimen sides.	
Measure the specimen. Record 6 diameter measurements at third points of the specimen at 90 degree increments. Record 4 height measurements at 90 degree increments.	
Immediately wrap the specimen in plastic wrap or enclose it in a membrane to prevent moisture loss.	
Repeat until 6 specimens have been produced.	
Allow the specimens to sit undisturbed at 77°F for 24 hours.	
Procedure for Confined Compressive Strength Test	
Remove the specimen from the plastic wrap or membrane and record the mass to the nearest 0.1 g.	
Place the specimen in the center of the triaxial cell bottom platen.	
Place the top platen on the specimen and center it.	
Place the tubular membrane around the specimen and assemble the external shell.	
Place the assembled triaxial cell beneath the loading frame and center the top platen with the load shaft.	
Zero the load cell.	
Carefully apply a contact load of about 20 lb. (100 N) to the top platen.	
Attach and zero the deformation measuring device.	
Attach the air line with the pressure regulator to the air inlet of the rubber membrane.	
Apply the desired confinement stress. Allow the pressure to stabilize. (The confinement pressures selected for the R-value study were 0, 3, 5, 10, 15, and 20 psi.)	
Apply a strain rate of 2% strain/min. Record the displacement and load every 0.2 in. Stop the test once 6% strain is reached or when the load starts decreasing.	
Record the peak load and confinement pressure.	
Unload the specimen and disassemble the triaxial cell.	
Break up the specimen and determine the moisture content according to AASHTO T 265.	
Post-Procedure	
Verify that all necessary data were acquired. Make notes when the procedure was adjusted for certain samples.	
Make sure the area is clean and all tools are returned to their respective location.	
Ensure all necessary data are reported.	
Safety Notes	
Follow all current UCPRC safety procedures.	

When sampling or testing in the field, always yield to construction traffic.			
Wear thick nitrile gloves to keep hands dry and to protect from sharp aggregate.			
Sit or stand straight to prevent back injury.			
Personal Protective Equipment			
Always wear required PPE including safety eyewear, nitrile gloves, long pants, sturdy shoes, oven gloves.			
PPE is available at the following: common use in the lab cabinet of room 126 and some workstations. Individual use, at the request of a lab supervisor and in personal lockers.			
Hazardous Materials and Disposal			
This test method may include the following hazardous materials:			
<ul style="list-style-type: none"> • Silica dust and organic materials 			
This test method may include the following physical hazards:			
<ul style="list-style-type: none"> • Hot ovens or materials • Sharp objects • Falling objects 			
Place all reusable oil rags (gray or blue) and reusable general rags (Wipeall, white from rolls) into the designated bins for washing/reuse.			
How to dispose: Dispose of waste soil in the appropriate soil waste containers. Dispose of all wash water down the drain.			
Potential Accidents or Near Misses			
Best practices to avoid accidents and near misses:			
<ul style="list-style-type: none"> • Wear heat-resistant gloves when working with ovens. • Be aware of equipment placement (do not place equipment near edges or on uneven surfaces). 			
Hard copies of the SDS sheets are located in the main laboratory file cabinet, Room 126.			
There are 3 eyewashes and 2 showers available on the north and south ends of the building, and main lab Room 126.			
If ever in doubt regarding an accident, dial 911 for emergency services.			
First aid kits are available near most fire extinguishers and a large supply in the PPE Cabinet in the main lab Room 126.			
SOP Refresher Date			
This SOP must be renewed every 3 years, or when updated by the lab, whichever is less.			
Lab Supervisor	Date	Lab Operator	Date

APPENDIX C DENSITY RESULTS

This appendix includes the Modified Proctor and CT 216 density results for the materials tested in this study.

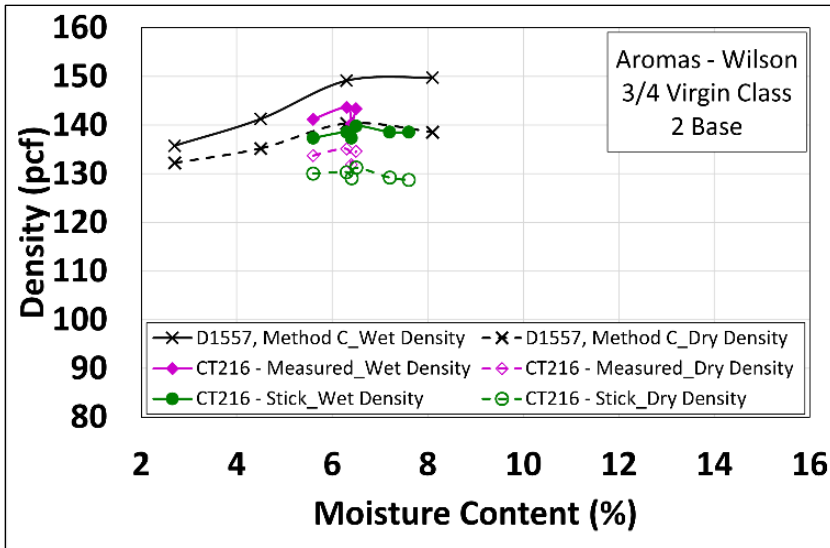


Figure C.1: Density results for Material #1.

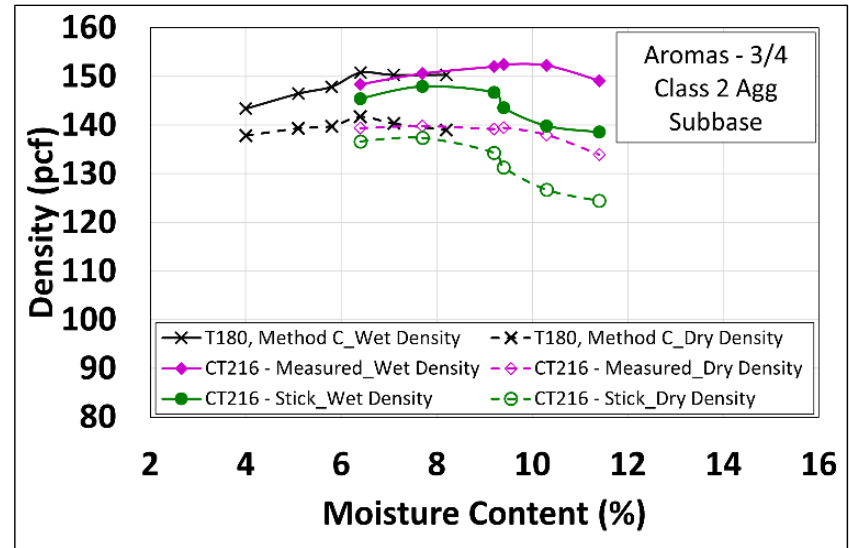


Figure C.2: Density results for Material #2.

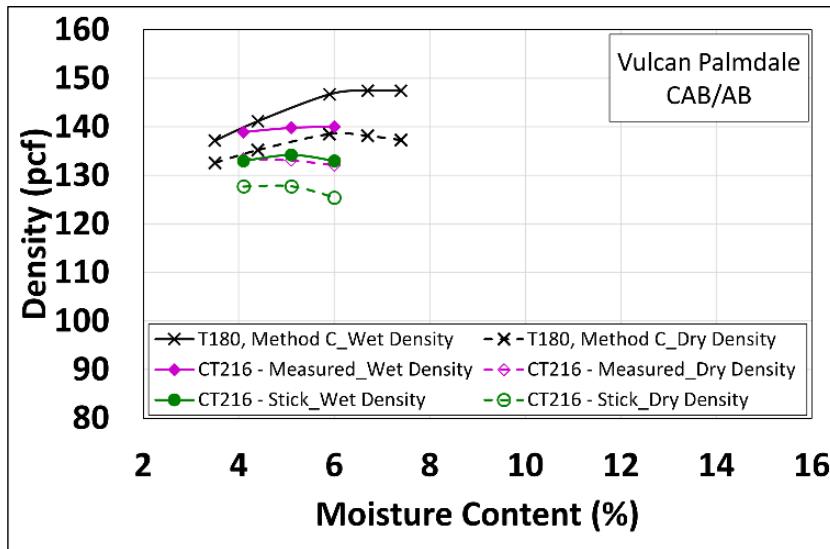


Figure C.3: Density results for Material #3.

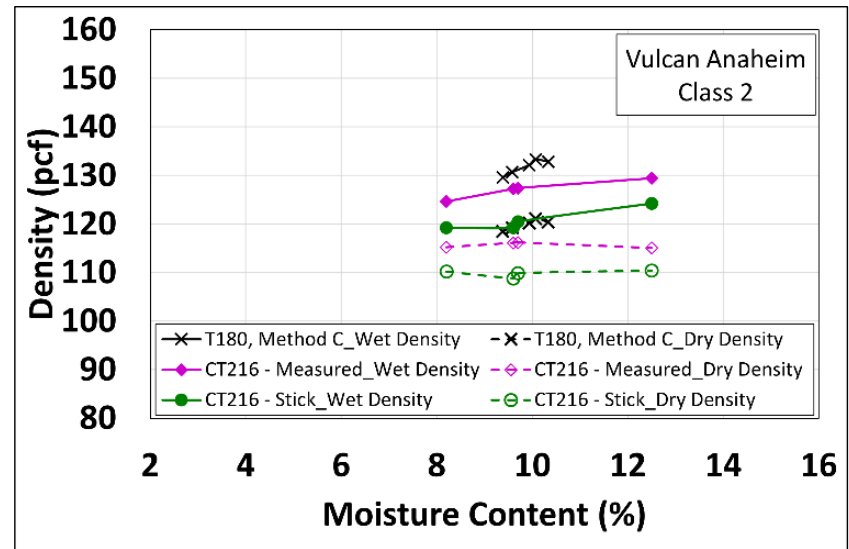


Figure C.4: Density results for Material #4.

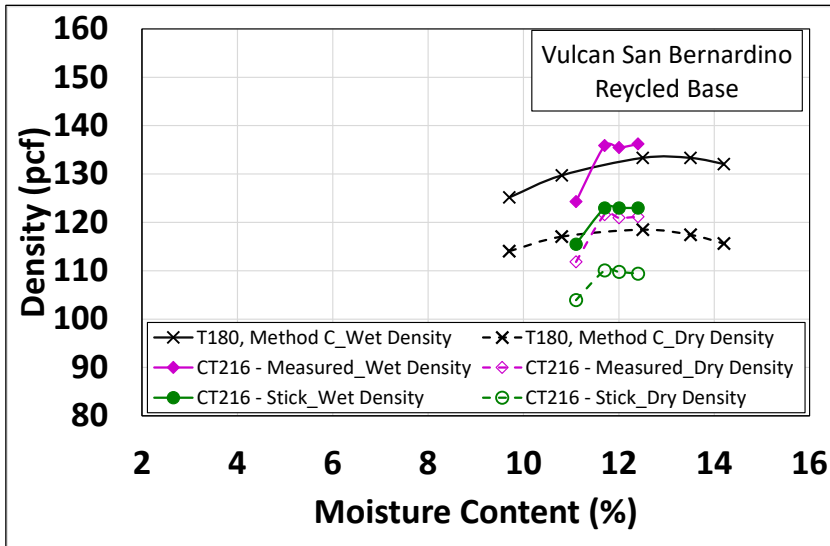


Figure C.5: Density results for Material #5.

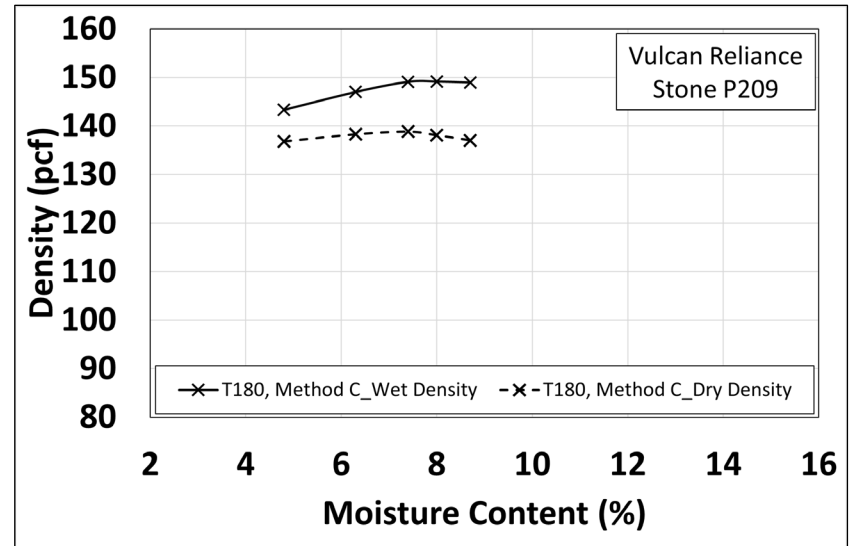


Figure C.6: Density results for Material #6.

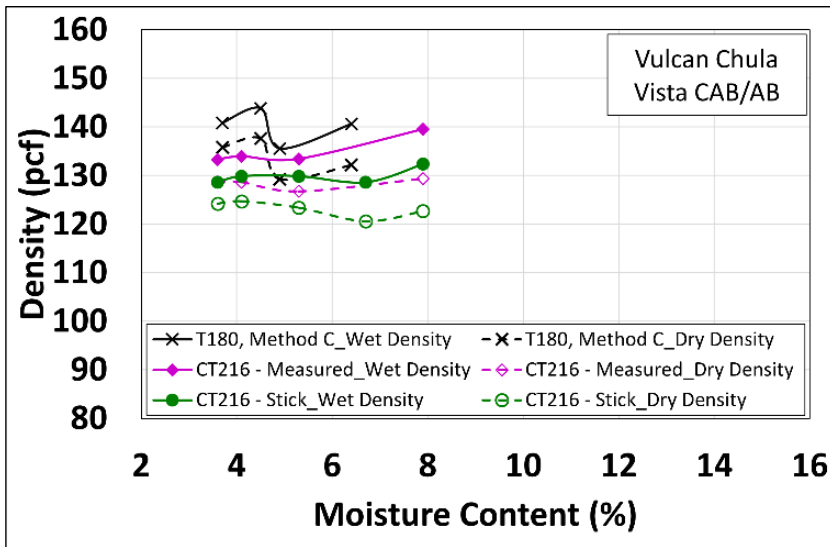


Figure C.7: Density results for Material #7.

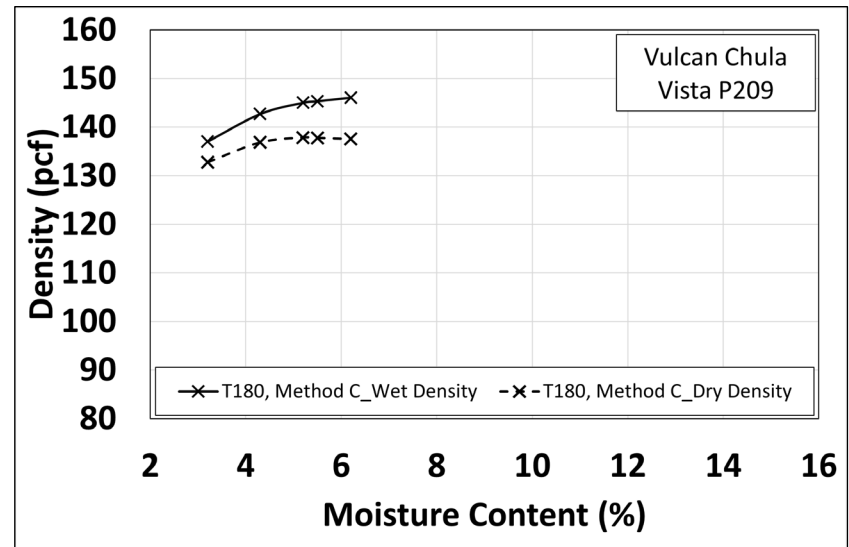


Figure C.8: Density results for Material #8.

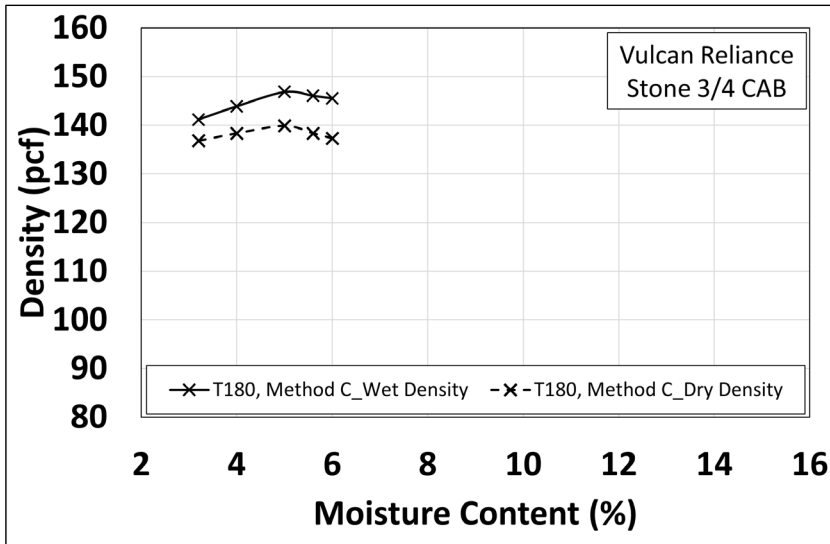


Figure C.9: Density results for Material #9.

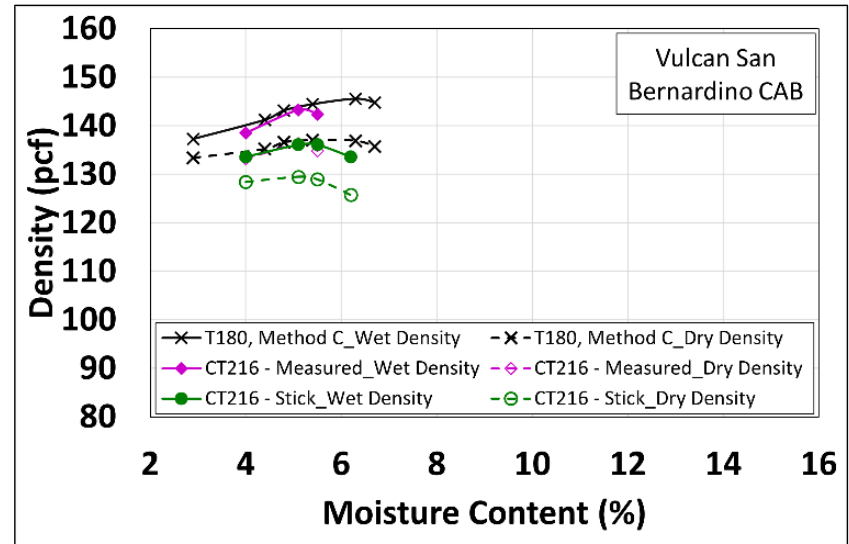


Figure C.10: Density results for Material #10.

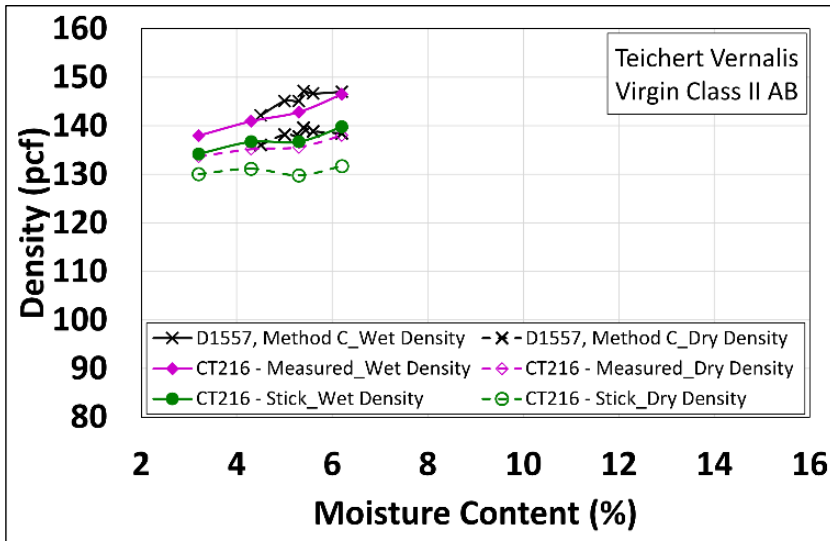


Figure C.11: Density results for Material #11.

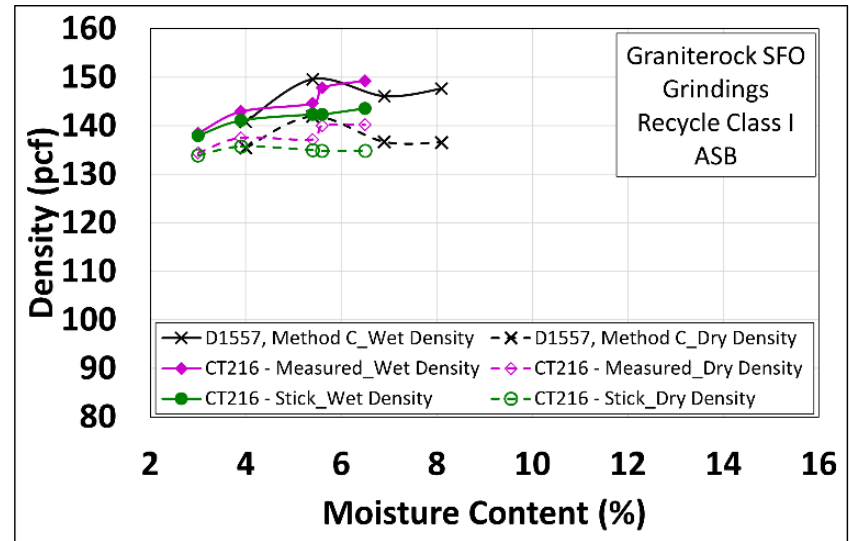


Figure C.12: Density results for Material #12.

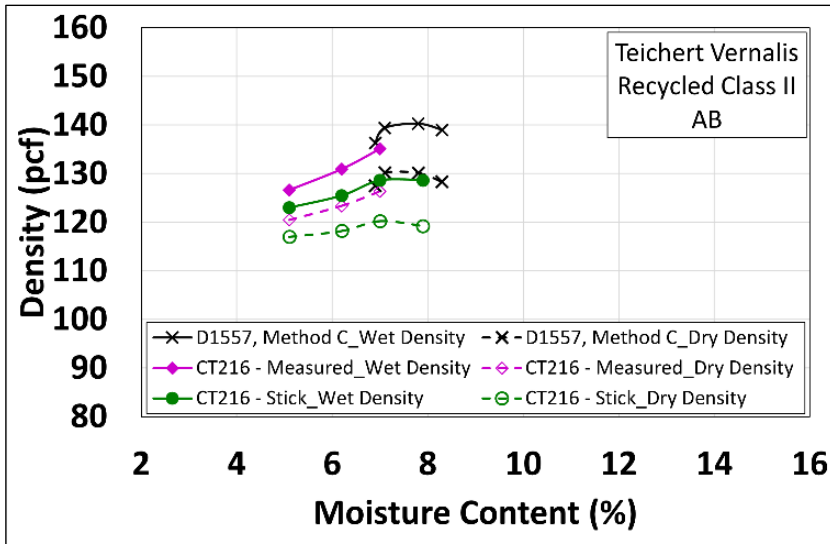


Figure C.13: Density results for Material #13.

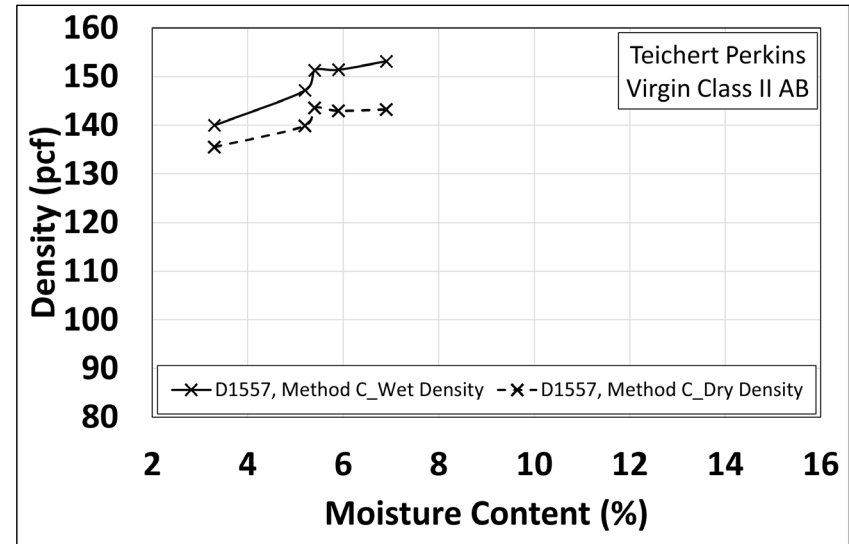


Figure C.14: Density results for Material #14.

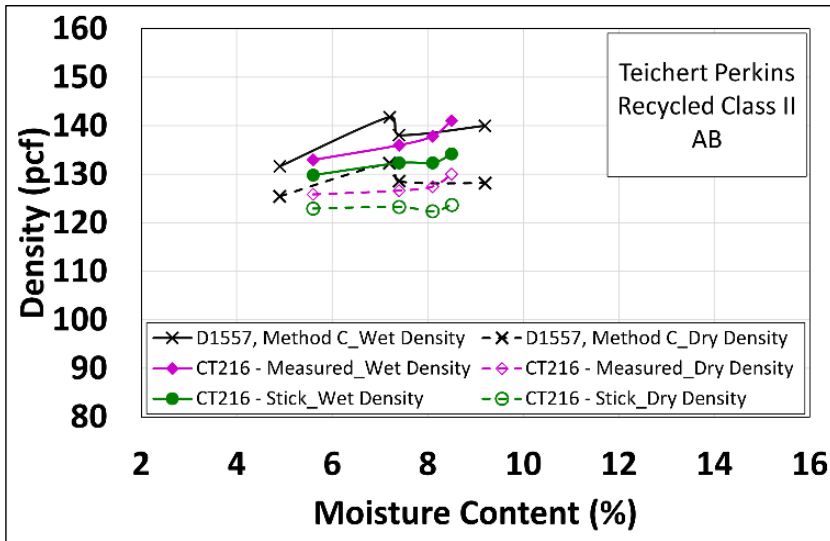


Figure C.15: Density results for Material #15.

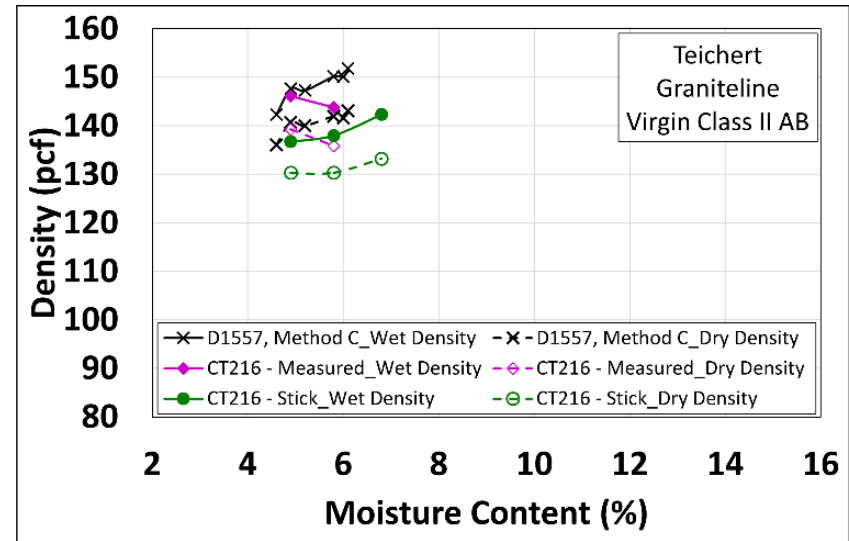


Figure C.16: Density results for Material #16.

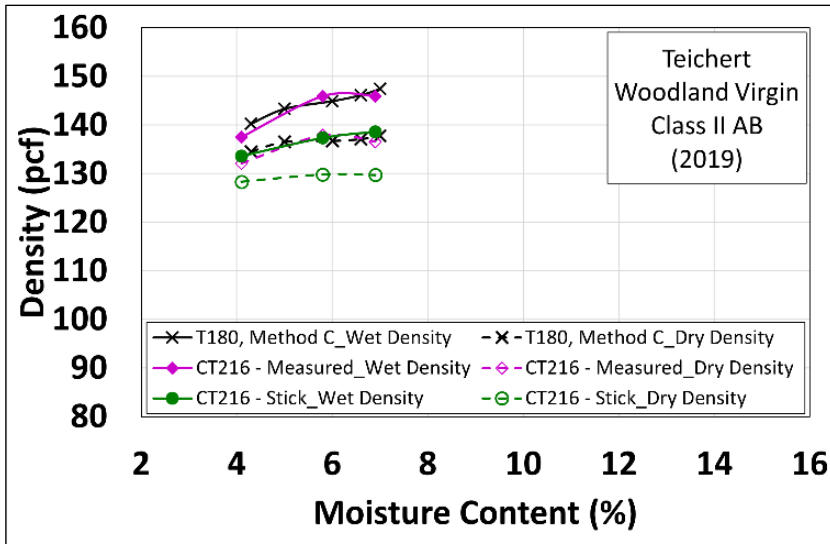


Figure C.17: Density results for Material #17.

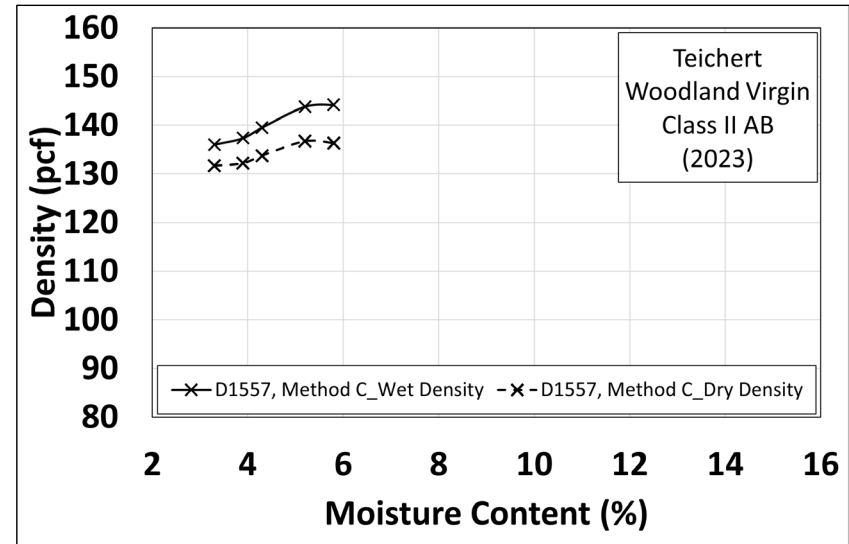


Figure C.18: Density results for Material #18.

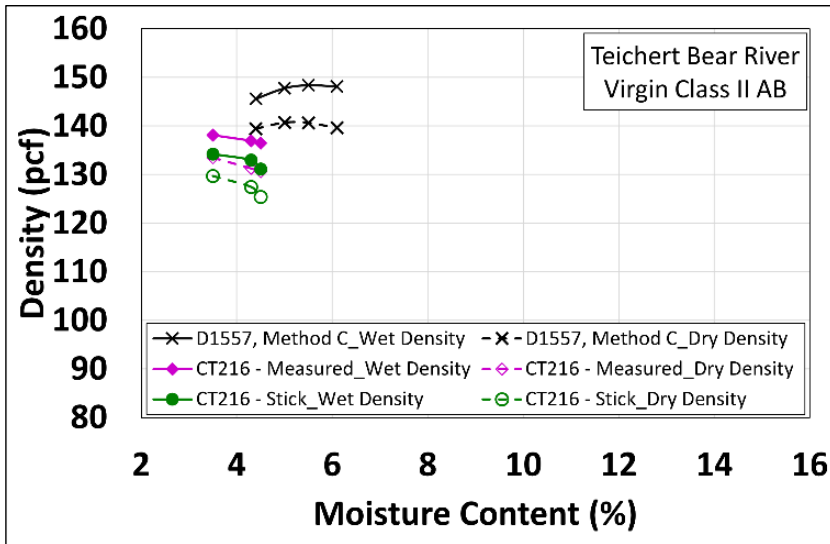


Figure C.19: Density results for Material #19.

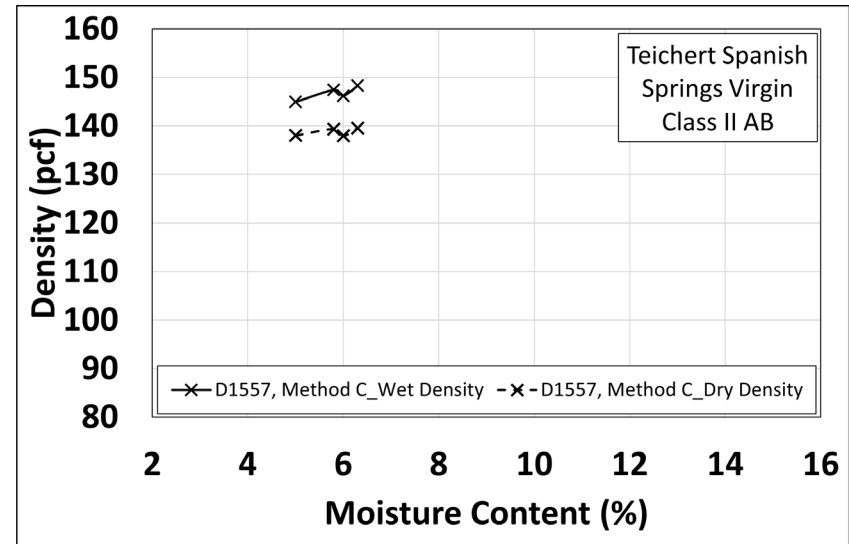


Figure C.20: Density results for Material #20.

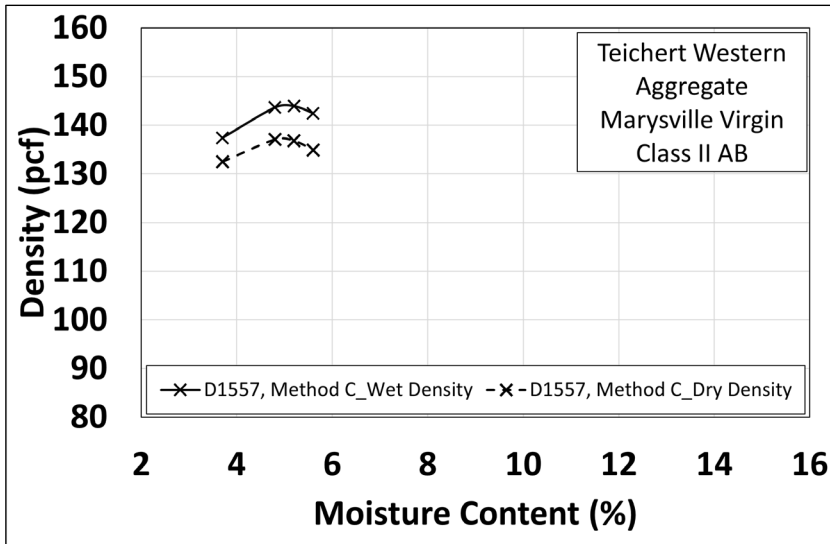


Figure C.21: Density results for Material #21.

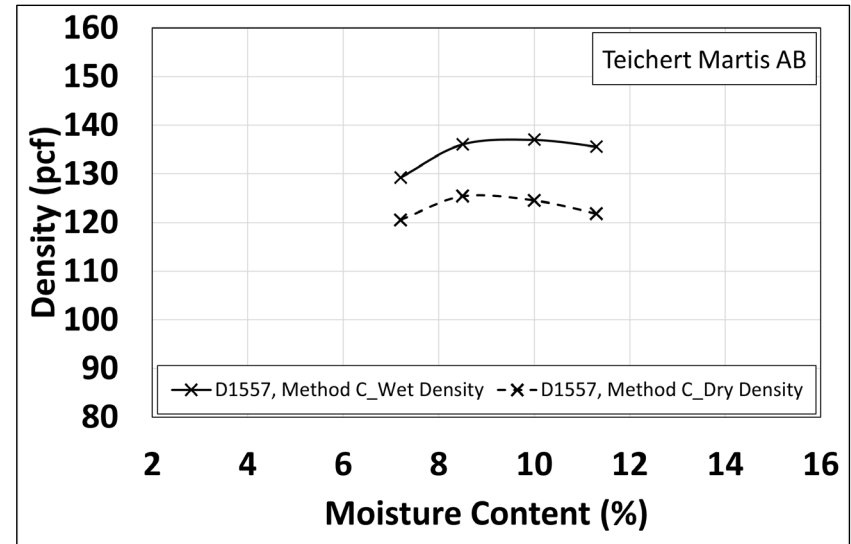


Figure C.22: Density results for Material #22.

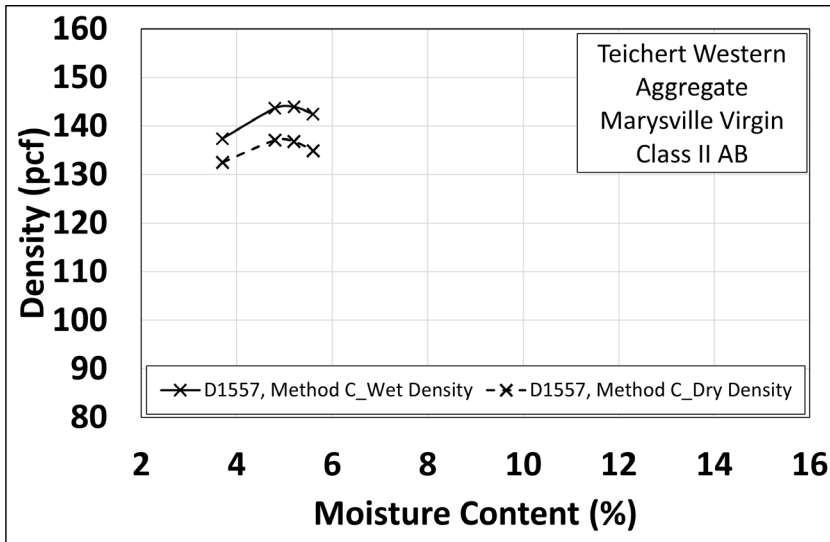


Figure C.23: Density results for Material #23.

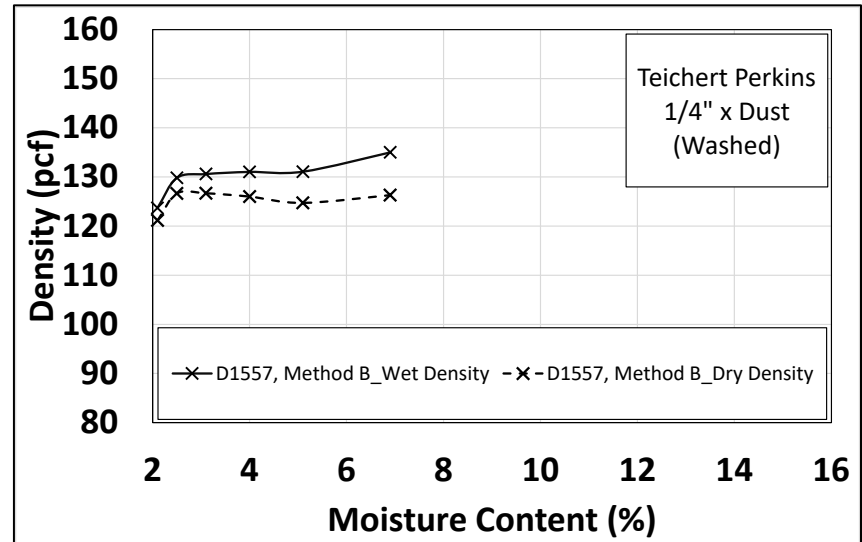


Figure C.24: Density results for Material #24.

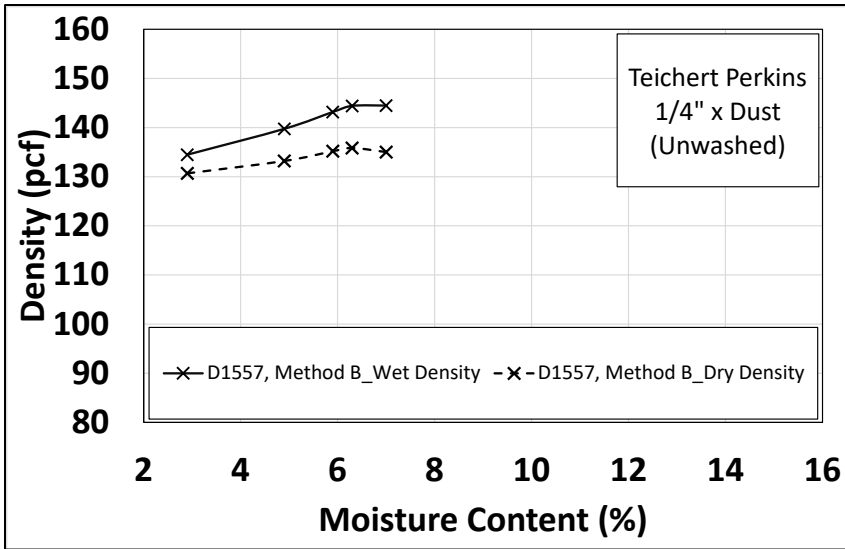


Figure C.25: Density results for Material #25.

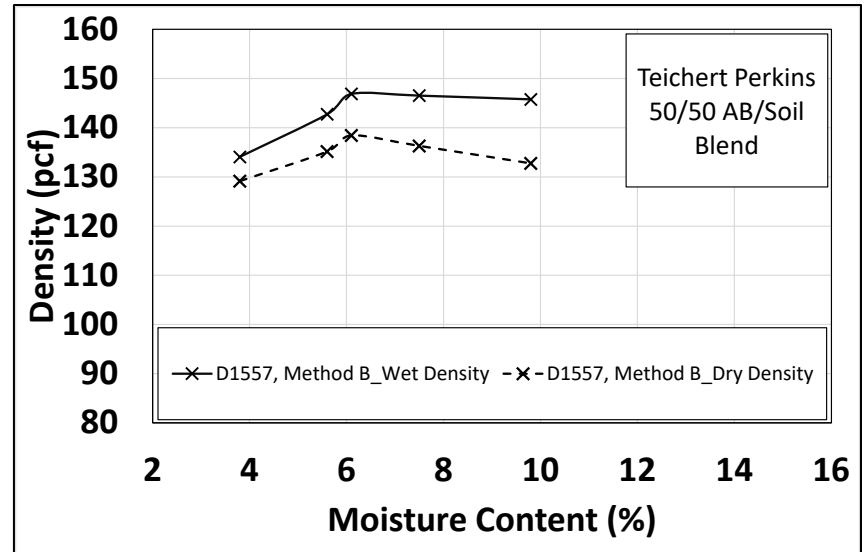


Figure C.26: Density results for Material #26.

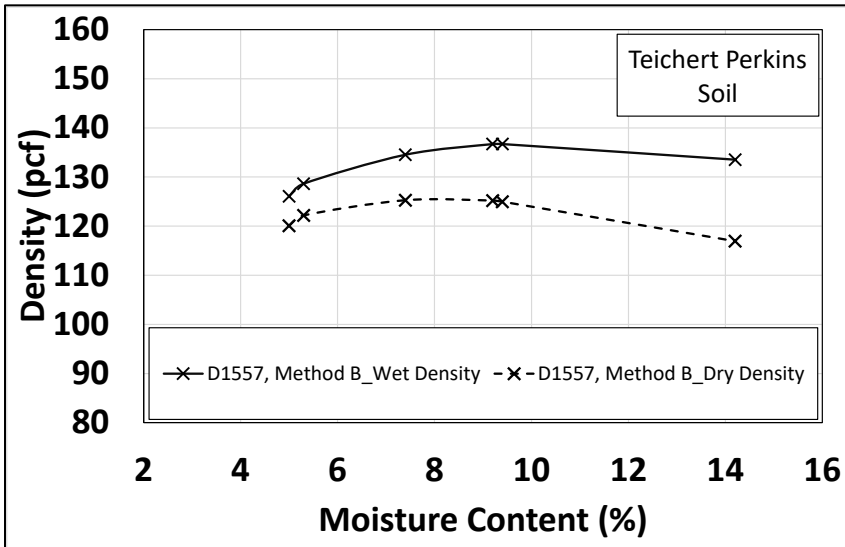


Figure C.27: Density results for Material #27.

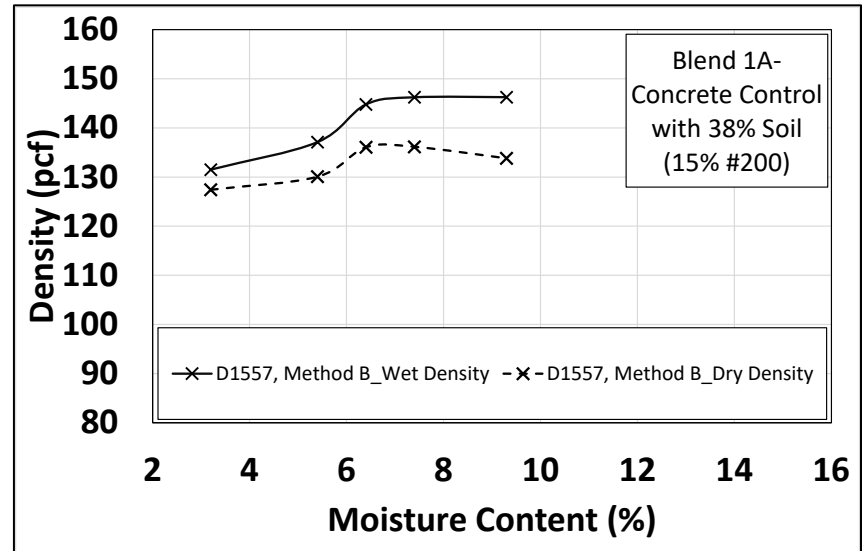


Figure C.28: Density results for Material #28.

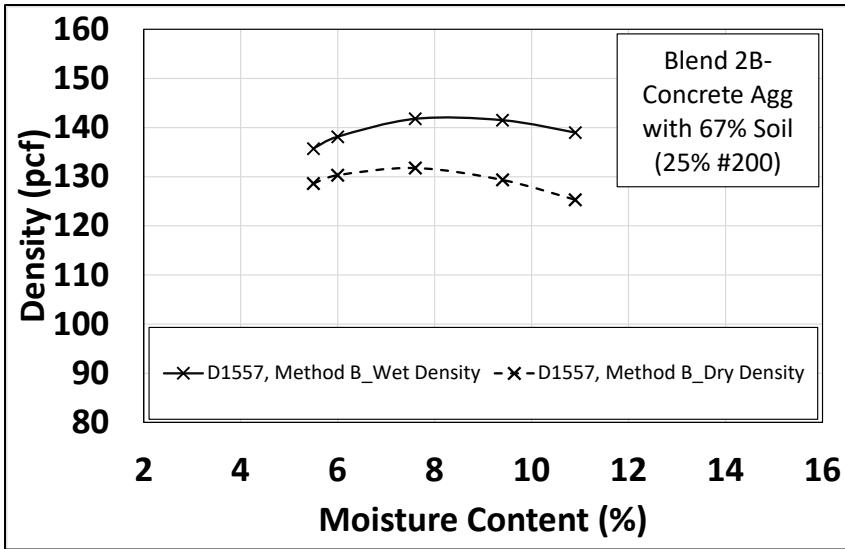


Figure C.29: Density results for Material #29.

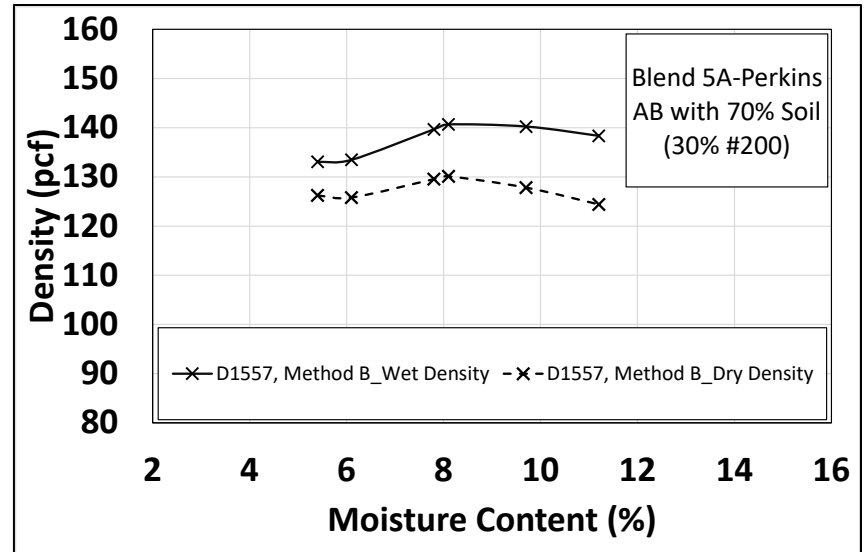


Figure C.30: Density results for Material #30.

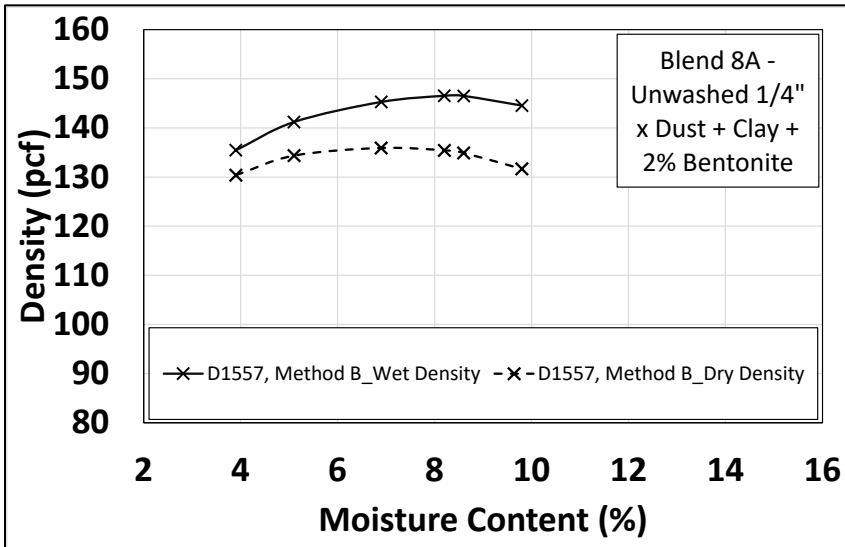


Figure C.31: Density results for Material #31.

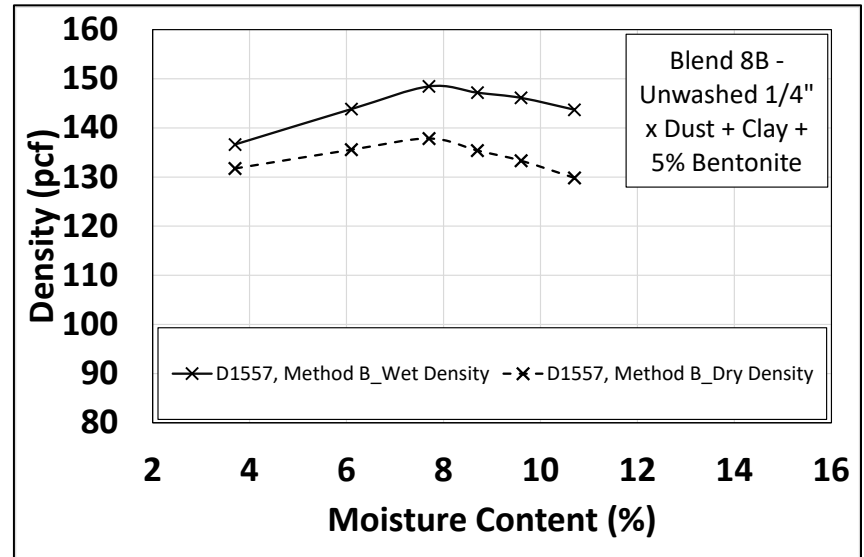


Figure C.32: Density results for Material #32.

Not tested

Figure C.33: Density results for Material #33.

APPENDIX D CONFINED COMPRESSIVE STRENGTH TEST RESULTS

This appendix includes the Mohr-Coulomb diagrams for each of the materials tested in this study.

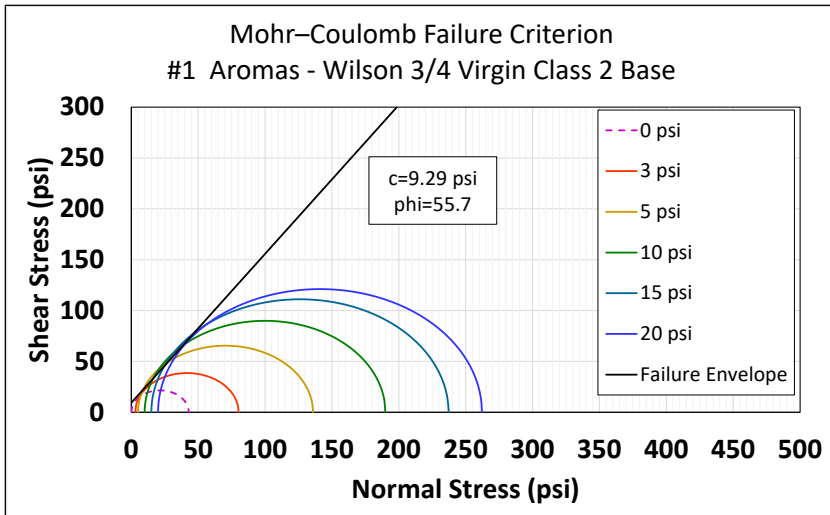


Figure D.1: Mohr-Coulomb plots for Material #1.

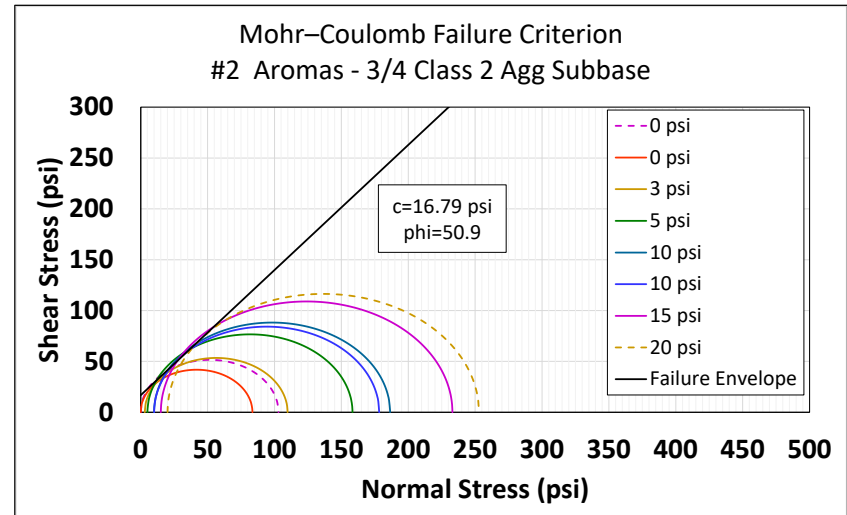


Figure D.2: Mohr-Coulomb plots for Material #2.

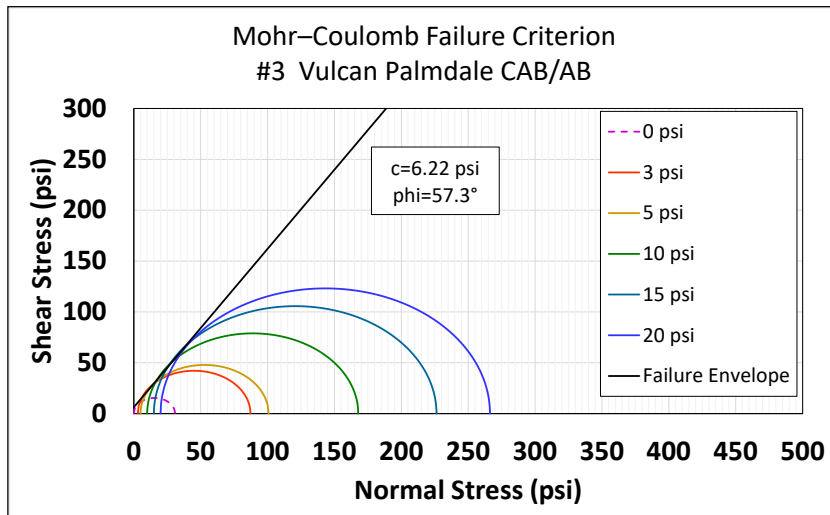


Figure D.3: Mohr-Coulomb plots for Material #3.

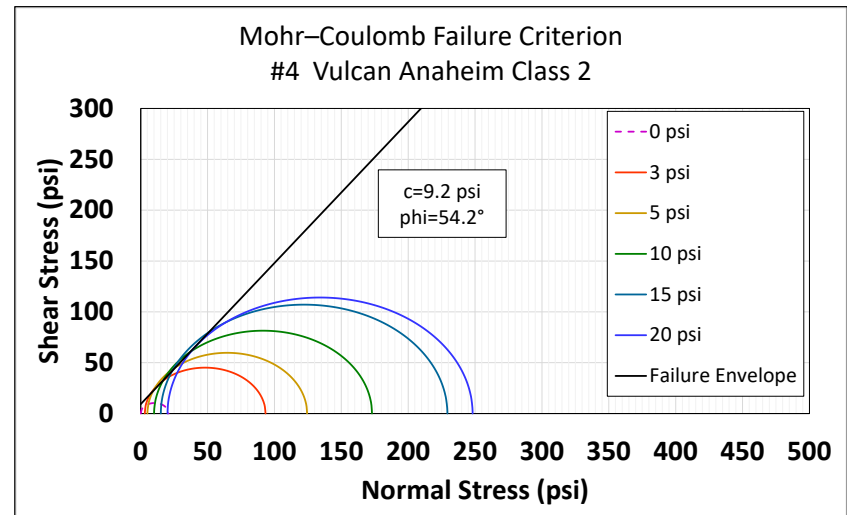


Figure D.4: Mohr-Coulomb plots for Material #4.

Not tested

Figure D.5: Mohr-Coulomb plots for Material #5.

Not tested

Figure D.7: Mohr-Coulomb plots for Material #7.

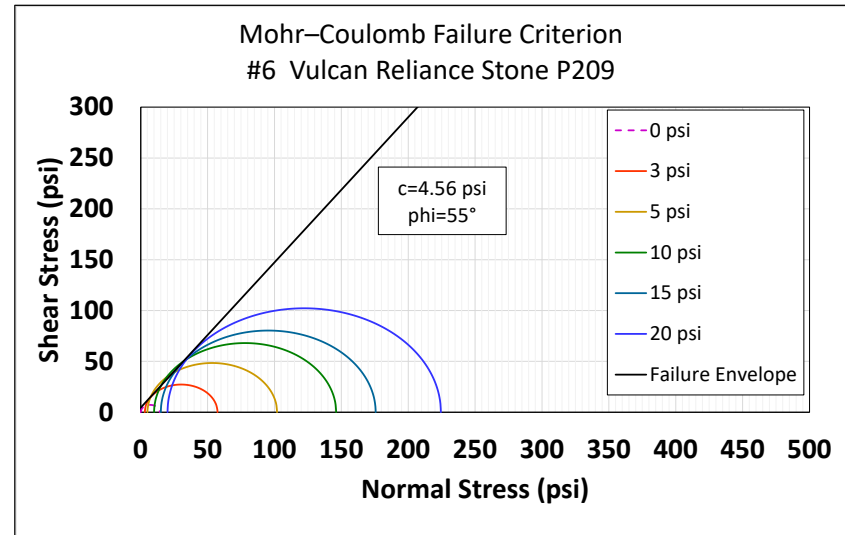


Figure D.6: Mohr-Coulomb plots for Material #6.

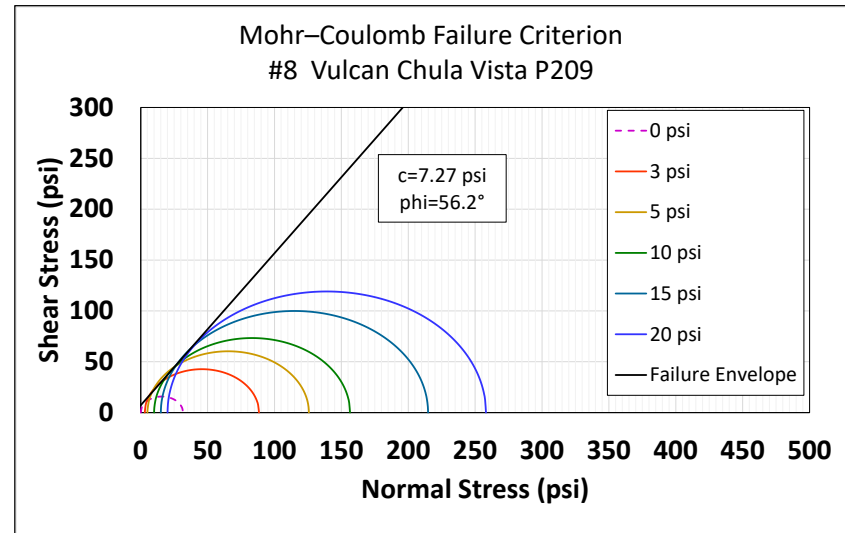


Figure D.8: Mohr-Coulomb plots for Material #8.

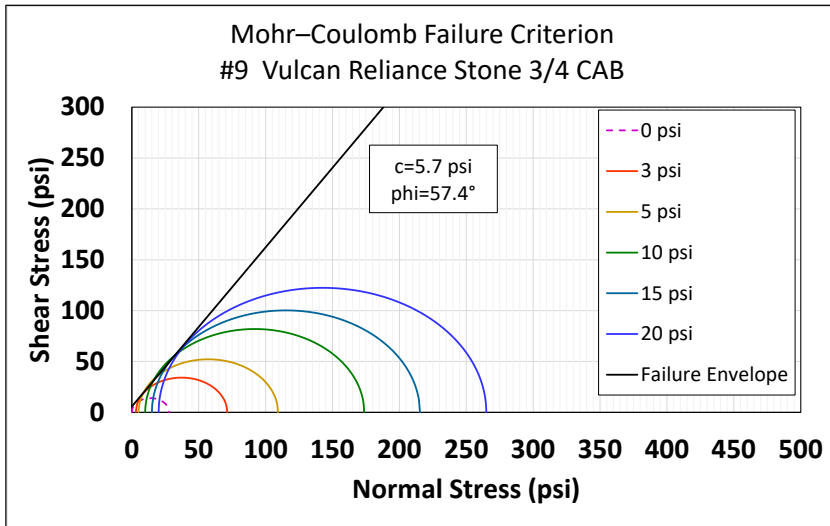


Figure D.9: Mohr-Coulomb plots for Material #9.

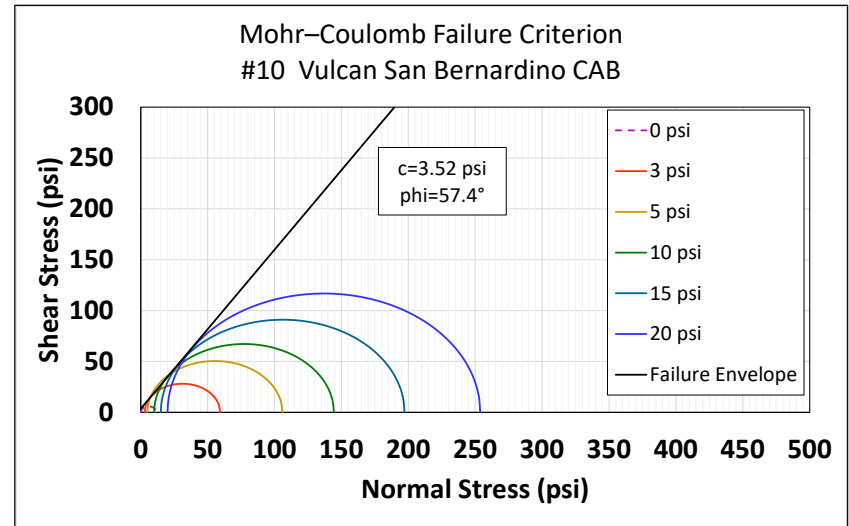


Figure D.10: Mohr-Coulomb plots for Material #10.

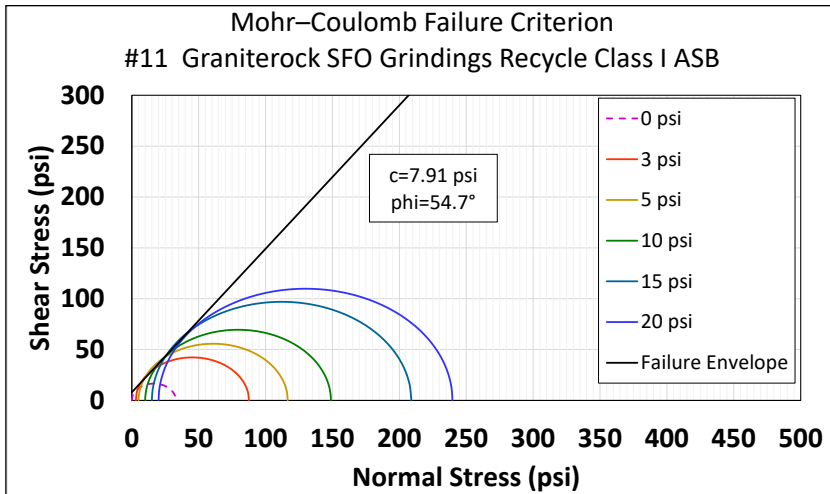


Figure D.11: Mohr-Coulomb plots for Material #11.

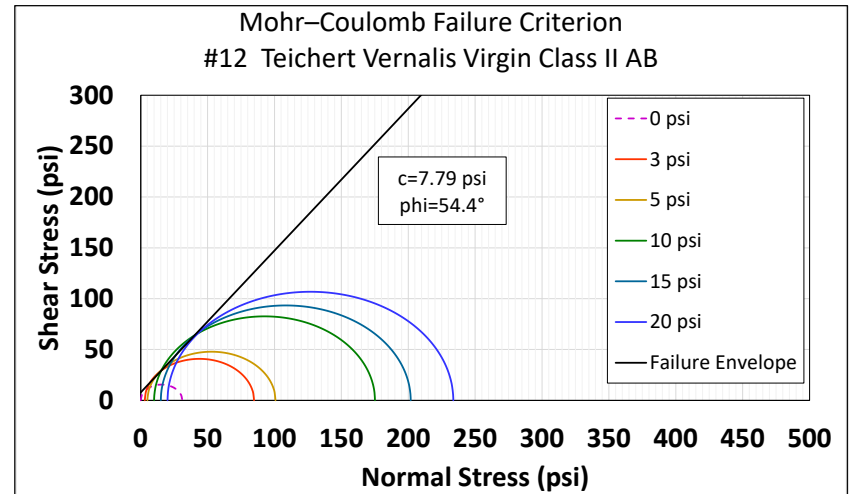


Figure D.12: Mohr-Coulomb plots for Material #12.

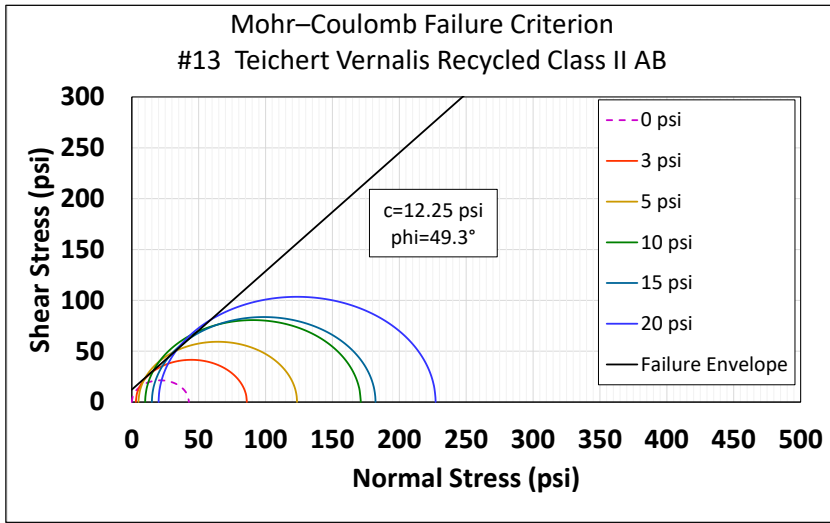


Figure D.13: Mohr-Coulomb plots for Material #13.

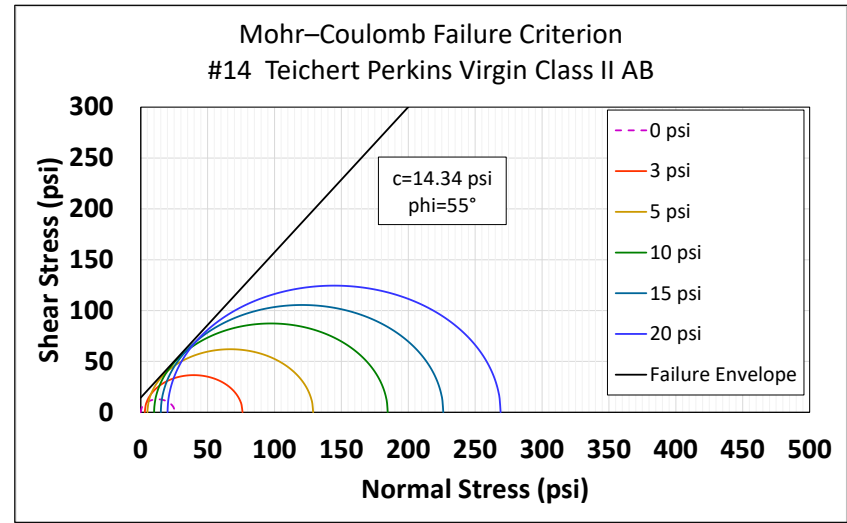


Figure D.14: Mohr-Coulomb plots for Material #14.

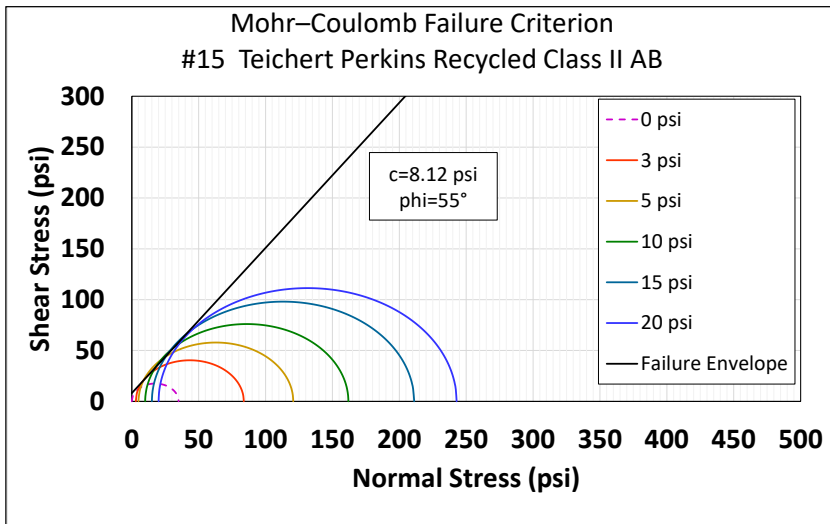


Figure D.15: Mohr-Coulomb plots for Material #15.

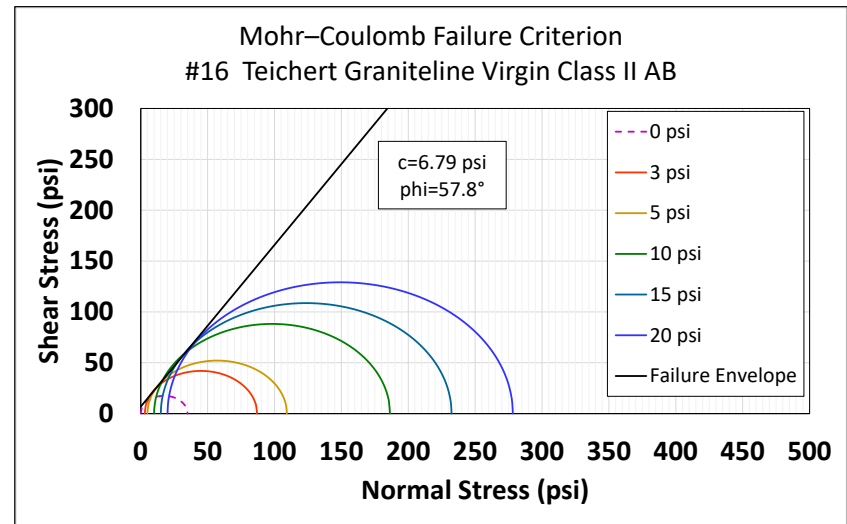


Figure D.16: Mohr-Coulomb plots for Material #16.

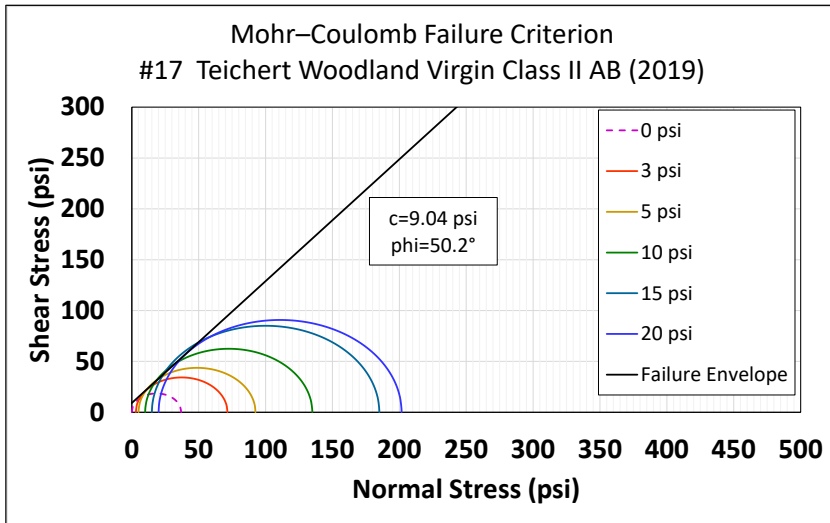


Figure D.17: Mohr-Coulomb plots for Material #17.

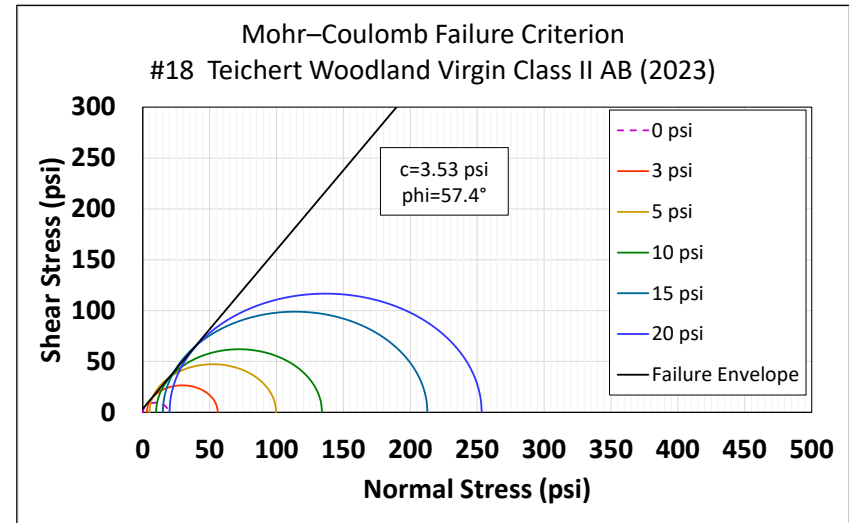


Figure D.18: Mohr-Coulomb plots for Material #18.

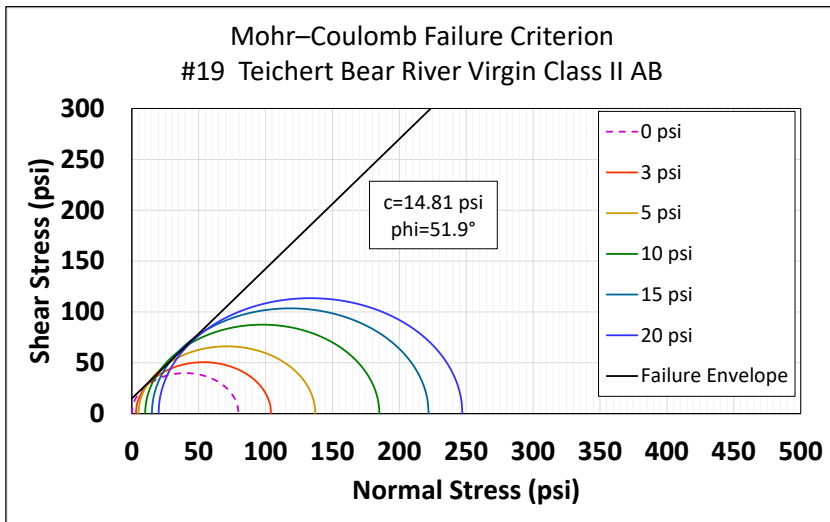


Figure D.19: Mohr-Coulomb plots for Material #19.

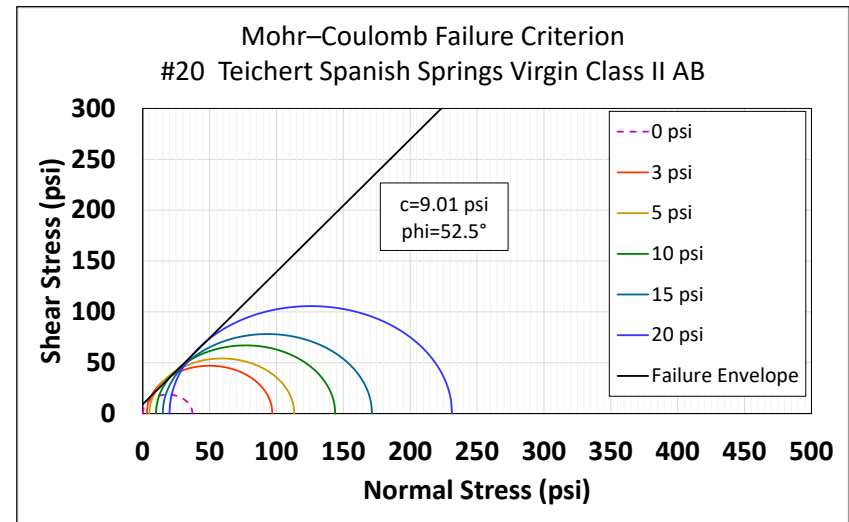


Figure D.20: Mohr-Coulomb plots for Material #20.

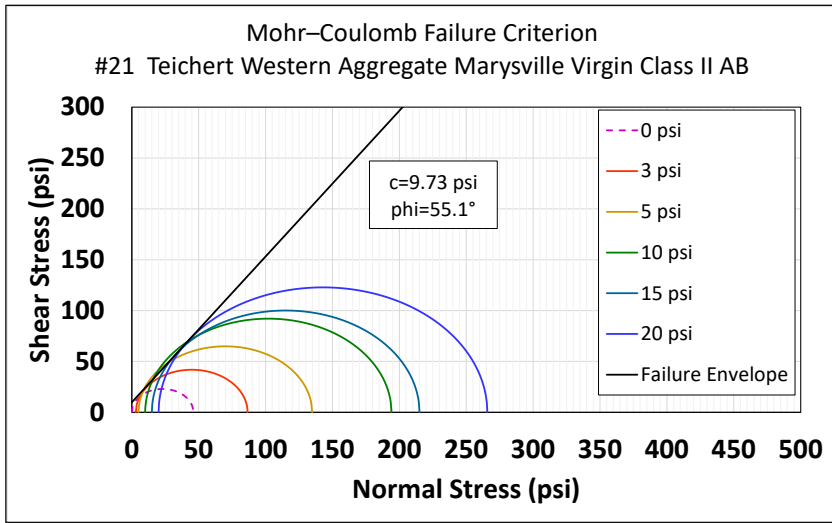


Figure D.21: Mohr-Coulomb plots for Material #21.

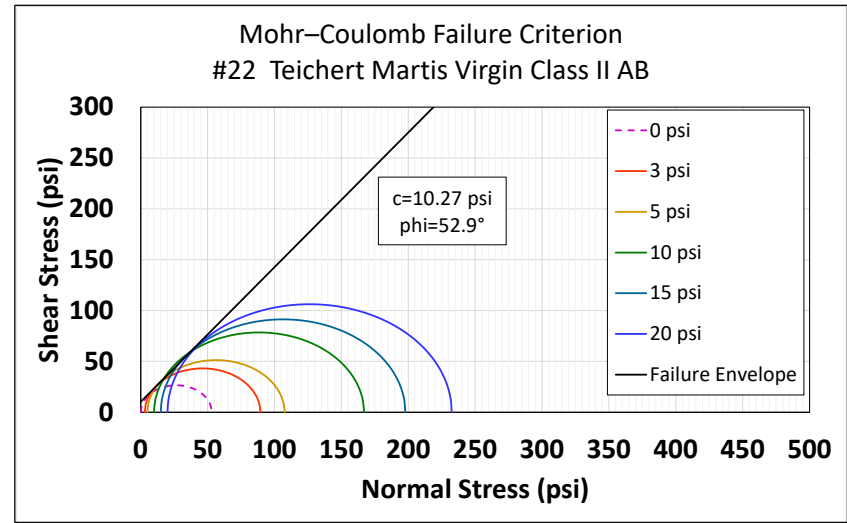


Figure D.22: Mohr-Coulomb plots for Material #22.

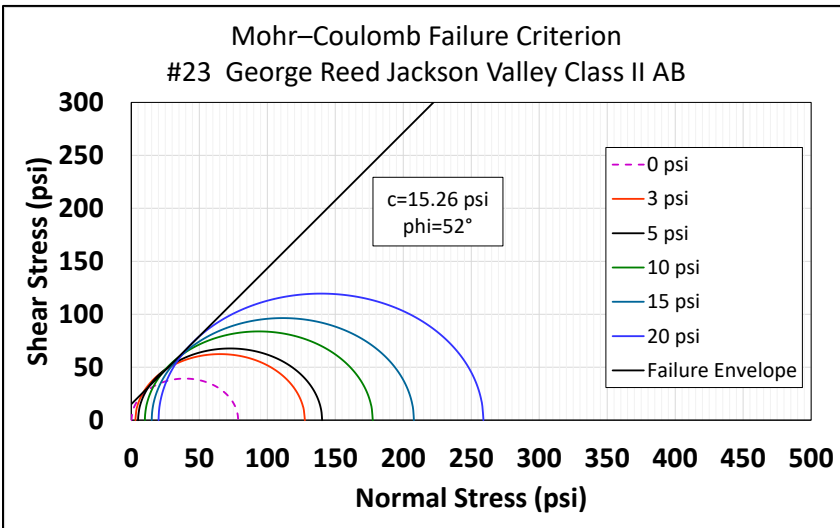


Figure D.23: Mohr-Coulomb plots for Material #23.

Not tested

Figure D.24: Mohr-Coulomb plots for Material #24.

Not tested

Not tested

Figure D.25: Mohr-Coulomb plots for Material #25.

Figure D.26: Mohr-Coulomb plots for Material #25.

Not tested

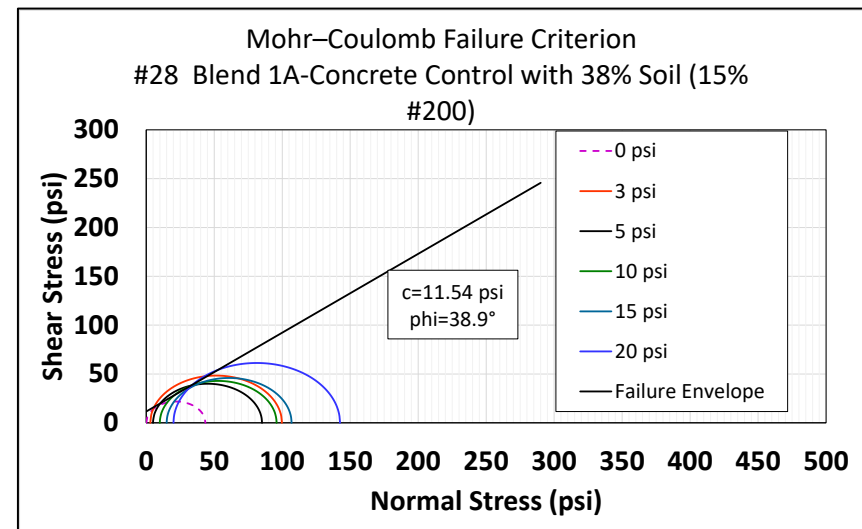


Figure D.27: Mohr-Coulomb plots for Material #27.

Figure D.28: Mohr-Coulomb plots for Material #28.

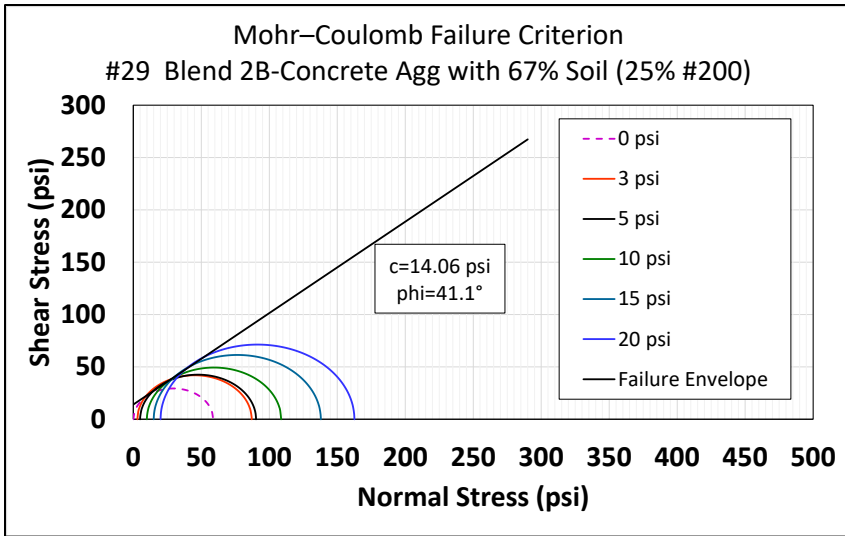


Figure D.29: Mohr-Coulomb plots for Material #29.

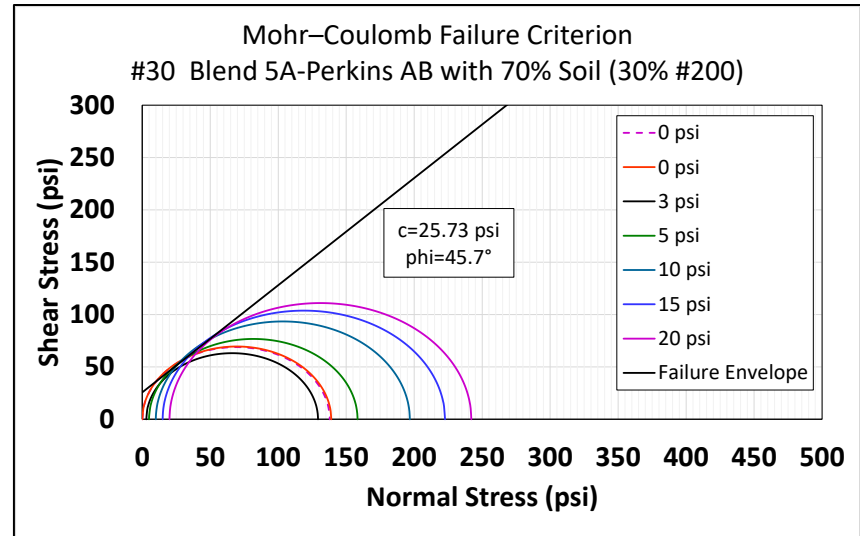


Figure D.30: Mohr-Coulomb plots for Material #30.

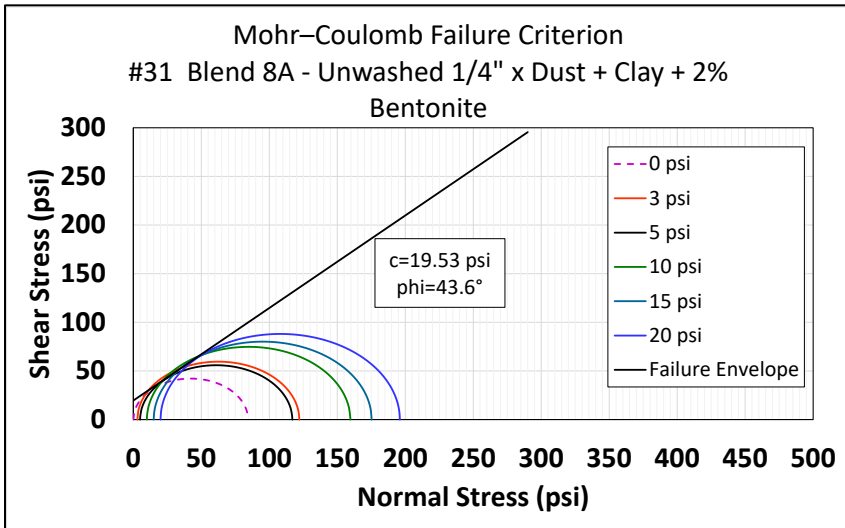


Figure D.31: Mohr-Coulomb plots for Material #31.

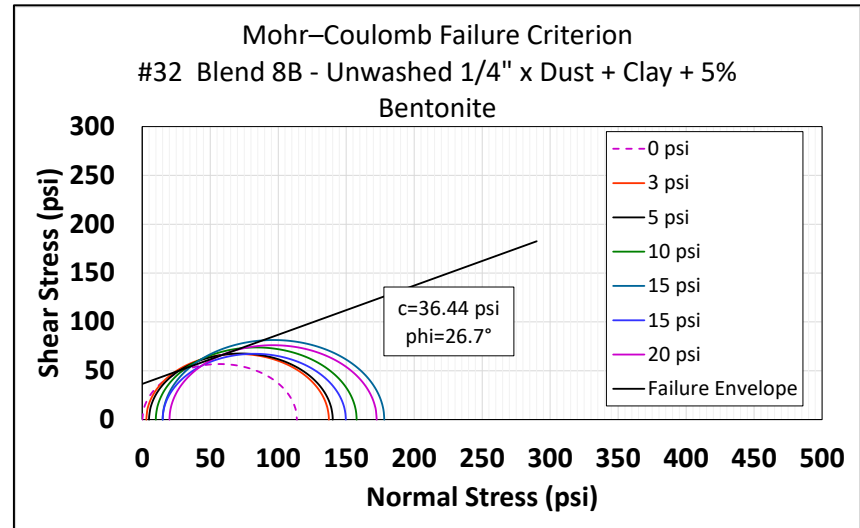


Figure D.32: Mohr-Coulomb plots for Material #32.

Not tested

Figure D.33: Mohr-Coulomb plots for Material #33.